REGULATION OF RYANODINE RECEPTOR BY NITRIC OXIDE

by

Eunji Cheong

BS, Yonsei University, 1993

MS, Yonsei University, 1995

Submitted to the Graduate Faculty of

School of Engineering in partial fulfillment

of the requirements for the degree of

Doctor of Philosophy

University of Pittsburgh

2003

UNIVERSITY OF PITTSBURGH

SCHOOL OF ENGINEERING

This dissertation was presented

by

Eunji Cheong

It was defended on

October 13, 2003

and approved by

Dr. Harvey Borovetz, Professor, Bioengineering

Dr. Daniel Farkas, Professor, Bioengineering

Dr. William Walker, Assistant professor, Cell Biology and Physiology

Dissertation Director: Dr. Guy Salama, Professor, Cell Biology and Physiology

REGULATION OF RYANODINE RECEPTOR BY NITRIC OXIDE

Eunji Cheong, PhD

University of Pittsburgh, 2003

The control of redox state of free thiols on ryanodine receptor (RyR) has been implicated as an important mechanism to regulate RyR channel activity and tune its responses to the physiological modulators. Both the skeletal and cardiac RyRs have been shown to be activated by S-nitrosylation of free thiols on them by a chemical process analogous to the oxidation of "critical" or "hyperreactive" thiols on RyR proteins. Inositol 1,4,5-triphophate receptors (IP_3Rs) that control Ca^{2+} release from internal stores in non-excitable cells were found to be activated by oxidation, which emphasizes the redox reaction as a common mechanism to regulate intracellular Ca^{2+} channels. Therefore, the study on nitric oxide-mediated regulation of these ion channels will be important to understand the regulation of Ca^{2+} homeostasis in all cells including excitable and non-excitable cells since it regulates internal Ca^{2+} stores via RyR and /or IP_3 receptors.

The aims were to investigate the chemical reaction underlying the thiol-oxidation and activation of ryanodine receptors (RyRs) by various types of NO donors namely authentic $NO^{\bullet}$, S-nitrosothiols and other $NO^{\bullet}$ species such as nitroxyl anions (i.e. HNO). The different actions of these various $NO^{\bullet}$ species were used to better evaluate the physiological significance of RyR activation by biologically relevant forms of NO, to investigate the role of oxygen on these

chemical reactions and to identify the critical cysteine residues involved in redox mediated regulation of RyRs.

The main findings are that RyRs are direct targets of S-nitrosothiols which *trans*-nitrosate hyper-reactive thiols and activate RyRs at biologically relevant concentration. In contrast, $NO^{\bullet}$ gas cannot modify RyRs at biological circumstances found in cells. HNO is considerably more potent activator of RyR1 than $NO^{\bullet}$, activates RyRs at nM concentrations. The study with truncated RyR1 indicated that all of transmembrane domains are located close to the C-terminus of the protein and the 'critical' regulatory thiols are part of conserved cysteines residing in it.

Further studies will be required to elucidate the interplay of oxidants and reductants found in the cytosolic milieu of all cells and how these activators and inhibitors act to regulate the opening and closure of Ca^{2+} release channels.

TABLE OF CONTENTS

ACKNOWLEDGEMENTS xvi

1.0 INTRODUCTION 1

1.1 MUSCLE CONTRACTION 3

1.1.1 Ultrastructure of Muscle Fiber 3

1.1.2 Excitation-Contraction Coupling 5

1.1.3 Difference in E-C Coupling in Skeletal and Cardiac Muscle 7

1.1.4 Ryanodine Receptors in Smooth Muscle 9

1.2 STRUCTURE AND TOPOLOGY OF RYRS 10

1.2.1 Structure of RyRs 10

1.2.2 Conductance Properties of RyRs 15

1.3 OVERVIEW OF RYRS' REGULATION 16

1.3.1 RyR Modulators 16

1.3.2 Proteins Associated with RyRs in the SR 19

1.3.3 Redox-medicated Regulation of RyRs 21

1.4 NITRIC OXIDE MEDIATED REGULATION OF RYRS 23

1.4.1 Nitric Oxide 23

1.4.2 NO Synthases 24

1.4.3 Function of NO in Various Muscles 25

1.4.4 Activation of RyRs by Various Nitric Oxide Donors 28
1.5 LOW MOLECULAR WEIGHT S-NITROSOTHIOLS 30
1.5.1 Physiological Forms of NO 30
1.5.2 S-nitrosothiols Trans-nitrosate Protein Thiols 33
1.6 HNO INDUCED ACTIVATION OF RYRS 34
1.7 REGULATORY CYSTEINES ON RYRS 34
1.7.1 Identification of Regulatory Cysteines on RyRs 34
1.7.2 Cysteine Residues Involved in Channel Gating 36
1.8 SUMMARY AND AIM OF STUDY 40
2.0 METHODS 42
2.1 PREPARATION OF RYRS 42
2.1.1 Preparation of SR Vesicles from Muscle (Skeletal and Cardiac) 42
2.1.2 Purification of RyRs from SR Vesicles 42
2.1.3 Preparation of Membrane Vesicles from HEK 293 Cells 43
2.2 TRANSIENT EXPRESSION OF RYRS IN CHO CELLS 43
2.2.1 Construction of cDNA to Express Truncated RyRs 43
2.2.2 Transient Expression in CHO Cells 44
2.3 CONSTRUCTION OF HEK CELLS EXPRESSING TRUNCATED RYRS 45
2.3.1 Construction of Truncated RyR cDNA 45
2.3.2 Stable Expression of RyRs in HEK Cells 46
2.4 MEASUREMENT OF RYR ACTIVITY VIA SR CA^{2+} TRANSPORT 48
2.5 MEASUREMENTS OF CA_I IN ISOLATED CHO CELLS 50
2.6 STUDY OF SINGLE CHANNEL ACTIVITY 50
2.6.1 Planar Lipid Bilayer Technique 51
2.6.2 Overview of the Planar Bilayer Apparatus 52

2.6.3 Analysis of Single Channel Activity Recordings 56

2.6.4 Statistics 62

2.7 EPR MEASUREMENTS 62

2.8 MEASUREMENT OF CREATINE KINASE ACTIVITY 63

2.9 MATERIALS 63

3.0 CHEMICAL REACTION OF S-NITROSOTHIOLS THAT ACTIVATE RYRS 65

3.1 CYS-SNO NITROSYLATES REGULATORY THIOLS ON RYR 65

3.2 EFFECT OF COPPER (I) AND CA^{2+} CHELATOR ON THE DECOMPOSITION OF CYS-SNO 65

3.3 S-NITROSOTHIOLS ELICIT RAPID CA^{2+} RELEASE FROM SR WITHOUT $NO^{\bullet}$ LIBERATION 69

3.4 POTENCY OF VARIOUS NO DONORS 73

3.5 EFFECT OF CYS-SNO ON SINGLE CHANNEL ACTIVITY 76

3.6 EFFECT OF OXYGEN LEVEL ON $NO^{\bullet}$ AND S-NITROSOTHIOLS-INDUCED ACTIVATION OF RYR 79

3.7 GATING OF RYR 87

3.8 EFFECT OF CYS-SNO ON CREATINE KINASE ACTIVITY 92

3.9 SUMMARY AND CONCLUSION 95

4.0 HNO-INDUCED ACTIVATION OF RYR 96

4.1 GENERATION OF HNO 96

4.2 HNO INDUCES CA^{2+} RELEASE FROM SKELETAL SR 99

4.3 HNO ACTIVATES SINGLE RYR1 CHANNEL 102

4.4 SUMMARY 104

5.0 IDENTIFICATION OF REGULATORY CYSTEINES ON RYRS 105

5.1 CYTOSOLIC AND LUMINAL SIDE ACTIVATION OF RYR BY NO 105

5.2 TRUNCATED RYR 108
5.2.1 Transient Expression of Truncated Form of Ryanodine Receptors in CHO Cells 109
5.2.2 Permanent Expression of Truncated RyRs in HEK Cells 114
5.2.3 p75 RyR1 Forms a Functional Channel 116
5.3 SUMMARY 118
6.0 DISCUSSION 120
6.1 MEASUREMENT OF RYR ACTIVITY 120
6.1.1 Single Channel Recording 120
6.1.2 Use of Purified RyR 121
6.2 REDOX REGULATION OF THE RYANODINE RECEPTOR 121
6.3 ACTIVATION OF THE RYR BY S-NITROSOTHIOLS 123
6.3.1 S-nitrosothiols Activate the RyR by Transnitrosation 124
6.3.2 Cys-SNO versus GSNO 125
6.3.3 NO-function and Oxygen 126
6.3.4 Gating of the RyR 129
6.3.5 NO Inhibits CK 131
6.4 HNO-INDUCED ACTIVATION OF THE RYR 132
6.5 TRUNCATED RYR (P75) FORMS A FUNCTIONING CHANNEL 134
6.5.1 Transient Expression of RyRs in CHO Cells 134
6.5.2 Permanent Expression of p75 RyR1 137
6.5.3 Single Channel Study of p75 RyR1 138
6.6 REVISITING NO-INDUCED RELAXATION OF SMOOTH MUSCLE 138
6.7 LIMITATION OF THE CURRENT STUDY AND FUTURE WORK 140
7.0 SUMMARY AND CONCLUSIONS 142

BIBLIOGRAPHY 144

LIST OF TABLES

Table No.		Page
1	Cysteine residues conserved in mammalian ryanodine and IP_3 receptors…….	38
2	CK activity in the presence of cys-SNO……	94

LIST OF FIGURES

Figure No.		Page
1	Ultrastructure of muscle fibers and Triad Junction	4
2	Excitation-contraction coupling event	6
3	Comparison of excitation-contraction coupling in skeletal and cardiac muscle	8
4	Cryo-electron Microscopy and 3-D reconstruction of skeletal RyR	13
5	Proteins interacting with RyRs	20
6	L-cysteine potentiate nitric oxide to induce Ca^{2+} release from SR vesicles	32
7	Topology of RyR according to 8 transmembrane domain model	39
8	Schematics of RyR Constructs driven by T7 Promoter	43
9	Generation of Flp-in HEK 293 cells stably expressing truncated RyR1	47
10	Spectrophotometric measurement of Ca^{2+} transport across SR vesicle membrane	49
11	Schematic representation of black lipid membrane apparatus	52
12	Schematics and picture of planar bilayer apparatus	54
13	Reconstitution of RyR channels by fusion of SR vesicles with planar lipid bilayer	56
14	Calculation of open probability of single channel	58
15	Four simple Markov models	60
16	Interactions of cys-SNO with thiols on RyR	66

17 Absorption spectra of cys-SNO in the presence and absence of BCS and EGTA……68

18 Cys-SNO induces Ca^{2+} release from skeletal SR……..70

19 GSNO and SNAP induce Ca^{2+} release from skeletal SR without $NO^{\bullet}$ generation……..71

20 Authentic NO• requires high concentration to induce Ca^{2+} release from SR vesicles…….……..72

21 Rate of Ca^{2+} release as function of NO donor concentration…….……75

22 Cys-SNO activates RyR1 via a trans-nitrosation reaction ….……...77

23 Open probability (P_o) calculated from single channel recording of purified RyR1…..…78

24 pO_2 level do not alter $NO^{\bullet}$ and cys-SNO induced Ca^{2+} release from SR vesicles…..…...80

25 pO_2 does not alter RyR1 single channel activity triggered by $NO^{\bullet}$ or cys-SNO……83

26 Open probability of purified RyR1 channel……...84

27 pO_2 does not affect activation of RyR1 channel induced by $NO^{\bullet}$ and cys-SNO in the absence of calmodulin……...86

28 Open and closed dwell times of a RyR channel……89

29 Markov Model for the purified RyR1 channel at pCa=5……..90

30 Markov Model for the purified RyR1 channel activated by cys-SNO…….91

31 UV- and EPR-spectra monitor the hydrolysis of ANGS……..98

32 HNO-induces Ca^{2+} release from Ca^{2+}-loaded SR vesicles……..100

33 HNO-, not hydroxyl radical, released from ANGS induces Ca^{2+} release from Ca^{2+}-loaded SR vesicles…….……..101

34 HNO increases P_o of purified RyR1 reconstituted in planar bilayers……..103

35 Cys-SNO activates RyR channel … ……..107

36 Immuno-analysis of full-length and truncated RyR1 expressed in CHO cells……110

37 Effect of ryanodine (10 μM) on control and transfected CHO cells……..……..112

38 Cai elevation induced by cys-SNO in CHO cells transformed to express ryanodine receptor in the absence of external Ca^{2+}…… ……113

39 Immuno-analysis of truncated RyR1s expressed in Flpin-HEK293 cells…….……..115

40 Cys-SNO increases Po of truncated (p75) RyR1 reconstituted in planar bilayer……117

ABBREVIATIONS

ANGS	sodium trioxodinitrate ($Na_2N_2O_3$; Angeli's salt)
AP III	Antipyrylazo III
BK_{Ca} channel	large conductance calcium activated potassium channel
CaM	calmodulin
cGMP	cyclic guanosine monophosphate
CHAPS	3-[(3-cholamidopropyl) dimethyl-ammonio]-1-propanesulfonate
CICR	calcium induced calcium release
CK	creatine kinase
CP	phosphocreatine
Cys-SNO	S-nitrosocysteine
DHPR	dihydropyridine receptor (L-type Ca^{2+} channel)
E-C-coupling	excitation-contraction coupling
EGTA	ethylene glycol bis(β-aminoethyl ether)-N,N,N',N'-tetraacetic acid
GSNO	S-nitrosoglutathione
IP_3Rs	inositol 1,4,5-triphophate receptors
NO	nitric oxide
NOS	nitric oxide synthase
ODQ	1H-[1,2,4]oxadiazolo[4,3-a]quinoxaline-1-one

PC	phosphatidyl choline
Pdf	probability density function
PE	phosphatidyl ethanolamine
PS	phosphatidyl serine
PKA	cAMP dependent protein kinase
PKG	cGMP dependent protein kinase
ROS	reactive oxygen species
RyR	ryanodine receptor
SNAP	S-nitroso-N-acetyl penicillamine
SOD	superoxide dismutase
SR	sarcoplasmic reticulum

ACKNOWLEDGEMENTS

Millions of Thanks are to my advisor, Dr. Guy Salama, who has taught me how to formulate scientific questions and approach to answer them. I would like to thank you for sharing your enthusiasm and love for science with me. Your support and guidance will always be appreciated.

I would also like to thank Dr. Harvey Borovetz for support, suggestions, and guidance from the beginning and during my graduate career. In addition, I would like to thank Dr. Willy Walker for teaching me molecular biology and giving me guidance on my work. Also, I would like to thank Dr. Daniel Farkas for agreeing to serve on my committee and to offer your helpful comments to the project.

I would like to thank Dr. Detcho Stoyanovsky for advices and support on my work for years. I am grateful to my research group including Dr. Bum-Rak Choi, Dr. Tong Liu, Dr. Linda Baker and Dr. Elizabeth Menshikova for their friendship and helpful input over the years. I appreciate the professional work done by the electronic (Jim Von Hedemann and Greg Szekerves) and machine (William Hughes and Scott McPherson) shops for their help in bilayer system used in this project. I would like to acknowledge the financial support of American Heart Pre-Doctoral Fellowship and the University of Pittsburgh, Department of Bioengineering that helped me to pursue my graduate education.

Endless thanks to my father, mother and parents-in-laws for their patience and their continued love and support through the years. I also thank my brother and sister-in-law for taking care of my parents with all the way I should have done. Special thanks to my husband, Seungook Min and to my little guardian angel, Janice Jungbin Min, for always being there for me.

1.0 INTRODUCTION

The overall oxidation/reduction (redox) state of a cell is a consequence of the balance between the level of oxidizing and reducing equivalents. Intracellular environment is usually maintained at a highly reduced state, protecting the cell from free radical damages that are often associated with cell survival. The excessive production of oxygen and nitric oxide (NO) radicals is linked to pathological states [1, 2]. However, a wealth of data indicates that reactive oxygen species (ROS) and nitric oxide (NO) are continually generated in healthy cells and the thiol redox modulation of various cellular proteins by them has been attributed to important cell signaling processes responding to either external or intracellular stimuli [3-6].

By analogy of oxidation, reversible nitrosation of cellular proteins by nitric oxide acts to transduce molecular signals regulating diverse processes such as muscle contraction, neurotransmission, protein metabolism, immune reactions and apoptosis. Nitric oxide is a signaling molecule found in almost all organs including the nervous, immune, respiratory, urologic, gastrointestinal and cardiovascular and muscular systems [4, 7]. Since nitric oxide (NO) was first identified as the endothelial derived relaxing factor, most of the earlier studies on NO-related functions focused on its vasodilating effect via cGMP-dependent mechanism [8-12]. However, it was found that nitric oxide has a contradictory effect on the contractility of cardiac and skeletal muscle and that there is a cGMP-independent pathway involving S-nitrosation of the Ryanodine receptor, an intracellular Ca^{2+} release channel [13-17]. Recently, several studies have

demonstrated that the activities of various cellular proteins are regulated by the S-nitrosation of protein thiols [4, 18-22].

Nitric oxide's effect on muscle contractility is mediated mainly by either the cGMP dependent mechanism or the S-nitrosation of the RyR. Both skeletal and cardiac RyRs are activated by the S-nitrosylation of 'hyper-reactive' regulatory thiols on RyRs [14, 15]. Muscle contractility is dependent on intracellular Ca^{2+} concentration. Massive Ca^{2+} release from the SR via RyRs is most important in intracellular Ca^{2+} cycling during the muscle contraction-relaxation, which tunes muscle force and cardiac output [23-27]. The failure of normal Ca^{2+} cycling is most likely not compatible with life. In the cardiovascular system, the dysregulation of Ca^{2+} cycling from beat to beat has been provisionally linked to many pathological conditions such as myocardial infarction, hypertension, cardiomyopathy, and hypertrophy [16, 28-32]. In skeletal muscle, the spontaneous mutations of RyR1 have been linked to malignant hyperthermia and central core disease [27, 31, 33-36]. Therefore, the elucidation of RyR regulation would be crucial to understand the mechanism of muscle contraction and the related physiological and pathological phenomena.

Despite extensive studies on nitric oxide's effect on the RyR, there is little known about the chemistry underlying S-nitrosation. Therefore, this study investigated the physiologically active form of NO to activate RyRs and the cysteine residues of the RyR involved in S-nitrosation by NO. This chapter introduces the role of the RyR in excitation-contraction (E-C) coupling in striated muscle, the regulation of the RyR, and the chemical and biological functions of nitric oxide and NO-related molecules that might be physiologically active forms of nitric oxide.

1.1 MUSCLE CONTRACTION

It is essential to understand how muscle contracts and relaxes to appreciate the role of the ryanodine receptor in Ca^{2+} cycling and its importance in muscle contractility.

1.1.1 Ultrastructure of Muscle Fiber

The structure of muscle fiber is shown as a diagram in figure 1. The basic repeating contractile unit, from Z band to Z band, is called the sarcomere. The two major structural proteins of the myofibril are myosin (thick filaments) and actin (thin filaments). Muscle contraction occurs via interaction between actin and myosin that appears as the sliding of the thick filaments and thin filaments past each other. As the thin filaments are drawn into the center of the A band, the length of sarcomere shortens (contraction).

The cytoplasm of muscle fiber is bounded by the plasma membrane (sarcolemma) that has the properties of excitable cells, and that fire action potentials. Action potentials that propagate along the sarcolemma are the physiological signals that initiate contractions. The transverse tubular system (T-tubule) is lined by a membrane that extends from the sarcolemma and carries the extracellular space deep into the muscle cell. Sarcoplasmic reticulum consists of the longitudinal reticulum at the center of the sarcomere and terminal cisternae, which abut the T-tubules. An action potential propagating along the sarcolemma depolarizes the T-tubular membrane containing the voltage sensitive L-type Ca^{2+} channel, Dihydropyridine receptor, which elicits the Ca^{2+} release from the SR through RyRs, which mediate interaction between actin and myosin, resulting in muscle contraction.

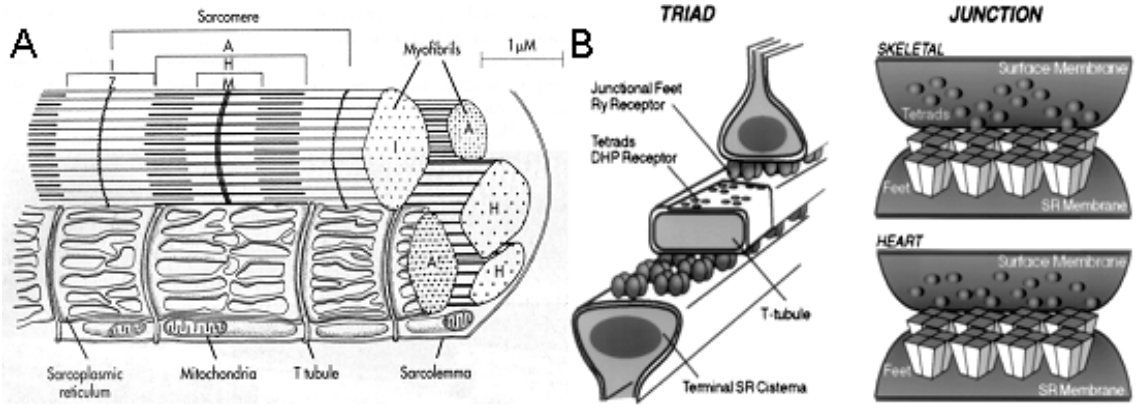

Figure 1. Ultrastructure of muscle fibers and Triad Junction.

A: Ultrastructure of muscle fibers. The dark band, A band, is a parallel array of thick filaments which are joined together at their centers by radially oriented M filaments. The thin filaments comprise the I band which are anchored to the Z band. H zone is the central part of the A band which is devoid of thin filaments. The basic repeating contraction unit, from Z band to Z band, is termed the sarcomere. The sarcoplasmic reticulum is a membrane network that surrounds the contractile proteins. B: Spatial line-up of Dihydropyridine receptors and RyRs between the T-tubule and terminal cisternae of SR. Dihydropyridine receptors in the skeletal muscle are shown to form tetrads corresponding to the RyR1 tetramer. However, Dihydropyridine receptors in cardiac muscle don't form the tetrads.

A: from Physiology (4th edition) p 272 by Berne, R.M. and Levy, M.N.

B from Flucher, BE, and Franzini-Armstrong, C. PNAS. 93(15): 8101-8106,1997.

1.1.2 Excitation-Contraction Coupling

Ryanodine receptors (RyRs) are Ca^{2+} release channels on the membrane of the sarcoplasmic reticulum (SR), a major Ca^{2+} storage compartment of striated muscles. Ryanodine receptors have considerable sequence and general structure similarities with inositol 1,4,5-triphophate receptors (IP_3Rs) that are another class of intracellular Ca^{2+} release channels formed in non-excitable cells [23-26, 37]. RyRs, however, have higher conductivity than IP_3Rs, a property required for fast release of large quantities of Ca^{2+} during excitation-contraction coupling. Rapid Ca^{2+} release from the SR via RyRs is the intermediate event between the excitation and the contraction of striated muscle, and Ca^{2+} binding to troponin-C, the regulatory protein, is the key step in regulating the actin-myosin interaction, the event of contraction [38].

The most important function of the RyR channel is probably its role in muscle excitation-contraction (E-C) coupling. In skeletal muscle, depolarization of the T-tubule membrane (i.e. excitation) induces conformational changes in DHPR that ultimately lead to the activation of the RyR channel on the SR membrane. In cardiac muscle, depolarization of the sarcolemmal membrane activates the DHPR to open, leading to Ca^{2+} entry through the DHPR, which activates the RyR channel. The activation of RyR channels leads to massive Ca^{2+} release from the SR, which in turn initiates contraction. This functional interaction between the DHPR and the RyR is commonly referred to as E-C coupling. When muscle contracts, myosin filaments slide between actin filaments by actin-myosin interaction. The globular heads of the myosin molecule bind to actin filaments and the ATPase catalytic site is localized at the globular end of the heavy chain of myosin. The actin-myosin interaction is regulated by the tropomyosin-troponin complex.

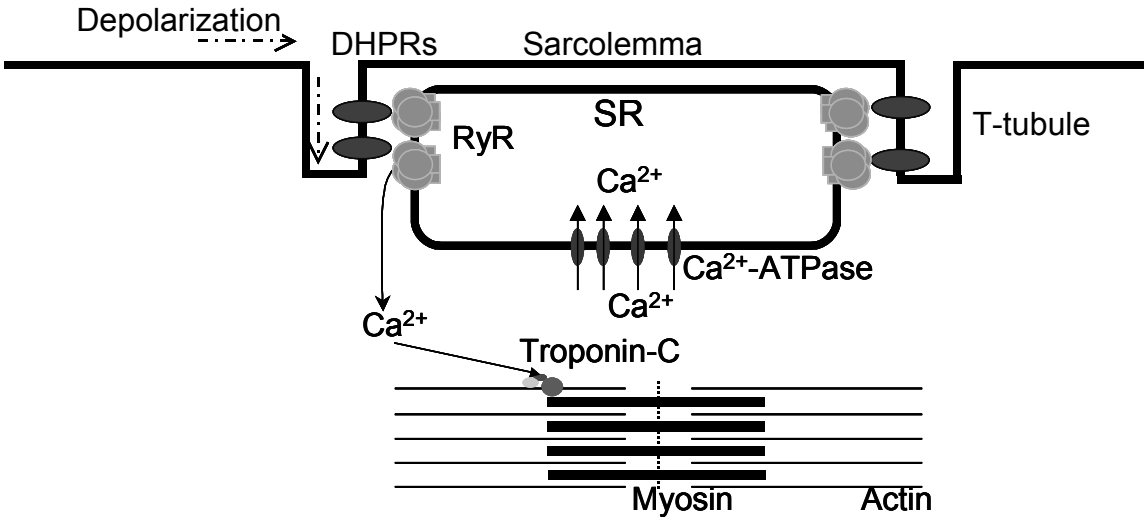

Figure 2. Excitation-contraction coupling event.

The propagation of action potential through the sarcolemma activates DHPRs, which in turn activates RyRs on the SR membrane. The activation of RyRs causes a massive Ca^{2+} release from the SR lumen to the cytosol of the muscle. Ca^{2+} binding to troponin-C initiates the sliding of myosin filaments and actin filaments, that is, the contraction of muscle. Ca^{2+}-ATPases on the SR membrane pump Ca^{2+} back into the SR lumen and the muscle goes back to a rest state.

Troponin is a complex of three subunits, troponin-C, I and T. Troponin C is the Ca^{2+} binding subunit with four Ca^{2+} binding sites. Troponin-I is the inhibitory subunit that is essential for the regulatory protein inhibition at low Ca^{2+} concentration. Troponin-T plays a role in binding the complex to tropomyosin. Changes in tropomyosin's position induced by Ca^{2+} binding to Troponin-C is the key step to initiate actin-myosin interaction. Activation of cross-bridge cycling only begins when the Ca^{2+} concentration rises high enough to effect lower affinity Ca^{2+} binding sites on troponin-C. The Ca^{2+} concentration in muscle cytoplasm at rest is less than 100 nM. Action potential propagates through the sarcolemma and activates DHPRs, which activates RyRs, resulting in very rapid Ca^{2+} release from the SR. Then, Ca^{2+} binding to troponin-C initiates the sliding of myosin and actin filaments, and the cycling of these cross-bridges shortens the sarcomere and generates force. Ca^{2+}-ATPases on the SR membrane pump Ca^{2+} back into the SR lumen and the muscle goes back to a state of relaxation.

1.1.3 Difference in E-C Coupling in Skeletal and Cardiac Muscle

The difference in excitation-contraction coupling in skeletal and cardiac muscles is illustrated in figure 3. In vertebrate skeletal muscle, Ca^{2+} current through DHPRs was not required to cause Ca^{2+} release from SR via RyR1 and the primary role of the DHPR acts as a voltage sensor that directly (perhaps physically) modulates the activation gate of the nearby RyR1 channel. [39] Electron microscopy studies show that the skeletal DHPRs in the t-tubules are arranged in clusters of four (tetrads) corresponding to the homotetramer of RyR, which indicates that there is a direct interaction between the skeletal RyRs and DHPRs [40, 41]. The membranes of the t-tubule and SR are juxtaposed and separated by a small ~10 nm gap [26].

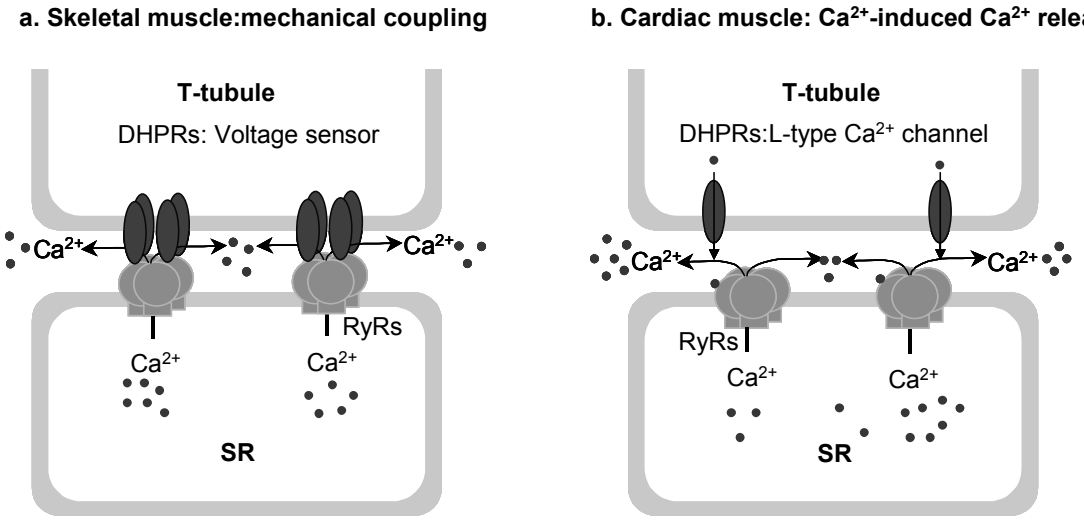

Figure 3. Difference in excitation-contraction coupling in skeletal and cardiac muscle.

In vertebrate skeletal muscle, DHPRs in the t-tubules are arranged in clusters of four (tetrads) corresponding to the homotetramer of RyR, which indicates that there is a direct interaction between the RyR1 and the DHPR. A lot of evidence supports that the DHPR and RyR1 communicate via physical protein-protein linkage and the activation of DHPR by membrane depolarization activates RyR1 to elicit the Ca^{2+} release from the SR. In cardiac muscle, Ca^{2+} release through RyR2 is elicited by the entry of Ca^{2+} through the L-type Ca^{2+} channel via a process called calcium-induced calcium release (CICR). Dihydropyridine receptors in cardiac muscle are located randomly relative to the RyR2 tetramer.

A lot of evidence supports that the DHPR and RyR1 communicate via physical protein-protein linkage, and the activation of the DHPR by membrane depolarization directly activates RyR1 to elicit the Ca^{2+} release from the SR. In cardiac muscle, Ca^{2+} release through RyR2 is elicited by the entry of Ca^{2+} through the L-type Ca^{2+} channel via a process called calcium-induced calcium release (CICR). Dihydropyridine receptors in cardiac muscle are located randomly relative to the RyR2 tetramer [42]. However, the exact coupling mechanism from the depolarization of the plasma membrane to the opening (activation) and closure (inactivation) of RyRs is not fully understood.

1.1.4 Ryanodine Receptors in Smooth Muscle

The contraction and relaxation of smooth muscle is regulated by a different mechanism from those in skeletal or cardiac muscles. A common feature is that high cytoplasmic Ca^{2+} level mediates contraction. However, the main source of Ca^{2+} to increase global cytoplasmic Ca^{2+} concentration in smooth muscle is Ca^{2+} entering through L-type Ca^{2+} channels on the sarcolemmal membrane, not Ca^{2+} released from internal stores (i.e. the SR network). Nelson et al. proposed that RyRs in smooth muscle SR, unlike their counterparts in cardiac and skeletal muscle, have a central role in relaxing muscle by activating large conductance K_{Ca} (BK_{Ca}) channels on the sarcolemmal membrane [43]. It was observed that the SR in smooth muscle is located right underneath the sarcolemmal membrane separated by a ~20 nm gap. They showed that outward current transients were observed with a time course similar to that of the Ca^{2+} sparks and were completely inhibited by the application of ryanodine and thapsigargin. Application of ryanodine and thapsigargin resulted in membrane depolarization and arterial constriction. The Ca^{2+} sparks caused from the opening of RyRs on the SR membrane in smooth muscle look quite the same as those in cardiac muscle in terms of duration and magnitude and

spatial extent. In cardiac muscle, the Ca^{2+} sparks are recruited throughout the cell to produce the global rise in cytosolic Ca^{2+} concentration that causes the synchronous activation of the contractile system and the consequent ejection of blood from the heart. However, the Ca^{2+} sparks in smooth muscle are generated in isolation principally near the cell surface, presumably reflecting the fact that SR enriched in RyR is near the cell surface in smooth muscle.

Nelson et al. proposed that local release of Ca^{2+} from the SR activates BK_{Ca} channels and the resulting K^+ efflux, observed in many smooth muscle cells periodically exhibiting spontaneous transient outward currents (STOC), causes membrane hyperpolarization. This decrease in membrane potential causes the voltage-sensitive Ca^{2+} channel on surface membrane to close, thereby causing a drop in cytoplasmic Ca^{2+} and diminished smooth muscle contraction [43].

1.2 STRUCTURE AND TOPOLOGY OF RYRS

1.2.1 Structure of RyRs

Studies on the identification, cloning, and molecular characterization of RyR isoforms have provided new details of the structure-function relationship of this large protein [44-47]. The RyR is a homotetramer of approximately 565 kDa subunits containing over 5000 amino acids consisting of a large cytoplasmic domain (the foot region) and a relatively small transmembrane domain that forms a Ca^{2+} pore. There are three RyR isoforms named according to where they were first isolated. RyR1, also called the skeletal type, is the isoform first purified, cloned and fully sequenced from first skeletal muscle; RyR2 is the dominant form in cardiac muscle; RyR3 is first purified in the brain. Sequence comparison of the three isoforms reveals a very high homology, over 67% among them [24, 26].

Hydrophobicity studies indicate a large hydrophilic NH_2-terminal region protruding into the cytoplasm, called a 'foot structure', and small, mostly hydrophobic, COOH-terminal region, predicted to form the intramembrane channel. The cytoplasmic domains of the RyR, make up the 'foot structure,' located at the junctional SR that form junctions with the surface and SR membranes to allow a direct connection between the RyR and exterior membranes. The COOH-terminal region, including a transmembrane region and COOH-terminal tail, is the most highly conserved domain of the molecule and has a strong similarity with the same region of the IP_3Rs. It has been reported that COOH-terminal amino acids are important for normal function of RyR channels [48]. Deletion of 3 amino acids from the COOH-terminus resulted in decreased activities, and the deletion of 15 amino acids yielded an inactive RyR [49].

A truncated version of the skeletal RyR (RyR1), which is translated using an alternate start site within the RyR1 mRNA, has been identified in the brain [45]. This shortened version of an RyR1 molecule, comprised of approximately ~700 C-terminal amino acids (~75 kDa), lacks the foot structure, but contains the transmembrane region required to form the Ca^{2+} channel pore. Consequently, this protein also may be a Ca^{2+} channel. But the role of this channel in brain tissue remains unknown.

Some details of the three-dimensional (3-D) general shape of the RyR have been predicted using cryo-electron microscopy and 3-D reconstruction techniques as shown in figure 4 [50-53]. The homotetramer of a functional channel was shown to have a quarterfoil shape (figure 4A). It showed that the RyR has two distinct domains (figure 4B). One is a large cytoplasmic assembly (~29 × 29 × 12 nm), consisting of loosely packed protein densities, and the other is a smaller transmembrane assembly that protrudes 7 nm from the center of the cytoplasmic assembly. This transmembrane assembly appears to have a central hole that can be occluded by a

pluglike mass. This hole and plug may correspond to the transmembrane Ca^{2+}-conducting pathway.

Transmembrane Domain of RyRs The detailed membrane topology of the transmembrane domain is unclear. Experimental evidence supports the cytoplasmic location of the NH_2- and COOH-terminus. Thus, the molecule requires an even number of membrane crossings. The number of transmembrane domains has been controversial, ranging from 4 to 12 [44, 46, 54]. All models to predict the number of transmembrane domains generally agree on the position of the most hydrophobic domains closest to the COOH-terminus. Takeshima et al. [45] suggested a 4 transmembrane domain model with 2 luminal regions, one between transmembrane domain 1 and transmembrane domain 2 (amino acid 4580-4640), the other between transmembrane domain 3 and transmembrane domain 4 (amino acid 4859-4917), a hypothesis supported by others [26, 37]. Antibodies (Abs) raised against amino acids 4581-4640 and 4860-4886 (luminal domains in Dr. Takeshima's model) could not reach their epitopes in isolated SR vesicles unless the vesicles were solubilized with detergent to allow access to the lumen of the SR, which supports that they are facing the luminal side of the channel [55].

Recently, Du et al. tried to define the topology of skeletal RyR. [56] They expressed RyR1 proteins containing N-terminal sequences of RyR1, but C-terminal sequences were deleted incrementally and tagged with enhanced green fluorescent protein (EGFP). The C-terminus ofRyR1 proteins were truncated at the end of each putative transmembrane domain in the 10 transmembrane model proposed by Zorzato et al. [44] and tagged with EGFP at the end of C-terminus of each protein. Confocal microscopy of intact and saponin-permeabilized cells was used to determine the subcellular location of truncated fusion proteins. Mapping by trypsin

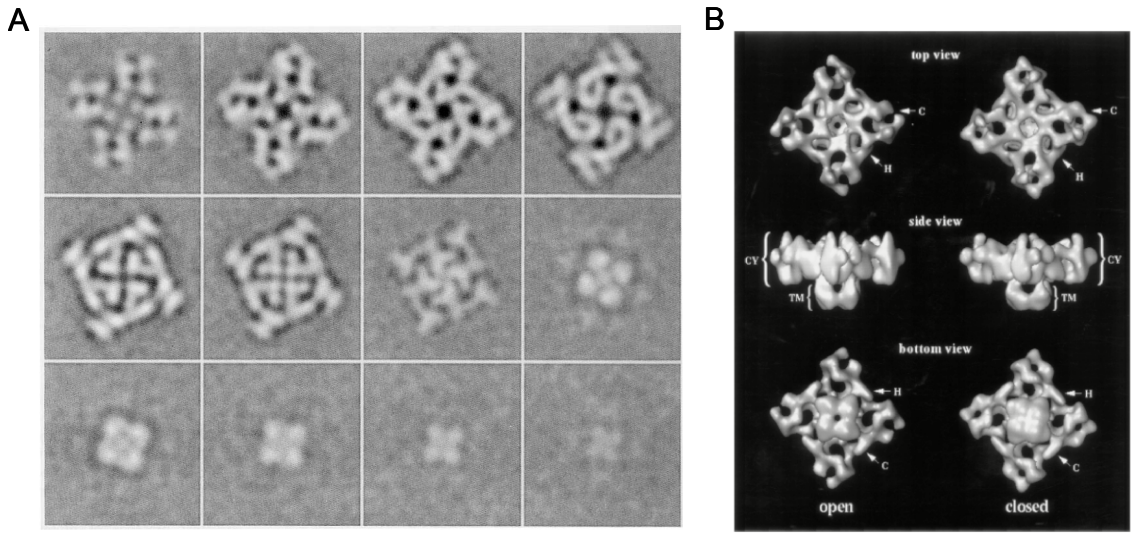

Figure 4. Cryo-electron Microscopy and three-dimensional reconstruction of skeletal RyR.

A.This is the selected z-slices spaced at 1.58-nm intervals (normal to fourfold symmetry axis, defined as the z-axis of the reconstruction) of the three-dimensional reconstruction of RyR1.
The first seven sections are from the cytoplasmic assembly, and the final five are from the transmembrane assembly.
B.3D reconstruction obtained for RyR in an open and closed state obtained with the angular reconstitution algorithm. T-tubule view (top), side view after tilting the structure around a diagonal of the cytoplasmic assembly (middle) and SR lumen view (bottom). The left column corresponds to the channel prepared in an open configuration, the right column to the channel in the closed configuration.
from Samsó, M. et al, *J. struct. Biol.* 121, 172-180 (1998).

digestion and extraction of isolated microsome revealed that EGFP positioned after M5, the N-terminal half of M7 or M8, was located in the lumen. Their results suggested that the M1- M2 (numbered from 1 to 10 according to Zorzato model) sequence is not membrane-associated and there are 8 transmembrane domains, although it is a little bit ambiguous if the M3/M4 domain (between amino acid 4277-4363) is membrane associated. It was shown that M5-M10 are membrane associated. It is important to notice that the transmembrane domain and the luminal loop confirmed in this study were similar to those in Takeshima's 4 transmembrane model, although they proposed an additional transmembrane domains.

Pore Forming Region of RyRs The pore-forming components of the RyR molecule are located in the carboxyl-terminal region of the molecule. Expression of a plasmid encoding the first 182 amino-terminal and the 1030 carboxyl-terminal amino acids of RyR1 yields a protein with a molecular weight of approximately 130 kDa, which, when incorporated into a planar phospholipids bilayer, functions as an ion channel displaying a number of properties characteristic of the RyR [57]. These authors reported that similar results were obtained following expression of a plasmid encoding the carboxyl-terminal 1377 amino acids of RyR1.

The luminal loop between transmembrane domain 3 and transmembrane domain 4 (amino acid 4859-4917) is believed to form the pore of the RyR1 channel. It has been noted that there is a striking similarity in the amino acid composition of the region in which this residue is located in RyRs and the equivalent region in IP_3Rs. It has been proposed that this luminal loop might fold back into the membrane to form the selectivity filter of RyR/IP_3R, or at least part of the conduction pathway of the channel [33].

The mutations in the pore forming region of RyRs found in humans were found to be linked to serious diseases. Lynch et al. reported a new mutation, I4898T, from a large Mexican

pedigree that is associated with central core disease (CCD) [58]. Balshaw et al. showed that a site directed mutation, I4898T, yielded greatly reduced [^{3}H]ryanodine binding levels, and responses to two RyR1 channel agonists, halothane and caffeine, was completely abolished [33]. Production of RyR channels with point mutations in this putative pore loop showed the serious alteration in the channel function. Gao et al. reported that the single substitution of a highly conserved amino acid motif significantly changed channel properties such as channel conduction and gating properties, and sometimes they were not successful in obtaining a functional channel [59].

Cytoplasmic Region of RyRs The rest of the RyR protein consists of hydrophilic domains corresponding to the large cytoplasmic region or "foot" structure that protrudes from the SR membrane into the cytosol and spans the gap between the T-tubules and the terminal cisternae. Why the cytoplasmic domain is so massive and complex is not clear. The cytoplasmic domain is known to contain regulatory sites that bind endogenous modulators and pharmacological agents to modulate the channel activity. The foot structure may be crucial to maintain compiling or communication between the RyRs and the DHPR via a direct physical interaction [26, 39-42]. It may also play a role in holding the architecture of the triad junction and/or facilitating Ca^{2+} diffusion from the SR [60].

1.2.2 Conductance Properties of RyRs

The ability of the RyR channel to mobilize intracellular Ca^{2+} depends on both its permeation and gating properties. Its permeation properties include its unitary conductance and ion selectivity. Its gating properties include its open probability (P_o) and the duration of individual open/closed events. It is generally assumed that the movement of the gate does not alter the nature of the pore, such as its diameter, length, charge and etc. It is in the pore where channel discrimination

between different ions occurs. The pore also contains determinants that define how quickly particular ions will pass.

The RyR channels are permeable to many different divalent and monovalent cations. In symmetrical solutions containing a monovalent cation (K^+, Na^+ or Cs^+ in a concentration of ~200 mM) as the main permeant species, the unitary RyR channel current-voltage relationship is linear with a slope conductance of ~500 pS. In asymmetric solutions containing a divalent cation (Ca^{2+}, Ba^{2+} or Sr^{2+} in ~50 mM) as the main permeant species, unitary RyR channel current-voltage relationships have a slope conductance of ~100 pS. These are very large conductance values [24, 26, 37].

The RyR channel is not a highly selective Ca^{2+} channel. RyR channels show very little selectivity between different monovalent cations, and they also show very little selectivity between different divalent cations. Intuitively, the apparent deficiency in Ca^{2+} selectivity may be related to its high conductance. A high conductance channel (i.e. ions passing rapidly) would have little time per ion to perform the steps needed to discriminate between ions.

1.3 OVERVIEW OF RYRS' REGULATION

1.3.1 RyR Modulators

A number of physiological signaling processes and pharmacological agents have been identified as activators and/or inhibitors of SR Ca^{2+} release channels. Many endogenous and exogenous effectors contribute to the regulation of RyRs [27, 61].

Calcium The action of Ca^{2+} on the RyR channel is complex. RyR1 is activated by Ca^{2+} binding to high affinity Ca^{2+}-selective sites in cytoplasmic domain and inactivated by Ca^{2+} and Mg^{2+} binding to low affinity, less selective sites, giving rise to the characteristic biphasic Ca^{2+}

dependence of channel activity [26]. An important functional difference between RyR1 and RyR2 is that both are activated by low (1-10 μM) Ca^{2+} and RyR1 is inactivated by high (1-10 mM) Ca^{2+}, but RyR2 shows little inactivation (> 100 mM Ca^{2+}). Ca^{2+} binding sites are also thought to be present within the regions of the channel exposed to the solution at the luminal side of the channel [62, 63], although the actions of luminal Ca^{2+} may occur as the consequence of the binding of Ca^{2+} to accessory luminal proteins like calsequestrin or junction.

Many attempts have been made to identify Ca^{2+} binding sites in the primary RyR sequence. Putative Ca^{2+} binding sites have been identified throughout the length of the RyR sequence from the use of site-directed antibodies, Ca^{2+} overlays [64], site-directed mutagenesis [58, 59, 65] and the construction of chimeras [66, 67].

Ryanodine Ryanodine is a plant alkaloid that gives the name 'ryanodine receptor' to this protein and is used to identify RyRs. Ryanodine binds to RyRs with high affinity (Kd ~2-5 nM), which results in an activation of channel activity locked up at the subconductance level when a lower concentration is added (up to ~ 10 μM), and inhibition of channel activity when a higher concentration is added (> 50 μM). The high-affinity binding site for ryanodine is only accessible when the channel is in an open conformation, and this observation has led to the suggestion that this binding site is located in the region of the pore of the channel. Recent investigations have demonstrated that mutations of residues located in the transmembrane domain of the RyR modify the ability of the RyR to bind ryanodine [48].

ATP and Mg^{2+} Cytosolic ATP is an effective RyR channel activator. Cytosolic Mg^{2+} is a potent RyR channel inhibitor. The cytosol of most cells contains ~5 mM total ATP and ~1 mM free Mg^{2+}. This means that most ATP is in its Mg^{2+}-bound form. Free ATP (~300 μM in the cytosol) is the species that binds to and activates the RyR channel. The action of ATP and Mg^{2+}

on single RyR channel function is isoform specific. Free ATP is a much more effective activator of the RyR1 channel than the RyR2 channel. The RyR3 channel is also less ATP sensitive than the RyR1 channel. In the presence of physiological levels of Mg^{2+} and ATP, the RyR1 channel requires less Ca^{2+} to activate than the RyR2 or RyR3 channels.

Caffeine Caffeine at the concentrations in the millimolar range induces muscle contracture and reduces the Ca^{2+} accumulation ability of SR. By acting directly on the RyR, it allows calcium-induced calcium release (CICR) to occur in skinned skeletal fiber even at Mg^{2+} concentrations that would normally inhibit this phenomenon and has become one of the exogenous agents used to locate the presence of RyRs in cells.

Ruthenium Red Ruthenium red is an agent that completely blocks CICR and is often used as a tool to check for RyR-dependent Ca^{2+} leaks from the SR.

Doxorubicin Doxorubicin is a widely used antineoplastic agent that causes a cardiomyopathy, possibly due to the sensitization of RyRs to activation by two physiological agents, Ca^{2+} and ATP.

Redox Mediated Regulation In addition to the modulators of RyR activity and SR Ca^{2+} release shown above, a number of sulfhydryl oxidizing and reducing agents have been shown to respectively activate or inactivate RyRs [19, 68-73]. Each monomer of an RyR contains about 100 cysteine residues and almost half of them are known to exist as free thiols, which are vulnerable for modification by sulfhydryl oxidants. The regulation of RyRs mediated via the modulation of the redox state of free thiols on it will be discussed in a detailed way in the later part of the chapter.

1.3.2 Proteins Associated with RyRs in the SR

Dihydropyridine Receptor RyR1 interacts with voltage-gated L-type Ca^{2+} channels called Dihydropyridine receptors on the T-tubule membrane. Depolarization of the surface membrane produces a conformational change in the α_1 subunit of the DHPR that is translated into a conformational change in RyR1 and results in the opening of the RyR1 channel. The use of dysgenic mice (lacking DHPRs) allowed investigations of the regions in the DHPR that interact with RyR1 by expression of chimeras of the skeletal and cardiac isoforms of the α_1 subunit of the DHPR [39, 74-76].

Use of dyspedic mice (lacking RyRs) has revealed a retrograde signal from RyR1 to the DHPR [40]. DHPRs in dyspedic mice can undergo voltage-driven conformational changes producing charge movement, but the L-type Ca^{2+} current is less than that seen in normal cells. Expression of RyR1 in these dyspedic cells restores both skeletal-type excitation-contraction coupling and Ca^{2+} current, while expression of RyR2 restores neither of these phenomena.

FK506-Binding Proteins FK506-binding proteins are known to stabilize the functional state of the RyR homotetramer and facilitate coordinated gating of RyRs [26, 37]. In the absence of FK506- binding protein in the single channel activity study, the channels show an increased open probability and extended opening events at subconductance levels, ¼, ½ and ¾ of the full open conductance level. More recently, it has been suggested that FKBP may synchronize the single channel function of neighboring RyRs. It is not yet understood how the same protein (FKBP) could both stabilize RyR monomer interactions within the RyR channel complex and synchronize the activity of neighboring RyR channel complexes.

Attempts have also been made to localize the binding sites for the FK506-binding proteins, FKBP12 (for RyR1, RyR3) and FKBP12.6 (for RyR2). Binding studies and cryo

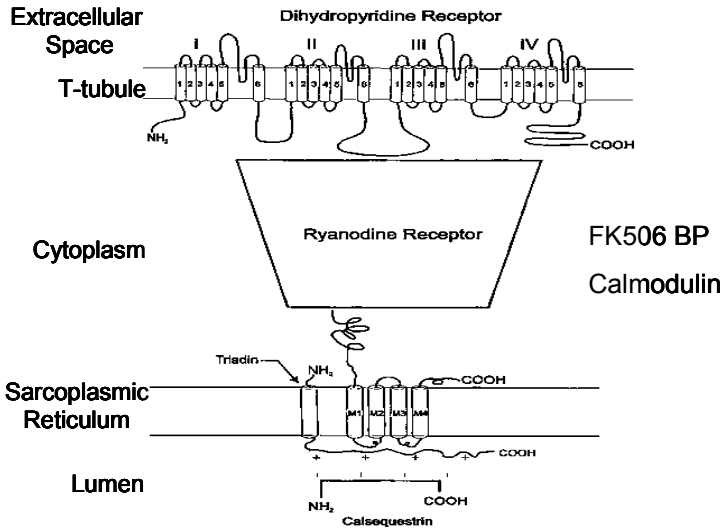

Figure 5.Proteins interacting with RyRs.
Franzini-Armstrong et al., Physiol. Rev.,vol 77, p713, 1997.

electron microscopy have revealed that each RyR monomer possesses a single FKBP binding site [24, 26, 53]. Recently, the FKBP12.6 binding site of RyR2 was identified as an isoleucine-proline sequence, homologous to the proposed motif for FKBP12 binding site of RyR1 [77].

Calmodulin Calmodulin (CaM) was the first peptide found to interact with single RyR channels in the lipid bilayer [78]. Calmodulin can either activate (at low Ca^{2+} concentrations) or inhibit (at high Ca^{2+} concentrations) the RyR1 and RyR3 channels. For the RyR2 channel, only inhibitory effects of CaM have been reported [79, 80]. It was reported that oxidation modifies RyR1 channel behavior and yet it does not seem to alter RyR interaction with CaM [81, 82]. There have been some reports that calmodulin is required for the modulation of RyR activity by nitric oxide [83-86], but other reports showed that RyRs were activated by nitric oxide donors without calmodulin [15, 87, 88]. The role of CaM in the modulation of the RyR2 channel during E-C coupling remains controversial.

Luminal Proteins Calsequestrin is the main Ca^{2+} binding protein in the lumen of the SR. Calsequestrin has a large number of acidic amino acids that permit it to coordinately bind 40-50 Ca^{2+} per molecule. It has been suggested that Ca^{2+}- and pH-dependent conformational changes in calsequestrin may modulate RyR channel activity [62]. It has been suggested that calsequestrin action on the RyR channel may require the presence of triadin, providing an anchoring point for calsequestrin and possibly a functional connection between calsequestrin and RyR. But, there is disagreement concerning the nature of the calsequestrin-RyR interaction.

1.3.3 Redox-medicated Regulation of RyRs

Studies on modulation of RyR channel activity by sulfhydryl oxidation-reduction started from the toxicological viewpoint. Initial studies demonstrated that heavy metals [68, 69, 71-73, 89] and cysteine in the presence of catalytic concentrations of copper oxidize free thiol irreversibly and thereby activate ryanodine receptors in SR vesicles [71]. In skeletal and cardiac SR vesicles and in skinned psoas fibers, reactive disulfides caused a prompt release of Ca^{2+} via activation of RyRs that was fully reversed by sulfhydryl reducing agents, without affecting Ca^{2+}, Mg^{2+}-ATPases pumps [70, 71, 90-92]. Reactive disulfide compounds are absolutely selective to the oxidation of low pK_a thiols to form mixed disulfides, and they oxidized only 2-4% of the available thiols on RyR1, a reaction sufficient to fully activate RyRs [91]. These observations indicated that RyRs contain ‘hyperreactive’ or ‘critical’ thiols that could be selectively oxidized and reduced to reversibly open and close the channel [68, 91, 93, 94].

The hypothesis that redox modification of critical or hyperreactive thiols on RyRs is an important mechanism involved in the regulation of this intracellular Ca^{2+} release channel has become increasingly persuasive. Although the oxidation and reduction states of RyRs were found to modulate channel activity, these findings were first considered to be of pathological

interest but of little or no physiological significance with respect to normal muscle function because the sulfhydryl oxidants that activate RyRs were not physiological [95]. However, it was subsequently reported that nitric oxide ($NO^{\bullet}$) and S-nitrosothiols oxidize critical thiols in both skeletal and cardiac isoforms of RyR, resulting in channel activation, and the subsequent addition of a sulfhydryl reducing agent resulted in channel closure [15]. This was reproduced by other studies [13, 83-86, 88]. Since the nitrosylation of free thiol groups on RyRs by nitric oxide modulates the RyR channel activity reversibly, it has received attention from a physiological viewpoint and it's been suggested that sulfhydryl oxidation is a key step in channel activation. A series of studies have shown that the mammalian RyR isoforms and inositol(1,4,5)triphosphate receptors (IP_3Rs) are modulated by sulfhydryl oxidation-reduction [3], which suggests that redox-mediated regulation is a common mechanism to control the cellular Ca^{2+} homeostasis in all kinds of cells. Thus, redox regulation of Ca^{2+} channels controlling intracellular Ca^{2+} concentration may be fundamental for our understanding of Ca^{2+} homeostasis.

Recently, it was proposed that RyR1s are modulated by the transmembrane redox gradient of the molecule controlled by the ratio of reduced to oxidized glutathione (GSH/GSSG ratio), which is critical to control channel activity [6, 96, 97]. In line with such a mechanism was the identification of a glutathione transporter that co-localized with RyR1 on the SR membrane and may maintain a lower ratio of GSH/GSSG in the lumen than the cytosol to produce a redox potential gradient. The redox-state in the lumen of the SR appears to be at a redox potential of –180 mV under normal cellular conditions, which may be critical to normal channel responses to physiological modulators because the effects of cytosolic free Ca^{2+} and other modulators of RyR1 was found to depend on the redox state of RyR1 channel. Channel activity of P_o increases when the cytosolic redox potential increases from –210 to –180 mV, and P_o decreases when the

cytosolic redox potential decreases (-180 to –210 mV) while the luminal redox potential is fixed at –180 mV. These observations emphasized the importance of the redox regulation of RyRs and its critical role to understand its regulation on the response of RyRs to all the known modulators of the channel.

1.4 NITRIC OXIDE MEDIATED REGULATION OF RYRS

1.4.1 Nitric Oxide

Nitric oxide was first identified as the endothelial derived relaxing factor (EDRF) based on the observation that acetylcholine caused a relaxation of blood vessels with intact endothelium inside the vessel and a contraction of blood vessels with endothelium removed [9]. Later it was reported that the EDRF is identical to nitric oxide [8]. Nitroglycerin and related compounds that had been used as vasodilating agents even before nitric oxide effect was known were discovered to release nitric oxide and relax the muscle fiber via cGMP elevation [5]. Nitric oxide ($NO^{\bullet}$) originates from the guanidino group of L-arginine factors in biological systems and is synthesized by one of three nitric oxide synthases (NOS) via the conversion of L-arginine and oxygen to $NO^{\bullet}$ and L-citruline as a by-product [8, 98, 99]. But the intermediate steps between $NO^{\bullet}$ and its multifaceted biological activity remain a matter of debate.

The term of NO is used in a generic sense. Nitric oxide has unique chemical features. It is a paramagnetic molecule containing an odd number of electrons and can exist in different charge states ($NO^{\bullet}$, NO^{+}, NO^{-}). In oxygenated aqueous milieu, $NO^{\bullet}$ is very short lived as it reacts with O_2 to form a nitrosyldioxyl radical ($ONOO^{\bullet}$) that rapidly interacts with $NO^{\bullet}$ to form N_2O_4, NO_2, N_2O_3 and HNO_2 [19]. $NO^{\bullet}$ is readily inactivated by heme iron, nonheme iron, superoxide anion, oxygen and other interactions [19, 100, 101]. $NO^{\bullet}$ is degraded rapidly by oxyhemoglobin,

resulting in the formation of methemoglobin and HNO_3. Low molecular weight thiol molecules rapidly react with $NO^{\bullet}$ to form low molecular weight S-nitrosothiols. Molecules most closely identified with NO-related activity include authentic $NO^{\bullet}$ itself, S-nitrosothiols, metal-NO complexes that can release nitrosonium (^{+}NO), nitroxyl anions (HNO), and higher oxides of nitrogen (NO_X) including peroxynitrite [19-21].

1.4.2 NO Synthases

NO is synthesized by the enzyme NO synthase (NOS). There are three isoforms that are named either by the cell or tissue in which NOS was originally found or the historical order in which they were purified and cloned: Neuronal NOS (nNOS or NOS I), inducible NOS (iNOS or NOS II) and endothelial NOS (eNOS or NOS III). The expression and localization of NOS isoforms are dependent on age and developmental stage, innervation and activity, history of exposure to cytokines and growth factors, and muscle fiber type and species. The activity of nNOS, which is constitutively expressed, is regulated by fluctuations in the concentration of cytoplasmic Ca^{2+} that acts in concert with calmodulin. The activity of iNOS is independent of elevated Ca^{2+}. eNOS is a constitutive, Ca^{2+}/calmodulin-dependent enzyme. The NOS isoform that is most abundantly expressed in skeletal muscle is nNOS [4]. nNOS mRNA levels and enzyme activity were reported to be higher in human skeletal muscle than in human brain [4, 102].

Use of NOS Knockout Mice As it was known that nNOS, eNOS and iNOS have specific tissue localization, it was suspected that the specific action of nitric oxide might depend on its enzymatic sources. But, conventional pharmacological antagonists couldn't distinguish these enzymes or provide models of chronic nitric oxide depletion in whole animals. Therefore, the generation of NOS knockout mice ($nNOS^{-/-}$, $eNOS^{-/-}$, and $iNOS^{-/-}$) provided an elegant method to distinguish the roles of nitric oxide from each enzyme. Studies on these animal models also

revealed the consequences of a life-long deficiency of these enzymes and the compensatory pathways [103]. NO donors have been known to cause relaxation of vascular smooth muscle and vasodilation. Studies with knockout animals have established the role of both nNOS and eNOS in vasodilation. The main NOS isoform in the endothelium is eNOS. $eNOS^{-/-}$ mice have hypertension [104]. In contrast, mice with transgenic overexpression of eNOS are hypotensive [103].

1.4.3 Function of NO in Various Muscles

A number of functions have been attributed to NO in a variety of biological processes. Actions of nitric oxide in various muscles are found to be multifaceted.

NO in Smooth Muscle NO was first known as an endothelial-derived relaxing factor in blood vessels [9]. $NO^{\bullet}$ interacts with the heme moiety of guanylyl cyclase and activates the guanylyl cyclase, which converts GTP to cGMP. cGMP is degraded by the action of one of several phosphodiesterases (PDE). It is generally accepted that cGMP triggers relaxation of smooth muscle by activating an intracellular molecular cascade, which revolves around the activity of cGMP-dependent protein kinase (PKG). This cascade results in a reduction of cytosolic Ca^{2+} through a series of complex but poorly understood mechanisms [105]. It was suggested that cGMP exerts its effect by modifying the activity of three types of intracellular receptor proteins: several ion channels nitrosylated by NO, PKG and several phosphodiesterases [106]. cGMP-dependent protein kinase (PKG) is considered the principal mediator of cGMP-induced smooth muscle relaxation by phosphorylating a number of target proteins. It was proposed that phospholamban, when phosphorylated by PKG or PKA, dissociates from SR Ca^{2+}-ATPase, which leads to increased Ca^{2+} pumping and an elevated SR Ca^{2+} load, which increases Ca^{2+} spark frequency. The Ca^{2+} spark activates large conductance of the K_{Ca} (BK_{Ca}) channel,

causing potential hyperpolarization of the membrane, which closes L-type Ca^{2+} channels, which reduces Ca^{2+} influx, lowering the cytoplasmic Ca^{2+} concentration, and leads to vasodilation [107]. It was also suggested that PKG activates the BK_{Ca} channel, resulting in spontaneous transient outward currents [108]. Activation of RyRs directly by nitric oxide was not considered in this study, although it would a probable mechanism to cause the increase of Ca^{2+} sparks.

It was initially thought that the relaxation stimulated by NO was mediated only by the cGMP-dependent pathway. This led to the assumption that NO and cGMP actions were synonymous in smooth muscle. However, it is now known from work with several models that at least part of NO-induced smooth muscle relaxation is cGMP independent because the inhibition of guanylate cyclase did not abolish NO-induced smooth muscle relaxation completely [12, 109, 110].

NO in Cardiac Muscle Although different isoforms of nitric oxide synthase (NOS) were found within the defined spaces in the heart a decade ago, and NO production in the beating heart [111] or in isolated cardiac myocytes [99] besides the endothelium of the heart was directly measured, the role that nitric oxide (NO) plays in cardiac regulation remains highly controversial. There is a growing consensus, however, that NO modulates the activity of several ion channels involved in Ca^{2+} cycling in excitation-contraction coupling as well as mitochondrial respiratory complexes. It was reported that NO showed contradictory effects on myocardial contractility [112, 113], and it is suggested that NO produced from endothelium relaxes cardiac muscle and NO produced in myocytes exerts a different function on myocardial contractility. In the cardiovascular system, eNOS (endothelia isoform of NOS) is found to be localized at caveolae and nNOS (neuronal isoform of NOS) is localized at the sarcoplasmic reticulum where the RyR and perhaps SR Ca^{2+}- ATPase are [7, 17, 114]. RyR2 is found to be activated by nitric oxide,

which would tune the SR Ca^{2+} cycling and eventually tune the myocardial contractility [14, 15]. The contradictory effects of NO on myocardial contractility shown in several experiments can be explained by how NO was delivered. Continuous addition of NO at low concentrations will cause Ca^{2+} to leak from the SR through RyRs, resulting in decreased SR Ca^{2+} load, which would cause a negative inotropic effect when action potential elicits muscle contraction. On the other hand, addition of NO at high concentrations at the same time with action potential will have a positive inotropic effect by increasing Ca^{2+} release from the SR.

It has been observed that cardiac muscle contracts more forcefully after it has been stretched, which is called the Frank-Starling law. But there was no rational mechanism to explain how the stretch increases myocardial contractility. Recently, Petroff et al. reported that NO mediates the Frank-Starling effect of cardiomyocytes [17]. They suggested that nitric oxide generated from eNOS in caveolae increased Ca^{2+} release from the SR in cardiomyocytes in a stretch-dependent manner [17]. They showed that the stretching of myocytes modulated the elementary Ca^{2+} release process from the ryanodine receptor, Ca^{2+} sparks and the electrically stimulated Ca^{2+} transient. Stretching induced Ptdlns-3-OH kinase (PI(3)K)-dependent phosphorylation of both Akt and the eNOS, resulting in nitric oxide production and a proportionate increase in Ca^{2+}-spark frequency that was abolished by inhibiting NOS or adding the sulfhydryl reducing agent dithiothreitol, which is consistent with the underlying mechanism being the S-nitrosylation of regulatory thiols on RyRs. It was proposed that this cardiac PI(1)3K-Akt-eNOS axis serves as a physiological sensor of cardiac stretch, a role served by the localization of eNOS in plasmalemmal caveolae close to the SR-T-tubule junction.

NO in Skeletal Muscle It has been known that cGMP effects are generally modest in skeletal muscle, and guanylate cyclase activity is relatively low compared with other muscles [4].

Actively contracting muscles generated increased levels of NO and reactive oxygen species that increased force markedly [115]. There have been different observations on the nitric oxide-derived modulation of RyRs. It was observed that nitric oxide inactivates skeletal RyR [116], but others observed that nitric oxide activates skeletal RyR [15, 83, 86, 88]. Generally it is agreed that nitric oxide activates skeletal RyR.

NO in Pathological Conditions It has been known that NO regulates many aspects of myocardial function, not only in the normal heart but also in ischemic and nonischemic failing heart. Most physiological NO actions on the normal heart are attributed to the NO generated by the constitutive NOS (eNOS and nNOS), which are Ca^{2+}/Calmodulin dependent. In contrast, iNOS is not regulated by Ca^{2+}/calmodulin and, once induced, generates NO continuously over longer periods of time leading to most of its detrimental effect [117]. iNOS has been reported absent in the normal human heart. However, during the acute ischemia and initial stages of heart failure, NO production generally increases by the induction of both eNOS and iNOS. During chronic diseases, such as end-stage failing ischemic or dilated cardiomyopathies, iNOS may remain overexpressed, whereas eNOS is progressively downregulated [118]. NO also contributes to late ischemic preconditioning. The late phase of ischemic preconditioning, lasting 3 to 4 days and protecting against both infarction and stunning, enhances the recovery of left ventricular function and includes activation of iNOS [119].

1.4.4 Activation of RyRs by Various Nitric Oxide Donors

Authentic nitric oxide ($NO^{\bullet}$) and various NO-donors were found to nitrosylate free thiols on RyRs to promote the opening of the RyR channel and Ca^{2+} release from skeletal and cardiac SR vesicles [13-15, 83-86]. NO-induced activation of RyRs was reversed by sulfhydryl reducing agents (e.g. the reduced form of glutathione (GSH), dithiothreitol (DTT)) [15, 88]. Conflicting

studies reported that NO inhibited, rather than activated, SR Ca^{2+} release (i.e. inhibiting Ca^{2+} release by caffeine or N-methyl maleimide) and reduced the open probability of RyRs reconstituted in planar bilayers [116, 120]. However, the consensus is now that low molecular weight S-nitrosothiols and NO-donors increase the open probability (P_o) of skeletal and cardiac RyRs in single channel recordings and that only activation was observed at low NO concentrations, whereas higher concentrations of cys-SNO were required to decrease open probability (P_o) [14, 15, 83-86].

Mechanistically, the activation of RyRs induced by $NO^{\bullet}$ and S-nitrosothiols reflects the occurrence of nitrosation of critical thiols on RyRs and suggests that $NO^{\bullet}$ may play a physiological role in the regulation of muscle force [13, 15]. The rate of RyR activation via S-nitrosation, however, strongly depended on the structure of the nitrosating agents [16]. The latter suggests that under physiological conditions, different forms of NO, including $NO^{\bullet}$ itself, S-nitrosothiols, metal-NO complexes that can release nitrosonium (^{+}NO), nitroxyl anions (HNO) and higher oxides of nitrogen (NO_X) including peroxynitrite, may exert, both kinetically and mechanistically, distinct effects on RyRs [19].

Recently, Thomas et al. reported that $NO^{\bullet}$ and O_2 can preferentially partition hydrophobic cellular compartments, suggesting that the concentration and subsequent oxidation of nitric oxide in phospholipid membranes could trigger a site-specific nitrosation of trans-membrane proteins [121]. This observation was extended to the nitrosation of the skeletal RyR by Eu et al., who proposed that $NO^{\bullet}$ can activate RyRs only at low pO_2 [83], and Sun et al., who proposed that $NO^{\bullet}$ nitrosylates C3635 residing within a calmodulin-binding domain [84]. A mechanistic interpretation of this phenomenon, however, has not yet been proposed.

Nonetheless, low molecular weight S-nitrosothiols can activate skeletal and cardiac RyRs, which suggests that S-nitrosothiols formed during the oxidation of $NO^{\bullet}$ in the presence of GSH and/or cysteine could substantially stabilize $NO^{\bullet}$ and mediate its physiological activity [8, 18]. It has been found that S-nitrosoglutathione (GSNO) is present in rat cerebellum and human plasma, airways and white blood cells at relatively high concentrations [10, 122]. Therefore, it would be fundamental to study the mechanism of low molecular weight S-nitrosothiols on RyR activation to understand the NO-induced RyR activation. Currently, however, the activation of RyRs via trans-S-nitrosation by low molecular thiols is not well studied. Hence, the current project has carried out experiments for assessing the ability of S-nitrosocysteine (cys-SNO) and S-nitrosoglutathione (GSNO) to reversibly activate RyRs. The discrimination between $NO^{\bullet}$- and *trans*-S-nitrosation-dependent activation of RyRs was one of major focuses of this study and the effect of the O_2 concentrations on the activation of RyRs by $NO^{\bullet}$ and S-nitrosothiols was investigated.

1.5 LOW MOLECULAR WEIGHT S-NITROSOTHIOLS

1.5.1 Physiological Forms of NO

Although the production of NO in cells was linked to the activation of RyRs and RyR isomers found to be activated by S-nitrosation, the amount of $NO^{\bullet}$ required to activate RyR in *in vitro* experiments was too high to be physiologically realistic, which weakens the hypothesis that S-nitrosation of RyRs by nitric oxide gas should be the key mechanism to regulate RyR activity. Second, $NO^{\bullet}$ is short lived and is rapidly neutralized to nitrates or nitrites in oxygenated aqueous medium. This fact limited the diffusion and access of $NO^{\bullet}$ as a signaling molecule to very short distances from where the nitric oxide synthases are located. However, substantial evidence

suggests that LMW S-nitrosothiols serve as intermediate molecular species that stabilize $NO^{\bullet}$ and may be the biologically active forms of NO [8, 18]. Moreover, there have been suggestions that LMW S-nitrosothiols are generated in the cytosol from $NO^{\bullet}$, in the presence of oxygen and LMW thiols at pH 7.0 [123], or that they could be generated with Fe-hemoglobin at low (sub-micromolar) $NO^{\bullet}$ concentrations, in the absence of oxygen and at neutral pH (7.4) through the formation of nitrosonium ions (NO^{+}) [124].

As shown in figure 6, Stoyanovsky et al. reported that high concentrations of authentic $NO^{\bullet}$ (up to 100 μM) failed to cause Ca^{2+} release from SR vesicles, but the same amount of $NO^{\bullet}$ elicited rapid Ca^{2+} release from SR vesicles with reaction medium containing cysteine (50 μM). The activation of RyRs in this experiment was induced by S-nitrosocysteine (cys-SNO) produced from cysteine and $NO^{\bullet}$, and cys-SNO is more potent than authentic $NO^{\bullet}$. This observation showed that low molecular weight S-nitrosothiols can be generated very rapidly in the presence of $NO^{\bullet}$ and LMW thiol molecules, and that LMW S-nitrosothiols activate RyRs more efficiently than $NO^{\bullet}$. This suggested that S-nitrosylation of RyRs by cys-SNO is not via liberation of $NO^{\bullet}$ from it, and LMW S-nitrosthiols might be the biologically active forms to deliver NO-functions

There have been controversies about the role of pO_2 on NO-induced activation of RyRs. Eu et al. suggested that authentic $NO^{\bullet}$ activates RyRs only at low pO_2 (~ 10 mmHg) [83, 85, 86], but it was observed that authentic $NO^{\bullet}$ was not potent enough to cause the Ca^{2+} release from SR vesicles even at the low pO_2 in the study by Stoyanovsky et al. [15]. The oxygen effect on nitrosation reaction will be discussed in detail in the discussion section.

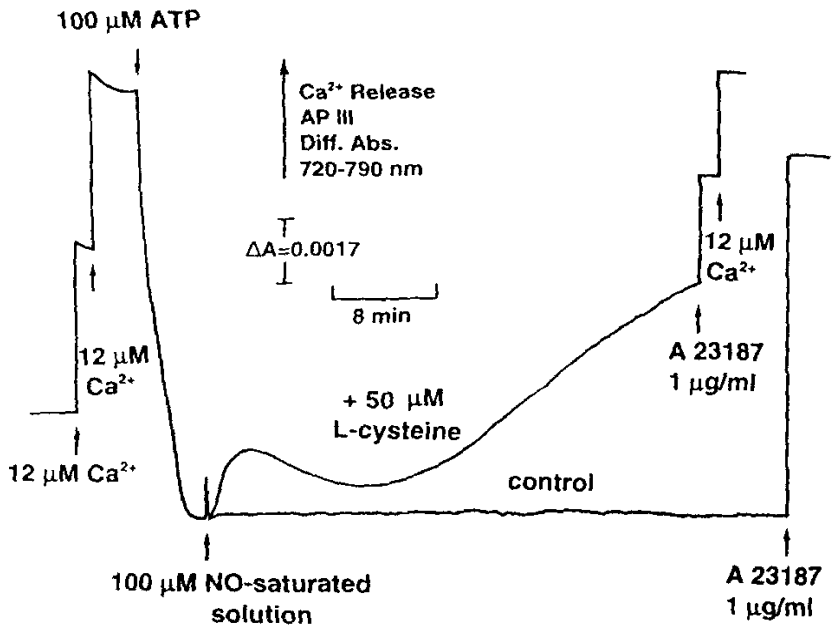

Figure 6. L-cysteine potentiates nitric oxide to induce Ca^{2+} release from SR vesicles.

from *Stoyanovsky DA et al. Cell calcium 21(1):19-29 (1997)*

1.5.2 S-nitrosothiols Trans-nitrosate Protein Thiols

It was presumed that S-nitrosothiols undergo homolytic cleavage of the S-N bond with the release of $NO^{\bullet}$. The biological activity of low molecular weight nitrosothiol compounds was often attributed to $NO^{\bullet}$ release [86, 125]. Marked variations have been reported for the rate of decomposition of different nitrosothiols, in aqueous solution at physiological pH, with half-lives ranging from minutes to hours (*e.g.,* G-SNO) [126]. Some studies show that S-nitrosothiols are stable in aqueous solutions and require trace amounts of copper to decompose thiol NO-donors to liberate $NO^{\bullet}$ [125, 127, 128]. Thus, copper (1) ions promote the decomposition of G-SNO, cys-SNO and SNAP [128-130].

Meanwhile, other reports suggested that the smooth muscle relaxing activity of S-nitrosothiol is independent of the liberation of $NO^{\bullet}$ [131]. Model studies suggest that low molecular weight (LMW) S-nitrosothiols may act as a nitrosonium cation (NO^{+}) in transnitrosation reactions between the LMW S-nitrosthiols and free thiols on peptides and large proteins [19]. GSNO has been shown to trans-nitrosate thiols on oxyhemoglobin in arterial blood, and reverse trans-nitrosation occurred between low molecular weight thiol compounds and S-nitrosohemoglobin in deoxygenated venous blood to produce S-nitrosothiols, which suggests the critical role of low molecular weight thiol compounds to deliver NO-related activity to the circulatory system [132]. Recent studies showed that S-nitrosothiols could exchange NO with the thiols according to the relative pK_a values of these two thiols by transnitrosation [19]. Thus, LMW S-nitrosothiols may serve to stabilize $NO^{\bullet}$ by gradually releasing the free radical and/or transferring NO^{+} to hyperreactive thiols on proteins to impart its biological activity.

1.6 HNO INDUCED ACTIVATION OF RYRS

In biological systems, $NO^{\bullet}$ participates in a complex equilibrium with S-nitrosothiols, nitroxyl (HNO) and metal-nitrosyl complexes that can release nitrosonium (^{+}NO) [98, 133, 134]. Recently, Kim et al. reported that HNO, in contrast to $NO^{\bullet}$, reacts with Cys-399 in the NR2A subunit of the N-methyl-D-aspartate (NMDA) receptor to limit excessive Ca^{2+} influx and thus provide neuroprotection from excitotoxic insults [21]. In *in vivo* experiments, Paolocci et al. observed that HNO exerts positive inotropic and lusitropic action, which, unlike $NO^{\bullet}$ and nitrates, is independent and additive to beta-adrenergic stimulation and stimulates the release of plasma calcitonin gene-related peptide [16]. These results lead to the thesis that HNO donors can be considered as prodrugs for the treatment of heart failure [16].

Whereas $NO^{\bullet}$ and $NO^{\bullet}$ donors oxidize thiols through nitrosation, HNO is known to convert thiols to unstable S-derived hydroxylamines that readily interact with a second thiol to form a disulfide bond, with the co-release of hydroxylamine [19, 20]. Hence, it is reasonable to predict that HNO may activate RyRs via an oxidation reaction followed by the formation of disulfide bonds. In this study, we have used sodium trioxodinitrate ($Na_2N_2O_3$; Angeli's salt; ANGS) as a donor of HNO to test its effects on the skeletal isoform of RyR.

1.7 REGULATORY CYSTEINES ON RYRS

1.7.1 Identification of Regulatory Cysteines on RyRs

Since it has become persuasive that the redox modification of critical or hyperreactive thiols on RyRs is a mechanism to regulate RyRs, attempts to identify the 'regulatory cysteines' on RyRs have been made by many researchers. The biggest challenge is the fact that there are ~100 cysteine residues on each monomer of RyRs and about half of them are known to exist as free

thiols that could be available for the redox modification. The reconstitution of RyRs from sheep ventricular muscle and frog and rabbit skeletal muscle has shown that sulfhydryl oxidizing agents increase channel activity through an increase in P_o without changing single channel conductance [70]. Eager et al. [87] reported that cardiac RyRs reconstituted from sheep heart were activated by either cytosolic or luminal oxidation using a membrane impermeable organomercurial agent, Thimerosal, which binds to free thiols on RyR protein to open the channel, and concluded that there are 'regulatory' cysteines on both sides of the channel protein. The studies by Feng et al. expanded the transmembrane nature of redox regulation because a transmembrane redox potential across the membrane appeared to regulate channel activity [96]. Thus, there is little doubt that cysteine residues facing the lumen of the SR are at least as important as cysteines facing the cytosolic side of the membrane. One report proposed that S-nitrosylation of C3635 on RyR1 activates the channel because a mutation of that cysteine residue produced a loss of NO-dependent activation [84]. Surprisingly, C3635 is part of the calmodulin binding site, yet mutated (C3635A) RyR1 exhibited normal calmodulin binding and calmodulin dependent regulation of the channel. Hence, NO activation of the channel should occur at C3635 and only in the presence of CaM. However, numerous reports indicate that calmodulin is neither required nor necessary to obtain sulfhydryl or NO-dependent activation of RyR1 in SR vesicles and RyR1 reconstituted in bilayers [15, 68, 69, 87, 88, 92, 135].

A critical issue that has not been resolved is the nature of the cysteine residues involved in the redox regulation of RyRs. It is important to note that only a fraction of these thiols are involved in redox regulation (2-4%) while there are over 100 cysteines per RyR monomer and almost half of them exist as free thiols. The thiols involved in the redox regulation of RyRs have been known to have low pK_a and to be readily oxidized by NO donors and other sulfhydryl

oxidants. For these reasons, the cysteines involved in the redox regulation of RyRs have been referred to as 'critical' or hyper-reactive' thiols to distinguish them as a subset of thiols that are unique in their function, reactivity, and reversible modulation of channel properties. Despite extensive progress in our understanding of the chemistry of these thiols, there is still little information regarding the location of this subset of cysteines and the linkage between cysteines accessible from the cytosolic versus the luminal side of RyRs. Thus, it is important to identify the cysteine residues that may be involved in RyR channel oxidation and/or S-nitrosylation.

1.7.2 Cysteine Residues Involved in Channel Gating

The identification of the regulatory cysteines of RyRs has been hindered by the fact that there are a large number of cysteines (~100 per monomer) and about half of them are known to be free thiols rather than form disulfide bonds. As discussed above, the redox-mediated regulation appears common across RyRs and IP_3Rs. From this, we hypothesized that the cysteines involved in the redox regulation of RyRs are conserved among all RyRs and IP_3Rs isoforms (see Table 1). Figure 7 shows the topology of RyR according to the 8 transmembrane domain model of Du et al. [56]. The 4 transmembrane model, suggested by Takeshima et al. [45], was the hypothesis supported by many other researchers. Recently, Du et al. tried to define the topology of skeletal RyR [56] by testing the 10 transmembrane model proposed by Zorzato et al. [44]. Their results suggested that the M1- M2 (numbered from 1 to 10 according to Zorzato model) sequence is not membrane-associated and there are 8 transmembrane domains, although it is a little bit ambiguous if the M3/M4 domain (between amino acid 4277-4363) is membrane associated. It was confirmed that M5-M10 are membrane associated. It is important to notice that the transmembrane domain (M5-M10) and the location of luminal loop confirmed in this study were very similar to those in Takeshima's 4 transmembrane model, although they proposed 8

transmembranes. Truncated p75 RyR1 staring at M4382 as shown in figure 7 contains a total of 8 cysteines: 4 cysteines fully conserved in 8 mammalian RyRs and IP_3Rs isoforms, and the other 4 cysteines are conserved in RyRs but not in IP_3Rs.

In figure 7, the dark gray amino acid represents 7 cysteines fully conserved in 8 mammalian RyRs and IP_3R isoforms and the light gray amino acid represents four cysteines conserved in RyRs but not in IP_3Rs residing in p75 RyR1. The cysteines conserved among 8 mammalian RyRs and IP_3Rs are referred as the fully conserved cysteines and the cysteines conserved only among 8 mammalian RyRs are referred as the partially conserved cysteines. Based on this topological map, there are 2 fully conserved cysteines and 3 partially conserved cysteines accessible from the cytosolic side of the RyRs and 2 fully conserved cysteines accessible from the luminal side of the RyRs. Two luminal fully conserved cysteines, C4876 and C4882, are located in the putative pore- forming region. Therefore, either or both of these cysteines in the pore region may be involved in luminal redox regulation. The study will avoid the site-directed mutations of the candidate cysteines (C4876 and C4882) for luminal redox regulation even though it will be a very straightforward approach to identify the regulatory cysteines because of the high possibility that a single substitution of a very conserved motif in the pore-forming region may cause the protein not to form functional channels or cause major alterations in channel characteristics other than redox regulation. Gao et al. reported that the single amino acid residue substitutions between amino acid 4894-4917 in the luminal loop could alter channel properties such as channel conductance and Ca^{2+}-dependent binding of [^{3}H]ryanodine, and sometimes they were not successful in obtaining functional channels, which highlighted the importance of this region to the normal channel behavior [59].

Table 1. Cysteine residues conserved in mammalian ryanodine and IP_3 receptors.
In dark gray are shown all 7 cysteine residues that are conserved across both the 9 mammalian RyRs and the 8 mammalian IP_3Rs. In light gray are shown the additional 10 cysteine residues conserved in RyRs but not in the IP_3Rs. The numbers prefixed by C are the cysteine residue numbers. The un-prefixed numbers (columns 3 and 5) are the i^{th} cysteine in the respective ryanodine receptor counting from the N-terminus.

	Rabbit RyR1		Rabbit RyR2		RyR Conserved	RyR + IP3R Conserved	Location
1	C 2232	53	C 2296	44	Yes	Yes	'Foot'
2	C 2237	55	C 2301	46	Yes	Yes	'Foot'
	Within RyR1 p170 (start is M3517)						
3	C 3635	82	C 3603	72	Yes	Yes	'Foot'
4	C 3733	84	C 3700	74	Yes	No	'Foot'
5	C 3839	86	C 3801	75	Yes	No	'Foot'
6	C 3892	87	C 3848	77	Yes	No	'Foot'
7	C 3973	89	C 3929	78	Yes	No	'Foot'
8	C 4114	90	C 4070	79	Yes	No	'Foot'
9	C 4238	91	C 4194	80	Yes	No	'Foot'
	Within RyR1 p75 (start is M4382) RyR1 p170 (start is M3517)						
10	C 4657	93	C 4588	82	Yes	No	Transmembrane
11	C 4663	94	C 4594	83	Yes	No	Transmembrane
12	C 4876	95	C 4808	84	Yes	Yes	'Pore'
13	C 4882	96	C 4814	85	Yes	Yes	'Pore'
14	C 4958	97	C 4890	86	Yes	Yes	'Tail'
15	C 4961	98	C 4893	87	Yes	Yes	'Tail'
16	C 5018	99	C 5050	88	Yes	No	'Tail'
17	C 5027	100	C 5059	89	Yes	No	'Tail'

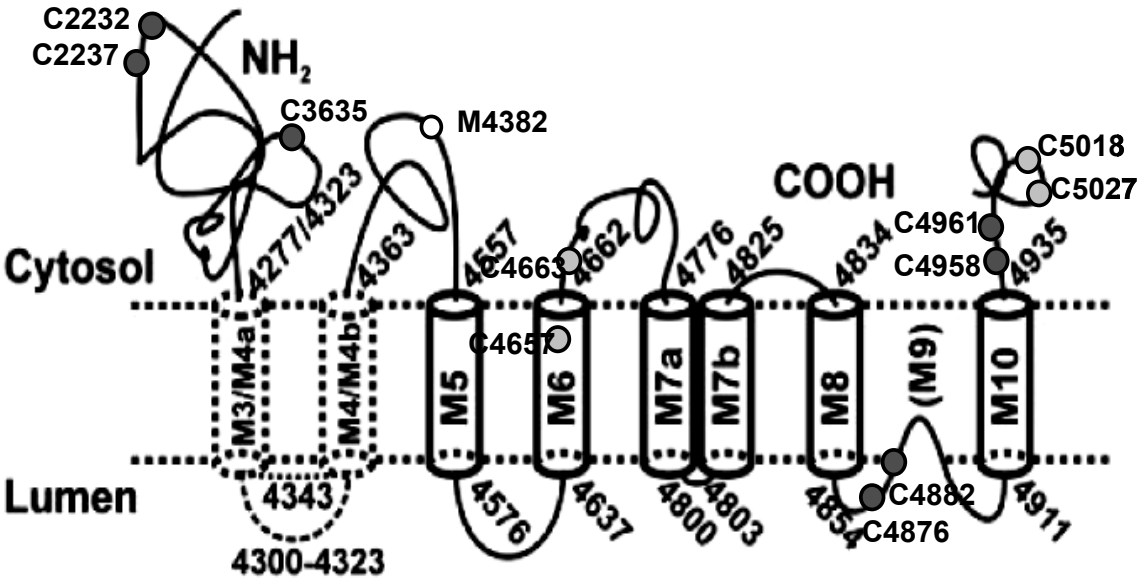

Figure 7. Topology of RyR according to 8 transmembrane domain model.

RyR can be divided into three regions: the N-terminus foot structure, the putative transmembrane domain including 2 luminal loops, and the C-terminal tail region. The dark gray circles represent 7 cysteine residues that are full-conserved across both the 8 mammalian RyRs and IP_3Rs. The light gray circles represent 4 partially-conserved cysteine residues within p75 RyR among 10 cysteine residues conserved in RyRs but not in IP_3Rs. p75 RyR consists of the transmembrane region and the C-terminal tail region starting from M4382 shown as a white circle. C3635 is the cysteine implicated as the CaM binding site. M4382 is the methionine, start site of truncated RyR1 found in brain tissue (Takeshima et al., Nature, 339(6224) pp439-45, 1989)

from Du, GG., et al, Proc. Natl. Acad. Sci. USA.,99(26) 16725-30, 2002

The channels with significant alteration in their characteristics will barely answer our questions about the NO regulation of RyRs. The study still will provide reasonably detailed information about the regulatory cysteine residues involved in NO-mediated regulation with truncated RyR first without mutations.

1.8 SUMMARY AND AIM OF STUDY

The ryanodine receptor carries out a central role in excitation-contraction coupling in a muscle cell and its activity is directly linked to the intracellular Ca^{2+} homeostasis in the cytosol of muscle cells. The hypothesis that redox modification of critical or hyperreactive thiols on the RyR is a key mechanism involved in the regulation of the intracellular Ca^{2+} channels has become increasingly persuasive. A series of studies have shown that both of the mammalian RyR isoforms and IP_3R isoforms are modulated by sulfhydryl oxidation-reduction, which suggests that the redox-mediated regulation is a common mechanism to control the cellular Ca^{2+} homeostasis in all kinds cells. Nitric oxide is a physiological sulfhydryl oxidant and known to activate RyRs. Thus, the study on nitric oxide-mediated regulation of these ion channels will be important to understand the regulation of Ca^{2+} homeostasis in all cells including excitable and non-excitable cells since it regulates internal Ca^{2+} stores via RyR and /or IP_3 receptors.

In a biological system, molecules most closely identified with NO-related activity include authentic $NO^{\bullet}$ itself, S-nitrosothiols, metal-NO complexes that can release nitrosonium (^{+}NO), nitroxyl anions (HNO) and higher oxides of nitrogen (NO_X) including peroxynitrite. The rate of RyRs' activation via S-nitrosation strongly depended on the structure of the nitrosating agents, which suggests that under physiological conditions different forms of NO may exert, both kinetically and mechanistically, distinct effects on RyRs. Currently, however, the modulation of

RyR activity by these NO-related molecules and the role of oxygen level on S-nitrosation reaction are not well studied. Also, there is still little information regarding the location of regulatory cysteines and the linkage between cysteines accessible from the cytosolic versus the luminal side of RyRs.

Hence, this study will attempt to answer the following questions:

1) What are the physiologically active form of nitric oxide?

The chemical reaction underlying the thiol-oxidation and activation of skeletal muscle ryanodine receptors (RyRs) by different types of NO donors, including authentic $NO^{\bullet}$, S-nitrosothiols and HNO, should be studied in order to better evaluate the physiological significance of RyR activation by biologically relevant forms of NO. The discrimination among $NO^{\bullet}$-, *trans*-S-nitrosation- and disulfide formation-dependent activation of RyRs will be one of major focuses of this study.

2) What is the role of oxygen on NO-mediated activation of RyRs?

The effect of the O_2 concentrations on the activation of RyRs by $NO^{\bullet}$ and S-nitrosothiols will be investigated.

3) Which is (are) the regulatory cysteine(s) involved in the NO-regulation of RyRs?

This study will test the hypothesis that cysteines involved in the NO regulation of RyRs are located in the highly conserved C-terminal region of the RyR where all the cysteine residues are found highly conserved among mammalian RyRs.

2.0 METHODS

2.1 PREPARATION OF RYRS

2.1.1 Preparation of SR Vesicles from Muscle (Skeletal and Cardiac)

SR vesicles were isolated from white muscle from the hind legs of New Zealand white rabbits, as described by Salama and Scarpa with modifications.[136] The procedures were as follows. The white muscles taken from the hind legs of New Zealand white rabbits are put into the ice-cold medium and chopped using blender. Muscle homogenate was differentially centrifuged to yield crude SR vesicles. SR vesicles were run on a discontinuous sucrose gradient to separate heavy SR vesicles from light SR vesicles. Heavy SR vesicles consist of terminal cisternae SR and contain a lot of RyRs. Light SR vesicles consist of longitudinal SR and contain a lot of Ca^{2+}-ATPase. Heavy SR vesicles were collected from the 35-40% interface and used for single channel recordings. Care was taken to avoid all sulfhydryl oxidants or reducing agents throughout the preparative steps to avoid changes in thiol oxidation-reduction of the vesicles.

2.1.2 Purification of RyRs from SR Vesicles

Ryanodine receptors were further purified from SR vesicles. SR vesicles were solubilized by incubating them in the medium containing 0.8 % CHAPS (3-[(3-cholamidopropyl) dimethyl-ammonio]-1-propanesulfonate) at 4 °C for 1 hour, which then was centrifuged at 34,000 rpm to spin down the non-solubilized vesicles. Continuous sucrose gradient (5~20%) was generated and the supernatant from the solubilized vesicles was loaded on the top of sucrose gradient and centrifuged at 20,000 rpm for 16 hours. The fraction was harvested and run on the

polyacrylamide gel to verify the fractions containing RyRs. The fractions with RyRs were fooled and run on the Amicon concentrators to concentrate the proteins and remove CHAPS. The solubilized proteins were put into the planar lipid bilayer for the single channel recordings.

2.1.3 Preparation of Membrane Vesicles from HEK 293 Cells

HEK cells stably expressing the RyRs were harvested and microsomal membrane vesicles were prepared. Briefly, harvested cells were resuspended in a hypotonic lysis buffer (10 mM Hepes-Tris, 1mM EGTA, pH 7.4) and Dounce-homogenized (10 strokes) and an equal amount of restoration buffer (500 mM sucrose, 10 mM Hepes-Tris, 1 mM EGTA, pH 7.4) were added. This were be then Dounce-homogenized (20 strokes) and centrifuged at 1000 g for 10 min to spin down the unbroken cells. The pellet were resuspended in lysis buffer to repeat the above Dounce-homogenization. Microsomal membrane vesicles were obtained by centrifugation of the supernatant collected at 100,000 g for 45 min. The pellet were resuspended in a buffer containing 250 mM sucrose, 10 mM Hepes-Tris and pH 7.4.

2.2 TRANSIENT EXPRESSION OF RYRS IN CHO CELLS

2.2.1 Construction of cDNA to Express Truncated RyRs

Derivatives of pBS (Strategene) plasmid carrying the rabbit skeletal muscle ryanodine receptor (RyR) full-length and truncated cDNAs were constructed by standard recombinant DNA techniques. Plasmid (pRRS18) contained the full-length (RyR) cDNA and was made by deletion of the neo^r gene from pRRS11 (figure 8). A 15.7 kb HindIII fragment carrying the RyR cDNA from pRRS18 was cloned into the HindIII site of pBS/KS in an orientation so that the T7 promoter directs the mRNA synthesis. The

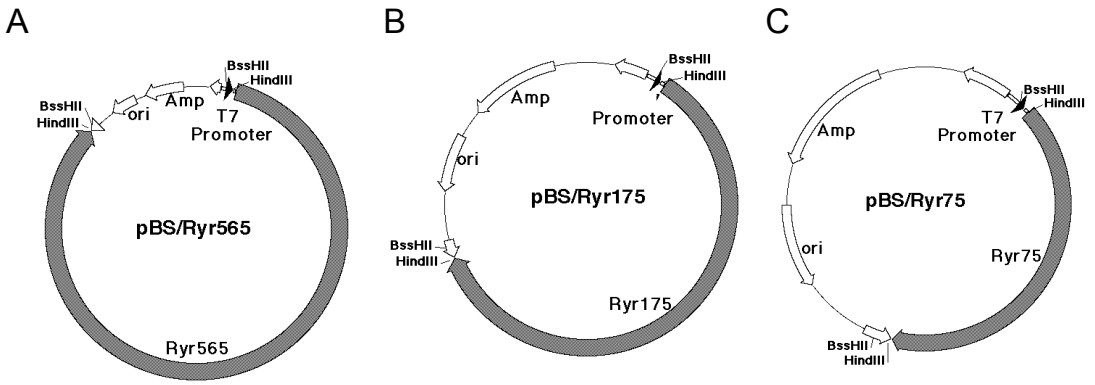

Figure 8. Schematics of RyR Constructs driven by T7 Promoter.

A. pBS/RRs18-p560 position –22 to the 3'-end

B. pBS/RRs3-p170 position 10,650 to the 3'-end

C. pBS/RRs13-p75 position 13,123 to the 3'-end

carrying this truncated RyR cDNA from pRRS3 was cloned into the HindIII site of pBS/KS in a way that transcription from the T7 promoter generates an mRNA for the truncated RyR molecule. This plasmid was designated pBS/Ryr170 (Figure 8B). Plasmid pRRS13 carrying a brain specific cDNA was shown to encode the carboxyl-terminal RyR molecule [45]. A 2.1 kb HindIII fragment carrying the brain specific RyR1 cDNA from pRRS13 was cloned into the HindIII site of pBS/SK. (Figure 8C) Its orientation was such that the T7 promoter directed the mRNA synthesis of a 75 kDa carboxyl-terminal RyR molecule to yield pBS/RyR75 (from 4382M to the C-terminus, a total of 656 residues).

2.2.2 Transient Expression in CHO Cells

CHO cells were obtained from American Type Culture Collection (ATCC) and maintained in a 1:1 mixture of Dulbecco's modified Eagles medium and Ham's F-12 medium (GIBCO BRL) containing 5% heat-inactivated fetal calf serum (HyClone) and kept in a water-saturated 5% CO_2

incubator at 37°C. The cells were grown to confluence in 75-cm^2 tissue culture flasks and passed at 1:5 split ratio. An avian host-range-restricted vaccinia virus encoding bacteriophage T7 RNA polymerase, MVA/T7 pol was used for the transient expression in CHO cells. Because it is replication-deficient in mammalian cells, MVA/T7 pol reduced cytopathic effects yet provides a high level of gene expression [137, 138]. For immunofluorescence and Ca^{2+} release assays, CHO ($\sim 10^4$) cells were seeded on a coverslip that was placed in a 35-mm plate. The cells were usually at 40-50% confluence when transfection was performed the next day. After removing the medium, MVA/T7 pol virus ($5x10^5$) in 1 ml of DMEM/F12 was added to each plate and incubated at 37°C in a CO_2 incubator for 60 minutes. Virus-containing medium was then replaced with 0.8 ml of DNA-lipid complexes in DMEM/F12 medium, which was prepared by mixing pBS/RyR plasmids with lipofectamine (BRL GIBCO) at a ratio of 1:6 (DNA to lipid) following the procedure recommended by the manufacturer. After 4 hours incubation at 37°C, 1.2 ml of growth medium was added to each plate and the incubation was continued for 16-20 hours. No severe cytopathic effects were observed when the cells were used 20-24 hours post transfection.

2.3 CONSTRUCTION OF HEK CELLS EXPRESSING TRUNCATED RYRS

2.3.1 Construction of Truncated RyR cDNA

The cDNA that encodes the carboxyl-terminal p75 RyR1 molecule kindly provided by Dr. Takeshima was cloned into eukaryotic expression vector pcDNA5/FRT (Invitrogen, CA) that is the part of Flpin system. A 2.1 kb fragment was cloned into KpnI and EcoRV sites in the multiple cloning site of pCDNA5/FRT for expression of the p75 (from M4382 to the C-terminus, a total of 656 residues) RyRs. Each single amino acid mutation was prepared by introducing a

double base change (TGC to GCC or GAC) by Pfu DNA polymerase-based chain reaction by using two mutagenic primers and the QuickChange site-directed mutagenesis kit (Stratagene). All of the constructs were confirmed by sequencing and restriction analysis.

2.3.2 Stable Expression of RyRs in HEK Cells

The perpetual cell line stably expressing wild type p75 RyR1 and p75 RyR1s with site-directed mutation were constructed. One of the biggest obstacles to study the structure-function relationship of a protein was often to obtain the stable production of proteins with the various mutations to be tested. It usually took about six months to obtain a perpetual cell line with stable and reasonable level of expression by the conventional methods. Yet, often the expression level went down in a couple of months after the transfection. On the other hand, the transient expression method allows the researchers to obtain proteins in a short time after the transfection, but one needs to carry out the transfection process every time a new batch of proteins needed and the concentration of the expressed protein in the membrane fraction often is not very high because of the limited efficiency of transfection. The use of FlpIn system (Invitrogen, CA) allows the perpetual cell lines to express various truncated and mutated RyRs in a relatively short time.

Flpin HEK 293 cells (Invitrogen, CA, U.S.A.) were grown in DMEM medium (Gibco BRL, MD, U.S.A.) with 10% fetal bovine serum. HEK cells before the transfection with the expression vector were grown in the medium containing Zeocin (100 μg/ml) according to the manufacturer's guide in a 5% CO_2 incubator at 37°C. HEK cells were transfected with pcDNA5/FRT/p75 RyR1 using liposome-based methods (Lipofectamine 2000, Gibco BRL, MD). 48 hours after the transfection, cells were exposed to Hygromycin (150 μg/ml) and selected for

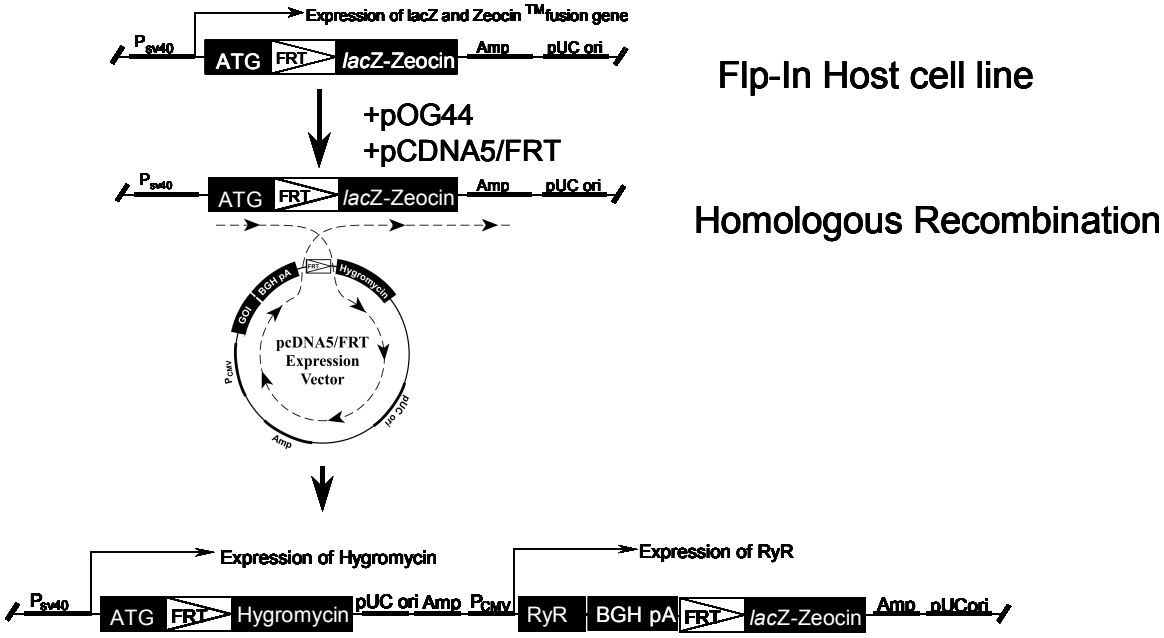

Figure 9. Generation of Flp-In HEK 293 cells stably expressing truncated RyR1.

Flp-in host cell line contains the vector inserted into the chromosome to express lacZ and Zeocin. The expression level of foreign proteins is optimized for the reference protein. After the initiation codon, there is so called flip in site (FRT). When the host cell line is transfected with the expression vector containing the gene of interested protein and pOG 44 vector to express the recombinase to promote the homologous recombination between the FRT site in the expression vector and the vector already existing in the chromosome of host cells. Because the location of FRT is right after the initiation codon, the homologous recombination of FRT sites turns off the expression of lacZ and Zeocin and turns on the expression of Hygromycin resistance. The expression of RyR is promoted by pCMV ubiquitously existing in mammalian cells.

stable transfectant clones. The expression level of proteins has already been optimized for the reference protein. Therefore, it doesn't require the subculturing, which allows the researcher to obtain a perpetual cell line within 3-4 weeks after the transfection. Immunofluorescence staining and Western blotting using Rat polyclonal antibody or monoclonal RR2 antibodies was used to monitor the expression of RyR proteins.

2.4 MEASUREMENT OF RYR ACTIVITY VIA SR Ca^{2+} TRANSPORT

Ca^{2+} uptake and efflux from SR vesicles were measured spectrophotometrically through the differential absorption changes of Antipyrylazo III (AP III) as an indicator of extravesicular free Ca^{2+}. Differential absorption of AP III was measured kinetically at 720-790 nm with a time-sharing dual-wavelength spectrophotometer (SDB-3A, University of Pennsylvania, Biomedical Instrumentation, Philadelphia, PA). All measurements were performed in a temperature-controlled cuvette under continuous stirring. Ca^{2+} uptake by SR vesicles was measured in a medium containing100 mM KCl, 200 μM AP III, 1 mM $MgCl_2$, 100 μM ATP, 2.5 U/ml creatine kinase (CK), 4 mM phosphocreatine (CP), 20mM HEPES-Tris, pH 7.0 at 37^{o}C. CK and CP provided an ATP regenerating system to maintain a constant concentration of ATP and free Mg^{2+} during Ca^{2+} transport [15, 135, 139, 140].

Differential absorbance normalizes the system by avoiding the artificial effect by particles in the reaction buffer. Addition of $CaCl_2$ to the reaction buffer at the beginning of each experiment to measure Ca^{2+} release from SR vesicles was used as calibration of differential absorbance to free Ca^{2+} concentration in reaction buffer for each experiment.

For experiments under deoxygenated conditions, the medium was degassed with N_2 gas for 20 min to deoxygenate the medium. The deoxygenated solutions and vesicles were added

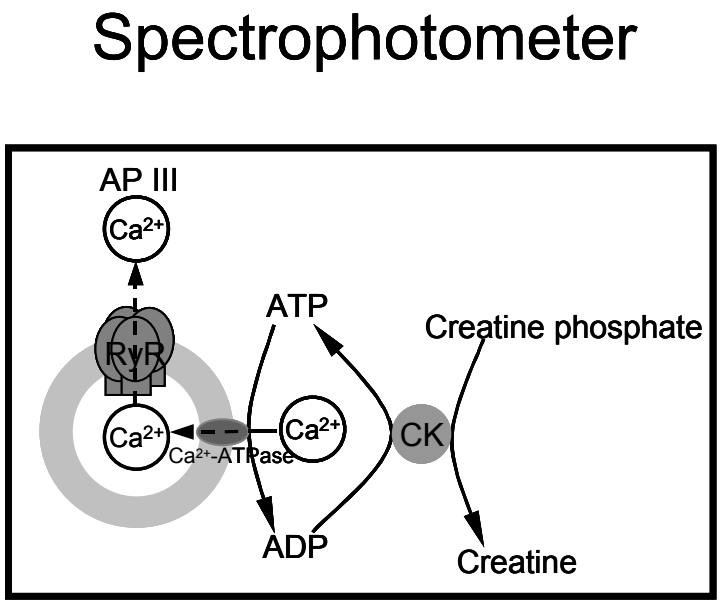

Figure 10. Spectrophotometric measurement of Ca^{2+} transport across SR vesicle membrane.

The Ca^{2+} influx into and efflux from SR vesicle were measured spectrophotometrically using AP III as a Ca^{2+} indicator. $CaCl_2$ was added to the media containing SR vesicles and the following addition of ATP (100 μM) and regeneration system consisting of creatine kinase and phosphocreatine promotes Ca^{2+}-ATPase to pump Ca^{2+} into the SR vesicles. After SR vesicles are loaded up with Ca^{2+}, an agent to activate RyRs is added and its effect monitored through Ca^{2+} release from SR vesicles.

into the cuvette under the N_2 gas stream and the cuvette was sealed with a cap and vacuum grease to prevent the medium from being oxygenated. Subsequent additions of ambient medium and the other solutions into the cuvette were made using Hamilton syringe to obtain the desired oxygen level in the solution. The oxygen level in each solution was measured using oxygen meter after each experiment (Fisher Scientific, Pittsburgh, PA).

2.5 MEASUREMENTS OF Ca_i IN ISOLATED CHO CELLS

CHO cells were plated on poly-L-lysine coated glass cover slips (25 mm) and cultured at 37^{o}C in 95% O_2 plus 5% CO_2 in a medium supplemented with fetal bovine serum (5%). Cells were loaded with the Ca^{2+} indicator in a saline solution containing (in mM): 140 NaCl, 4 KCl, 2 $MgCl_2$, 1 $CaCl_2$, 12 glucose, 10 HEPES-NaOH (pH 7.2) and 2 μM Fura 2-AM at 37^{o}C. After a 30-min loading period, cells were washed and placed in an incubator for 15 min at 37^{o}C. Ca_i measurements and calibration procedures were performed as described. [141] Cells loaded with Fura-2 were imaged with a 40 X fluor oil-immersion objective on an inverted microscope (Nikon Diaphot) and an intensified video camera with Metafluor software (Universal Imaging Corp., West Chester, PA) for image analysis. Fura-2 was excited with alternating epi-illumination (1 Hz) at 340 and 380 nm and the emission was collected at 505 nm. Ca_i was measured from the fluorescence ratio, $F_{340\,nm}/F_{380\,nm}$ assuming a K_d of 225 nM. [141] Data points were sampled every 5 s and a computer calculated Ca_i on line.

2.6 STUDY OF SINGLE CHANNEL ACTIVITY

Since the patch-clamp technique was introduced, single channel recording has made an enormous impact on our understanding of ion channel function and its role in membrane

transport and cell physiology. But, it has limitation on that ion channels on the intracellular membrane cannot be accessed by patch pipettes. The location of RyR in an intracellular membrane makes the characterization of channel function difficult. Unlike channel proteins in the cell surface membrane whose currents can be monitored using standard patch-clamp method, the ion translocation through RyR must involve the incorporation of the channel into some form of artificial membrane system such as a planar phospholipids bilayer. The incorporation of purified RyR channel proteins into a planar lipid bilayer results in an extremely powerful system for the investigation of the mechanisms involved in ion handling by this channel. The reconstituted system allows for free access and complete control of the ionic composition of the solutions at both sides of the channel protein and RyR incorporates into planar bilayers with a fixed orientation so that the cytosolic and luminal sides of the channel can be defined.

2.6.1 Planar Lipid Bilayer Technique

Synthetic planar lipid membranes were originally used as model systems for studying cell membrane structure. Miller and Racker discovered that SR vesicles isolated from muscle could be fused with artificial lipid bilayers and incorporate ion channels from muscle membranes into artificial membranes [142]. To study ion channels, bilayers are usually formed using a modification of the film drainage method developed by Mueller et al. [142] A solution of lipids in a hydrophobic solvent (usually n-decane) is smeared across a hole in a plastic septum to produce a thick lipid film separating two baths. The bilayer forms spontaneously from this thick lipid film. During bilayer formation, surface-active lipids aggregate into monolayer at the oil-water interfaces on each side of the thick film. The solvent drains away from between the two monolayers, thus allowing their apposition and formation of the bilayer structure. Draining of the solvent depends on the material used to make the partition.

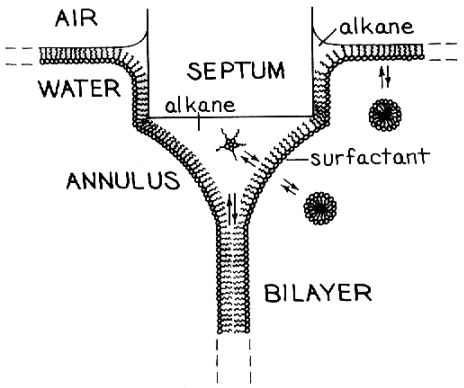

Figure 11. Schematic representation of black lipid membrane apparatus
The lipid in the annulus is represented as simple inverted micelles, but other much larger and complex aggregates are possible. The arrows indicate the equilibria between the various phases of the system. The drawing is not to scale. For bilayers formed by spreading from bulk nonpolar solutions, the mass of the annulus is a million times that of the bilayer. Therefore, the chemical potentials of the lipid and solvent (alkane) in the annulus determine the chemical potentials in the bilayer.
From: Ion channel reconstitution by Miller, C. 1986.

2.6.2 Overview of the Planar Bilayer Apparatus

The whole planar lipid bilayer system is divided into two main sections: (1) mechanical hardware, including chambers, electrodes, and interference shielding; (2) electrical hardware, covering pulse generators, current-to-voltage converter, and signal conditioning.

Mechanical Hardware The mechanical system consists of two membrane chambers (trans and cis chambers), electrodes, and salt bridges prepared with agar therein

which connect between the electrode chambers and membrane chambers. The membrane chambers consist of two parts. The one is a Kynar cup with a perforated hole and sidewall around the hole thinned.

The other is a Teflon block. Planar bilayers were formed using painted membranes by placing small amount of lipid solution, dissolved in n-decane, onto the aperture of a Kynar cup. As the lipid solution drains to the border of the aperture, a film is formed in the central part of the aperture. This film gets thinner and finally becomes a bilayer.

Electrical connection of the membrane chambers to the measurement equipment is done by Silver chloride electrodes. Silver-silver chloride electrodes are generally used to avoid polarization of the electrode tips and are easy to prepare. Silver chloride can be deposited by placing the electrode under preparation and another silver wire into 3 M KCl solution and passing a current over 10 mA for 2 min through the silver wires.

Interference Problems The membrane chambers and the current-measuring circuit must be enclosed in a Faraday cage to avoid current interference from RF signals generated alternating current in power lines and oscillator cages. Vibrations transmitted to the membrane chamber can cause serious interference when measuring small currents and are avoided. Floor vibrations are attenuated by placing the chamber on a vibration insulation table, which improve the signal-to-noise ration of the low-level current recordings.

Electrical Hardware The electrical equipment consists of a waveform generator, a current-to-voltage converter, a voltage amplifier, and a low-pass filter. The bilayer is connected to a function generator and a current-to-voltage converter. The electrical potential at one side of the membrane is the output of the function generator, and the other side is actively held at ground by the current-to-voltage converter. Current passing through the membrane is transduced into an analogue voltage signal by the current-to-voltage converter. The output is amplified by the signal-conditioning circuit before being displayed on an oscilloscope and then sent to the computer.

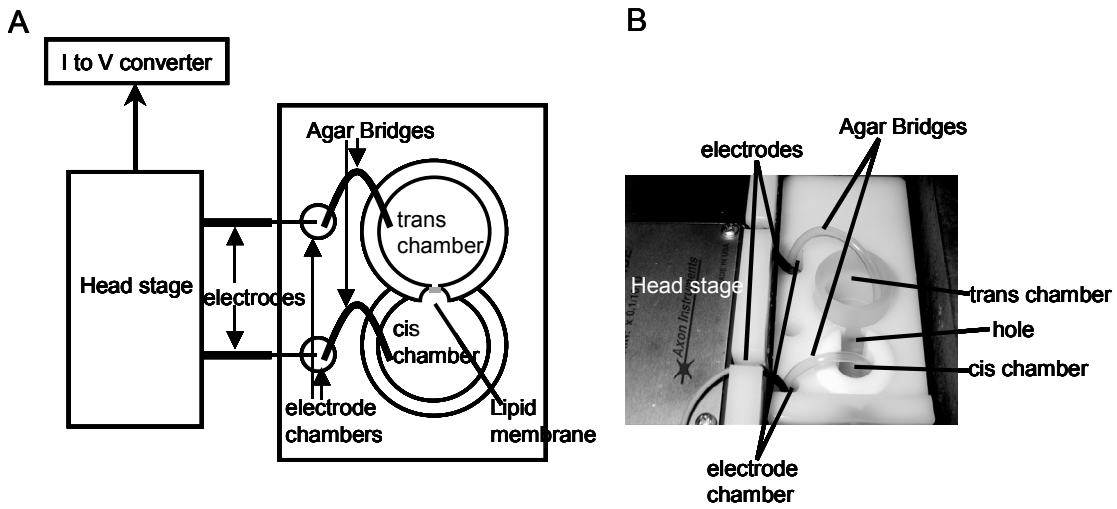

Figure 12. Schematics and picture of planar lipid bilayer apparatus.

A. Schematics of chambers to measure the single channel activity using planar lipid bilayer. The planar lipid membrane is formed on the small hole between the cis and trans chambers, which results in no current between these two chambers. The membrane chambers are connected to electrode chambers with the bridges filled with polymerized agar in saturated KCl solution. RyR channels are reconstituted in planar lipid bilayer by fusing SR vesicles or purified RyR proteins from cis chamber. Only when the reconstituted channel opens, there will be currents through this channel protein. The electrodes detect the currents across the membrane.
B. Picture of planar lipid bilayer chambers.

Formation of Planar Lipid Bilayer Lipid membranes were formed as described above. Lipids can be applied to the hole in the cup using either a small brush or a fire-polished glass rod. The lipid bilayers were formed using a mixture of phosphatidyl ethanolamine (PE) / phosphatidyl serine (PS) / phosphatidyl choline (PC) (5:3:2 by wt) (Avanti Polar Lipids, AL) dissolved in n-decane at a concentration of 50 mg/ml across an ~200 μm diameter aperture in a Kynar cup.

Reconstitution of RyR Channels in the Planar Lipid Bilayers The planar lipid bilayer is formed by making the membrane out of mixture of phospholipids in a small hole in kynar cup. Isolated SR vesicles are incorporated into the planar lipid bilayer, which reconstitutes RyR channels in the bilayer. In the ion channel reconstitution by using the fusion method, the most critical point is to control the fusion process itself. The fusion rates depend on the vesicle concentration in the aqueous solution, the area of the planar bilayer, the amount of hyperosmolarity of the cis side or the vesicles, and the amount of organic solvent in the planar bilayer. If there is increase in any of these parameters, the fusion rates are increased. Additional parameters to control and increase the fusion rates are the amount of negatively charged lipid in the planar bilayer together with the concentration of calcium in the aqueous solution, the amount of PE lipids in the planar bilayer and the temperature when a planar bilayer in the frozen state is used. Another important parameter to the fusion rate of the vesicles is the vesicle membrane composition that could be varied from one preparation from another.

The incorporation of ion-channel proteins into planar bilayers by fusion is a known technique and has been used for a quite long time. However, the fusion process itself is not fully understood. The microsomal membrane vesicles or heavy SR vesicles will be added to the cis chamber of a bilayer and fused in the presence of osmotic gradient, 200 mM/50 mM or 250 mM/50 mM (cis/trans) cesium gluconate in 10 mM Hepes-tris, 1 mM EGTA and pH 7.4. The

above solution condition hindered the conductance of K^+ channels and Cl^- channels which exist on the microsomal membrane because K^+ channel activity was blocked by Cs^+ and Cl^- channels are not permeable to $gluconate^-$.

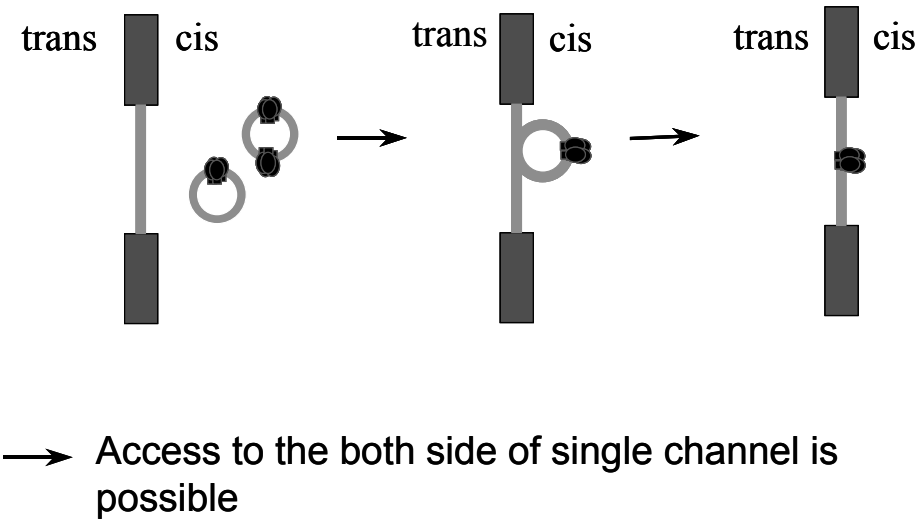

Figure 13.Reconstitution of RyR channels by fusion of SR vesicles with planar lipid bilayer.

The reconstitution of RyR channel from purified RyR protein was simpler than incorporating the heavy SR vesicles into the lipid bilayer. The osmotic gradient was not required. The channel activity was recorded in 250 mM KCl solution (symmetrical in *cis/trans* chamber) because there was no potassium channel or chloride channel current interferences.

2.6.3 Analysis of Single Channel Activity Recordings

Data Recording Single channel currents were recorded using an Axopatch 1D amplifier with a CV-4B head stage (Axon Instruments, Foster city, CA). Single channel currents were filtered through an eight-pole Bessel filter at 2 kHz. Data was digitized with an analog-to-digital converter and transferred to computer. Channel fluctuations were analyzed using pClamp

software (Axon Instruments) to determine the open probability, ionic conductance, subconductance states, and mean open and closed dwell times. Several approaches were used to analyze the channel activity.

Calculation of Open Probability of Single Channel Figure 14 shows a typical example of single channel recording from a single ryanodine receptor. Ideally, the current recordings should show stepwise jumps between discrete current levels of close and open states yet real data recorded in the bilayer setup is always distorted by experimental noise as shown in panel A. Therefore, the closed/open states are typically identified by computing a histogram of current values. Panel B is the histogram of channel currents showing two gaussian distributions. Threshold can be identified using k-means clustering or equivalent clustering algorithms. Peaks in the histogram correspond to current levels in each state (closed, full open and subconductance) and the width of the peaks is proportional to the size of the background noise and the area under each peak is proportional to the total time spent at that level. An overall measure of the channel activity can be obtained from the open probability (P_o). P_o is the fraction of time when the channel is in a conducting state and is calculated from the ratio of the number of data points in conducting levels and the total number of points in the record (assuming equally spaced data samples).

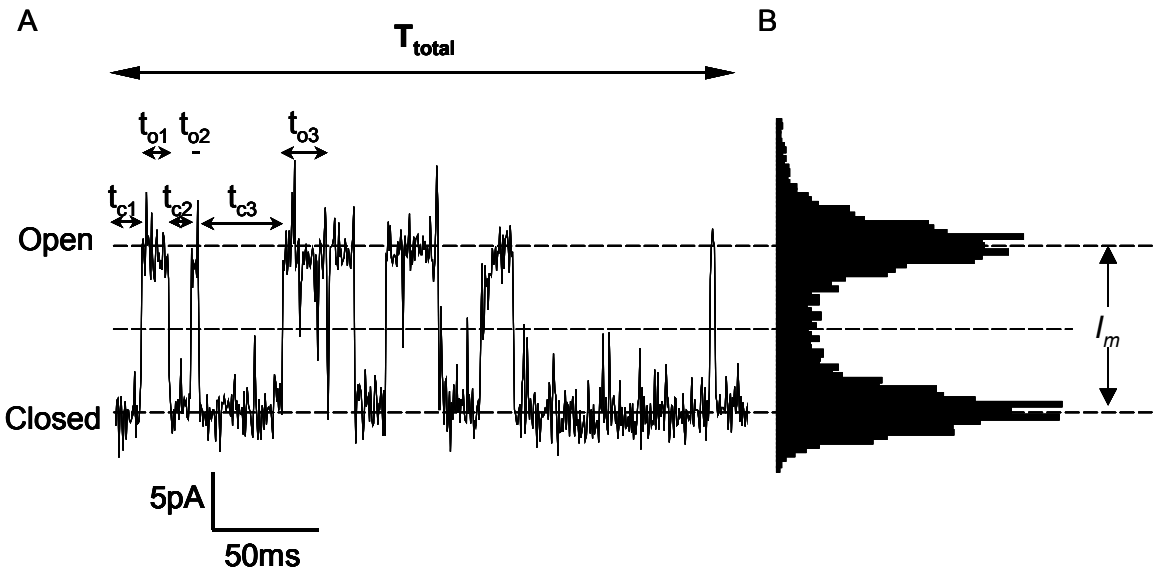

Open probability $P_o = \frac{t_{o1} + t_{o2} + t_{o3} \ldots\ldots + t_{on}}{T_{total}}$

$$P_c = \frac{t_{c1} + t_{c2} + t_{c3} \ldots\ldots + t_{cn}}{T_{total}}$$

$$P_o = 1 - P_c$$

Figure 14. Calculation of open probability of single channel.
A)A typical example of a current signal from a single ryanodine receptor where channel openings are marked by upward reflections in the current. The top and bottom dotted lines indicate the current levels corresponding to the open and closed channel.
B) An amplitude histogram of the date in (A) that shows a bimodal distribution with peaks corresponding to the open and closed states of the channel and the different current levels associated with those of the channel. The maximum unitary current is I_m.The open and closed dwell-times are given by the parameters t_{on} and t_{cn}, respectively.

An overall picture of channel gating rates is visualized in the mean open and closed dwell times (T_o and T_c). The mean open time T_o and the mean closed time T_c are calculated as follows.

Mean open time $$T_o = \frac{t_{o1} + t_{o2} + t_{o3} + \ldots + t_{on}}{n}$$

Mean closed time $$T_c = \frac{t_{c1} + t_{c2} + t_{c3} + \ldots + t_{cn}}{n}$$

A more detailed analysis of channel gating can be achieved from statistics of amplitudes and durations such as dwell times, i.e., the times spent at each current level before it jumps to a new level. Frequency histograms of open and closed dwell times graphically show the kinetic signature of the gating mechanism and provide clues to the underlying gating mechanism.

Stochastic Interpretation of Ion Channel Mechanisms The detailed kinetics of ion channels can be considered as a stochastic process from one state to the others and modeled by a Markov chain. The simplest model can be one closed state and one open state and the channel jumps form one to the other with fixed rate as shown in model 11(figure 15). When we assume that all the channels are open at the initial time (t=0), the number of channels in the open state will decrease exponentially as more channels jump to the closed state.

The same analogy can be applied to the single channel recordings. The dwell time (see page 66) of channel opening/closing will show an exponential decay if our two state Markovian model is correct. However, the actual distribution of dwell times often show more complex humps in dwell time histogram and disagree with this simple exponential decay (see figure 28), suggesting that the ion channel kinetics are more complex than the simple interpretation of shift from open to close state observed from the current measurements.

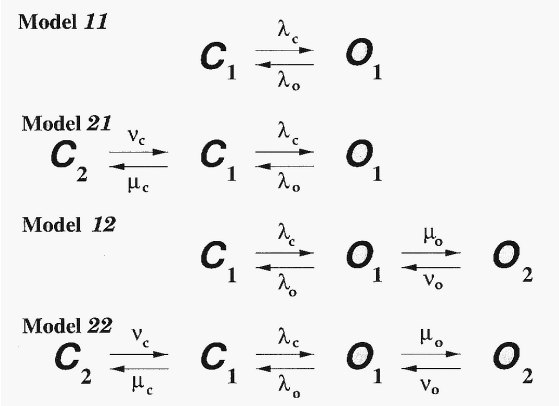

Figure 15. Four simple Markov models.
The state space of each Markov model is partitioned into an open class (*O*) and a closed class (*C*). Each edge is accompanied by the corresponding transition rate. Classes consist of either a single state or an 'inner' state (given the subscript 1) and an 'outer' state (subscript 2). As there is only a single pathway between the classes in all models, deriving the probability density function of the sojourn time in a two-state class is a simple exercise.

This is probably due to the fact that other distinct states of protein conformation or ligand binding are 'hidden' in either open or closed state observed from the current measurement in the bilayer setup. In other word, open/closed state may have additional states that cannot be discriminated from each other by just looking at the current values.

Although one cannot separate these hidden states from observed values, it is still possible to guess a model based on the outcome of dwell time distribution. Once the distribution of dwell time are constructed, one can choose the model and then calculate the probabilities (likelihood) that dwell time is distributed as data acquired by changing parameters (rate constant or transition probability) in the model. The rate constant can be determined by choosing the condition when the likelihood is at maximum (Maximum likelihood). [143, 144]

Several groups have developed algorithms to determine the most possible Markov model of ion channels from the observed data set using various optimization methods. [143-147] Due to the nature of data acquisition, the continuous Markov model is often replaced by discrete

Markov process. The discrete-time transition probability of the Markov model is related to the matrix of rate constants Q of the usual, continuous Markov model.

$P(t) = e^{Qt}$ where Q is the transition rate matrix.

The distribution of the length of an opening for the reversible mechanism can be shown to have a probability density function (pdf). [143] In simple cases, it is expected that the data should be fitted by an exponential distribution or a sum of exponentials.

$f(t) = \lambda e^{-\lambda t} = \tau^{-1} e^{-t/\tau}$ t>0 where λ is the rate constant, and τ is the time constant.

The exponential pdfs would not be expected if the transition probabilities between states vary with time, or if frequency resolution is limited. The pdf for a distribution that has the form of the sum of several (say k) exponentials can be written as

$$f(t) = w_1 e^{-\lambda_1 t} + w_2 e^{-\lambda_2 t} + \cdots + w_k e^{-\lambda_k t}$$

where the coefficients w_k are the amplitudes (at t=0) of each component.

Several methods have been used to compute likelihoods and estimate model parameters from single channel data. The likelihood of the hidden Markov model is defined as the probability of the observed data samples $Y(t)$= $\{y_t, t = 1,\ldots,T\}$,

$L = P(y_1, y_2, ..., y_T \mid \lambda)$

The likelihood L of the hidden Markov model can be calculated by summing the probability of the data and the state sequence over all possible state sequences.

Finding the best Markov model involves 1) the preprocessing of data including filtering or inverse filtering, adjusting baseline fluctuation, or data whitening, 2) clustering data points into several groups, 3) selection of possible models and 4) optimization of Markov model parameters [143-147].

Markov Model and Maximum Likelihood Analysis We used winmil program by Qin, Auerbach, and Sachs (QUB, Buffalo, NY) for the analysis of data idealized using the pCLAMP program. Open and closed experimental intervals were binned as the logarithm of their duration with 18 bins per log unit. Individual lifetimes were fitted to a probability density function using the method of maximum likelihood with a correction for missed events. Single channel data were analyzed with maximum likelihood estimation of rate constants. [145-147]

2.6.4 Statistics

A minimum of 4-5 experiments will be performed for each experimental groups. Mean open probability will be calculated by clustering the conductance of a channel, not by the threshold method. Values are given as means ± S.E.M. The open probabilities of different conditions were compared by Student's t tests for paired and unpaired data, where appropriate. Results were considered significant when $p<0.05$.

2.7 EPR MEASUREMENTS

ESR measurements were performed on a Bruker ECS106 spectrometer with a 50 kHz magnetic field modulation, at room temperature. EPR spectrometer settings were: modulation amplitude 0.7 G, scan time 40 s, time constant 0.64 s, microwave power 20 mW and receiver gain 1 x 10^5. ESR measurements (Supporting Information) were performed on a Bruker ECS106 spectrometer with 50 kHz magnetic field modulation at room temperature (25^o C). All experiments were carried out in phosphate buffer (0.1 M; pH 7.4). For spin trapping of $NO^{\cdot}$, ferrous ammonium sulphate and L-cysteine were used. S-centered radicals were spin trapped with DMPO. ESR spectra simulations were made using a program created by Philip D. Morse II and Richard Reiter (EPR Simulation System 2.01, Scientific Software Services, IL). The hyperfine splitting

constants (in G) used for simulation of the spectrum of DMPO/L-cysteine thiyl radical were as follows: $A_N = 15.3$; $A_H = 17.2$.

2.8 MEASUREMENT OF CREATINE KINASE ACTIVITY

The activity of Creatine kinase was measure in the presence of various concentration of Cys-SNO in the medium containing 100 mM KCl, 5 mM $MgCl_2$, 20 mM HEPES-Tris, 10 mM phosphocreatine, 1 mM ADP, 1 mM NAD^+, 20 mM glucose, 2 U/ml hexokinase (Sigma), 2 U/ml glucose-6-phosphate dehydrogenase, pH 7.0 at 37^{o}C. [22] The forward reaction of creatine kinase to form ATP from ADP was measured by NADH formation monitored by differential absorption measured at 310-340 nm using a time-sharing dual-wavelength spectrophotometer (SDB-3A, University of Pennsylvania, Biomedical Instrumentation, Philadelphia, PA). All measurements were performed in a temperature-controlled cuvette under continuous stirring.

2.9 MATERIALS

Cys-SNO was freshly prepared right before each experiment. Cys-SNO was synthesized and provided by Dr. Stoyanovsky. [148] Other chemicals were obtained from Sigma Chemical Co. (St. Louis, MO) or as described.

Making the NO Saturated Solution The solution saturated with NO· gas was prepared by deoxygenating the medium with N_2 gas for 20 min. and then gassing with authentic $NO^\bullet$ gas that was passed through a KOH-containing column and then bubbled into the solution containing 4 mM NaOH. $NO^\bullet$ was produced by dropping strong sulfuric acid (6M H_2SO_4) to sodium nitrite ($NaNO_2$) ($2NaNO_2 + 2FeSO_4 + 3H_2SO_4 \rightarrow Fe(SO_4)_2 + 2NaHSO_4 + 2H_2O + NO^\bullet$) as described. [149]

Measurement of $NO^{\bullet}$ Concentration in $NO^{\bullet}$ Saturated Solution The actual $NO^{\bullet}$ concentration in $NO^{\bullet}$ saturated solutions was measured for each batch of stock solution using Ellman's reagent describe in [150] although it was known that the average NO· concentration in the solution produced by this method is about 1.9 mM. Briefly, 5-thio-2-nitrobenzoic acid (TNB) quantified by its absorbance at 412 nm was used to measure the $NO^{\bullet}$ concentration. Oxidation of the SH group on TNB by NO· resulted in decrease in absorbance at 412 nm, and $NO^{\bullet}$ concentration in stock solution was calculated from the difference in absorbance before and after addition of $NO^{\bullet}$ to TNB solution.

3.0 CHEMICAL REACTION OF S-NITROSOTHIOLS THAT ACTIVATE RYRS

3.1 CYS-SNO NITROSYLATES REGULATORY THIOLS ON RYR

Figure 16 depicts the 2 possible chemical interactions of S-nitrosocysteine with hyperreactive thiols on RyR. Scheme (1) direct transnitrosation where NO^+ is transferred from the thiol on the cysteine to the thiol on RyR. Scheme (2): S-nitrosocysteine first releases $NO^\bullet$ then $NO^\bullet$ oxidizes RyRs.

3.2 EFFECT OF COPPER (I) AND Ca^{2+} CHELATOR ON THE DECOMPOSITION OF CYS-SNO

The biological activity of S-nitrosothiols has led to the assumption that these compounds are unstable under physiological conditions; decompose to liberate the free radical $NO^\bullet$ that modifies physiological functions. Several reports showed that S-nitrosothiols are stable, and require catalytic concentrations of copper to promote the decomposition and liberation of $NO^\bullet$. [125, 127, 128] To investigate the effect of copper on the decomposition of cys-SNO, the visible absorption spectrum of cys-SNO was measured in the absence or presence of copper (I) chelators (bathocuproine disulfonic acid or neocuproine), the non-selective iron chelator, desferal, or Ca^{2+} chelators (AP III or EGTA). Cys-SNO was freshly prepared and placed in the medium used for measurement of Ca^{2+} transport at final concentration of 200 μM. The S-N bond of cys-SNO has absorption at 334 nm. As shown in figure 17A, the absorption

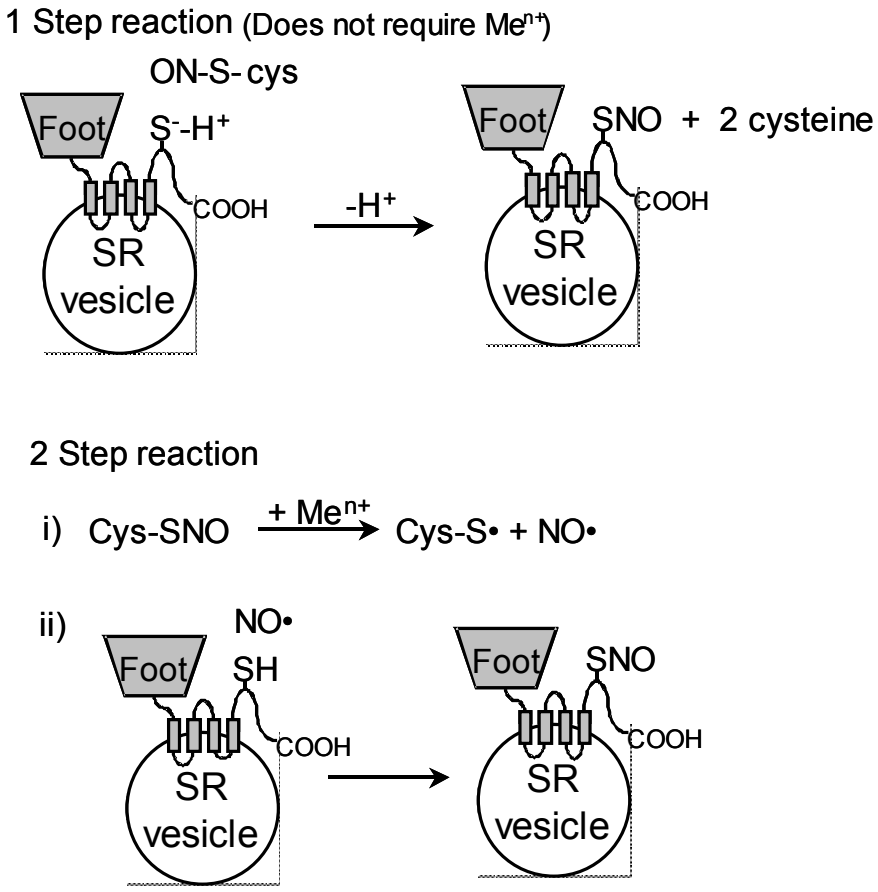

Figure 16.Interactions of cys-SNO with thiols on RyR.
Cys-SNO can nitrosylate free thiols on RyR via two possible reactions. The first one shows the 1 step reaction which is direct transnitrosation where NO^+ is transferred directly from thiol group of cysteine to the thiol on RyR. It doesn't require metal catalysis. The second scheme shows 2 step reaction. Cys-SNO undergoes homolytic fragmentation into cys-S • and NO• and NO• nitrosylate thiols on RyR.

decreased in a time-dependent manner as cys-SNO decomposes with the stoichiometric liberation of $NO^{\bullet}$. After ~ 60 min, the decrease in peak absorption was completed indicating the termination of cys-SNO decomposition.

In the presence of copper (I) chelators to eliminate copper contamination from the medium, the decomposition of cys-SNO was abolished and the peak absorption of cys-SNO remained stable for > 60 min with bathocuproine disulfonic acid (20-100 μM) (figure 17B) and neocuproine (20-50 μM)(data not shown). The iron chelator, desferal (20-100 μM) (data not shown) arrested the breakdown of cys-SNO. Surprisingly, the decomposition of cys-SNO was also arrested in the presence of EGTA (1 mM) and AP III (100-200 μM), Ca^{2+} chelators (Figure 17C). EGTA has been very widely used in planar lipid bilayer experiments in order to control the free Ca^{2+} concentration in the solution and AP III is used as Ca^{2+} indicator. The decomposition of other S-nitrosothiols was also blocked in the presence of theses copper (I) chelators and Ca^{2+} chelators. This showed that there was no $NO^{\bullet}$ liberation from S-nitrosothiols in the single channel experiments done with a solution containing EGTA.

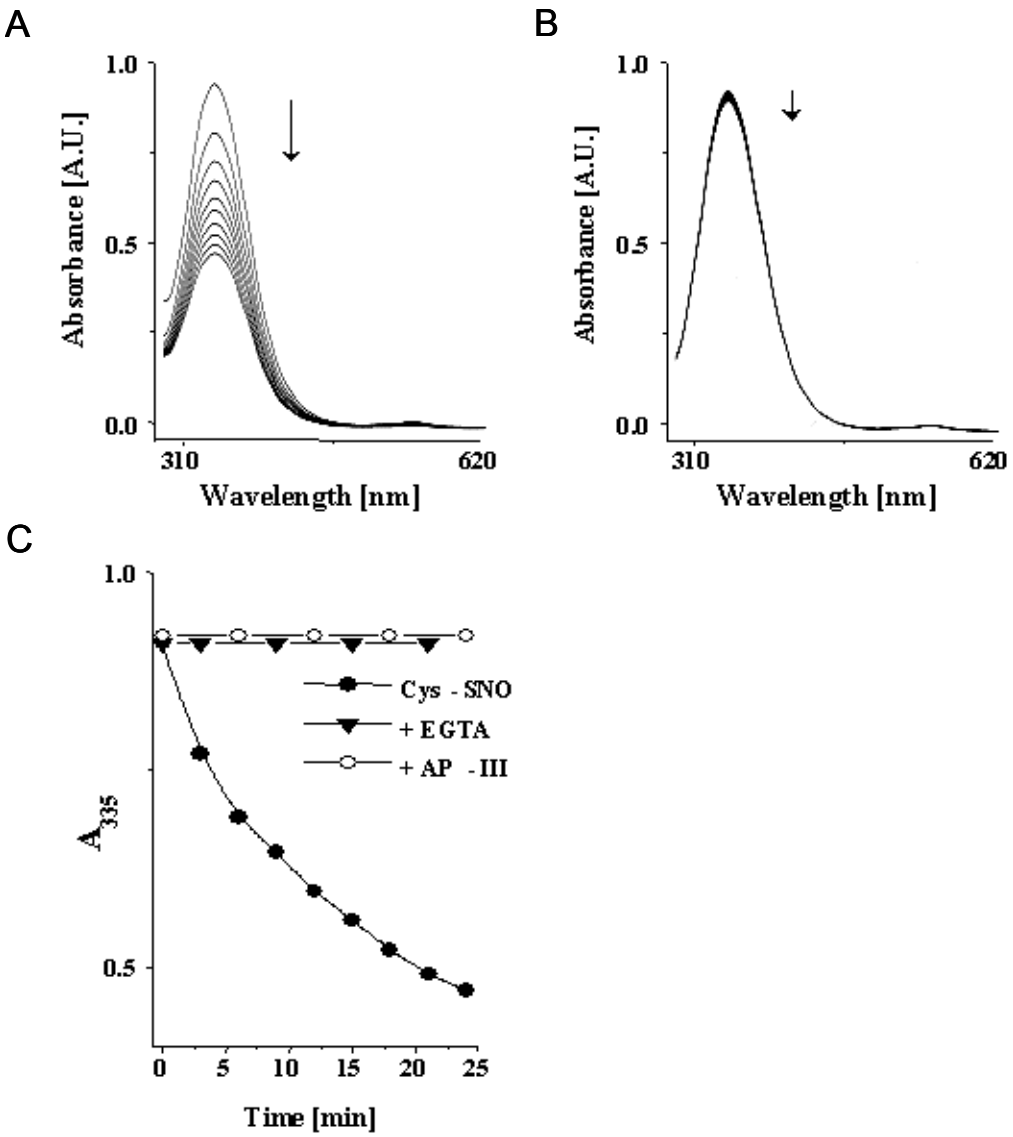

Figure 17. Absorption spectra of cys-SNO in the presence and absence of BCS and EGTA. Cys-SNO (200 μM) was added to a solution containing: 100mM KCl, 1mM $MgCl_2$, 20mM HEPES, at pH 7.0, 37°C. Absorption spectra were recorded with freshly prepared cys-SNO at the following time intervals: 0, 5, 10, 15, 20, 25 min. The peak absorption at 334 nm decreased with the aerobic decomposition of cys-SNO as indicated with arrow. A)Control; B)As in A, plus 100 μM BCS; C)The decomposition of cys-SNO was arrested by the presence of AP III and EGTA.

3.3 S-NITROSOTHIOLS ELICIT RAPID Ca^{2+} RELEASE FROM SR WITHOUT $NO^{\bullet}$ LIBERATION

The oxidation of hyper-reactive (low pK_a) thiols on RyRs of skeletal SR vesicles elicits the very rapid release of Ca^{2+} and the subsequent addition of sulfhydryl reducing agents reversed the oxidation resulting in active Ca^{2+} re-uptake via Ca^{2+} pumps. Figure 18A illustrates the assay of cys-SNO-induced Ca^{2+} release from skeletal SR vesicles (300 μg protein/ml). The Ca^{2+} transport across SR vesicle membrane was measured using Antipyrylazo III (AP III) as an ionized Ca^{2+} indicating dye in the reaction medium. AP III was found to block the decomposition of S-nitrosothiols to liberate $NO^{\bullet}$ (figure 17C). Therefore, there was no S-nitrosothiol-dependent generation of $NO^{\bullet}$ in these Ca^{2+} transport experiments unless $NO^{\bullet}$ was added directly to the reaction medium. As shown in figure 18A, two aliquots of Ca^{2+} (12 μM) were added to the reaction medium, then ATP (100μM) supplied energy for SR vesicles to actively load SR vesicles with Ca^{2+} via the Ca^{2+}-ATPase in the presence of the ATP-regenerating system with phosphocreatine and creatine kinase. Once Ca^{2+} uptake was completed, cys-SNO (5 μM) was added to elicit Ca^{2+} release. When the release of Ca^{2+} from SR vesicles reached plateau, an addition of a sulfhydryl reducing agent, DTT or GSH, caused a re-uptake of Ca^{2+} that most likely reflected the reduction of oxidized thiols on RyR. A subsequent addition of the ionophore A 23187 fully released the intravesicular calcium. Cys-SNO-induced Ca^{2+} release was measured in the presence of 100 μM of myoglobin, a heme iron protein that acts as a $NO^{\bullet}$ scavenger (figure 18B) to arrest any existing $NO^{\bullet}$ in the solution. Neither of the abolition of $NO^{\bullet}$

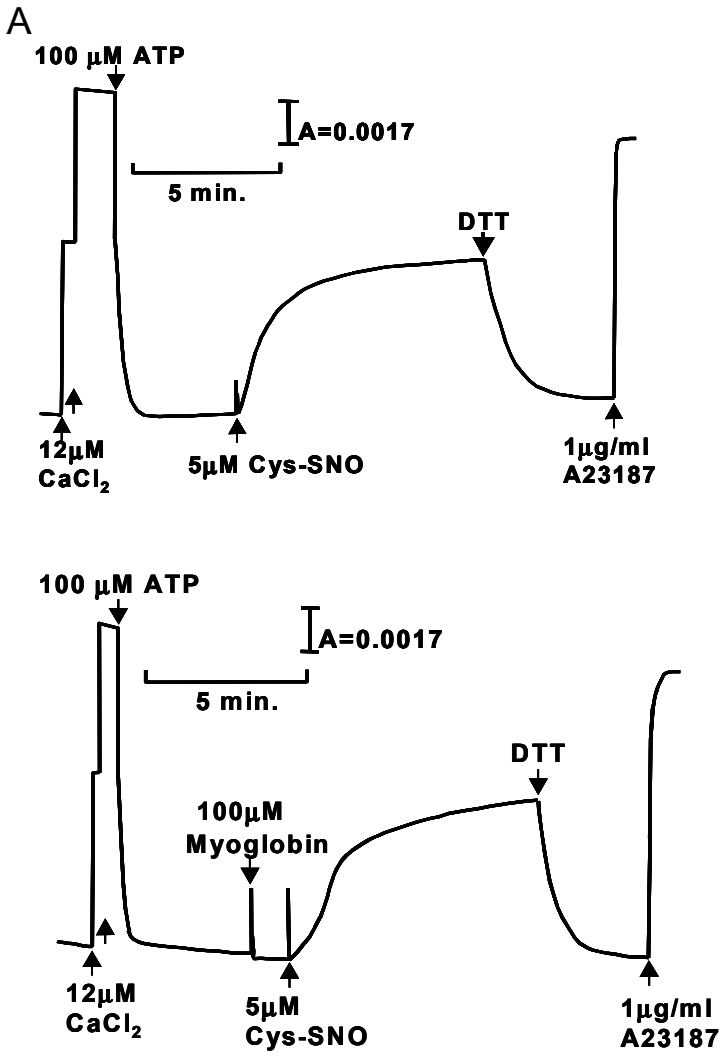

Figure 18. Cys-SNO induces Ca^{2+} release from skeletal SR.

Cys-SNO induces Ca^{2+} release from skeletal SR when the release of NO from it is blocked and NO scavenger is added to the reaction buffer to scavenge any possible NO released from it.

Skeletal SR vesicles (0.3 mg protein) were added to a cuvette containing a reaction mixture, two aliquots of Ca^{2+} (12 µM) were added to calibrate the signal and then ATP (100 µM) to initiate uptake. After the vesicles were actively loaded with Ca^{2+} using an ATP-regenerating system, cys-SNO was added to the reaction mixture to elicit Ca^{2+} release. After release was completed, DTT (1 mM) was added to reverse the effects of cys-SNO. Upon completion of the Ca^{2+} uptake, the Ca^{2+} ionophore A 23187 was added to the reaction mixture to determine the amount of intravesicular Ca^{2+}. A) 5 µM cys-SNO; B) Same as (A) plus 100 µM Myoglobin. Low concentration (5 µM) Cys-SNO caused very rapid Ca^{2+} release from SR vesicles even in the presence of APIII and myoglobin, which support our hypothesis that the $NO^{\bullet}$ released from cys-SNO is not a predominant pathway to induce Ca^{2+} release from SR vesicles.

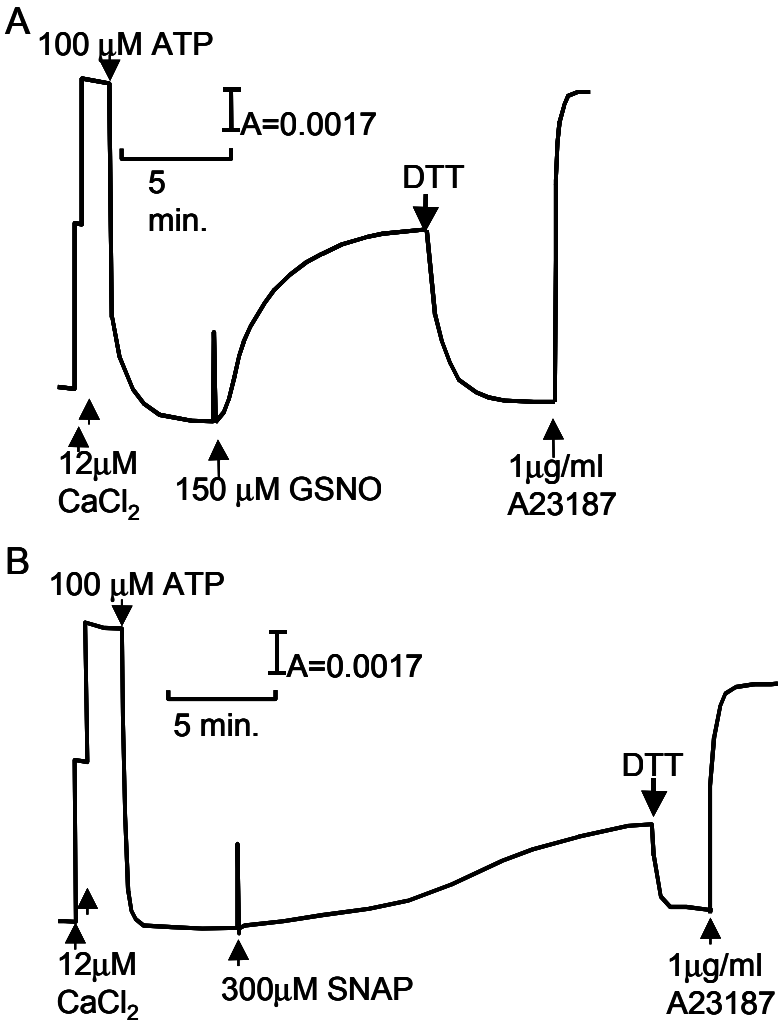

Figure 19 . GSNO and SNAP induce Ca^{2+} release from skeletal SR without $NO^{\bullet}$ generation. Skeletal SR vesicles (0.3 mg protein) were added to a cuvette containing a reaction mixture, two aliquots of Ca^{2+} (12 µM) were added to calibrate the signal and then ATP (100 µM) to initiate uptake. After the vesicles were actively loaded with Ca^{2+} using an ATP-regenerating system, GSNO or SNAP was added to the reaction mixture to elicit Ca^{2+} release. After release was completed, DTT (1 mM) was added to reverse the effects of cys-SNO. Upon completion of the Ca^{2+} uptake, the Ca^{2+} ionophore A 23187 was added to the reaction mixture to determine the amount of intravesicular Ca^{2+}. A)150 µM GSNO; B) 300 µM SNAP. Both of GSNO and SNAP induce Ca^{2+} release from skeletal SR when the release of $NO^{\bullet}$ from them was abolished by AP III.

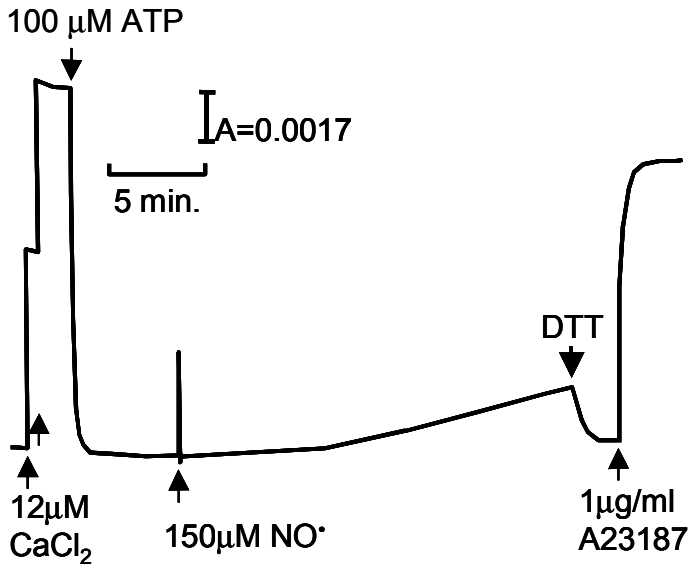

Figure 20. Authentic NO• requires high concentration to induce Ca^{2+} release from SR vesicles.

Skeletal SR vesicles (0.3 mg protein) were added to a cuvette containing a reaction mixture, two aliquots of Ca^{2+} (12 μM) were added to calibrate the signal and then ATP (100 μM) to initiate uptake. After the vesicles were actively loaded with Ca^{2+} using an ATP-regenerating system, authentic NO• was added to the reaction mixture to elicit Ca^{2+} release. After release was completed, DTT (1 mM) was added to reverse the effects of NO•. Authentic NO• was not a potent RyR activator and a high concentration of over 100 μM was required to initiate Ca^{2+} release from SR vesicles.

release from S-nitrosothiols nor the use of a $NO^{\bullet}$ scavenger, myoglobin, stopped S- nitrosothiols from inducing rapid Ca^{2+} release from SR vesicles, indicating that $NO^{\bullet}$ released from these NO donors is not a predominant pathway to activate RyR to cause Ca^{2+} release from SR vesicles. Similar results were obtained with GSNO and SNAP (figure 19).

As shown in figure 20, authentic $NO^{\bullet}$ elicits Ca^{2+} release from SR vesicles, but only at high concentrations. For these experiments, the stock solution saturated $NO^{\bullet}$ gas was prepared freshly each time as described in the method part and the actual concentration of the stock solution was measured using Ellman's reagent each time to insure a correct measurement of [$NO^{\bullet}$] [150]. The concentration of $NO^{\bullet}$ in the stock solution was in the range of 1.4-1.6 mM and the exact amount of stock solution to obtain the final concentration was calculated and added to the reaction buffer using a Hamilton syringe. There was a report that low pO_2 (~10 mmHg) is crucial to observe an activation of RyR by authentic $NO^{\bullet}$ via a nitrosylation of thiol groups on RyR. Therefore, we carried out Ca^{2+} transport across SR vesicles under controlled pO_2. However, $NO^{\bullet}$ did not induce rapid Ca^{2+} from SR vesicles under deoxygenated conditions (<2 mmHg) or low pO_2 (5-10 mmHg). Figure 20 shows a representative trace measured under the ambient oxygen level to keep the same condition for all NO donors used in figure 18-20. The fact that low molecular weight S-nitrosothiols such as cys-SNO and GSNO were more potent than authentic $NO^{\bullet}$ suggested that these NO donors activate RyR by some mechanism other than $NO^{\bullet}$ production from the donor compound.

3.4 POTENCY OF VARIOUS NO DONORS

The concentration dependencies of SR Ca^{2+} release rates induced by authentic $NO^{\bullet}$ and three S-nitrosothiols including cys-SNO, GSNO and SNAP are shown in figure 21. Cys-SNO was

considerably more potent than the other S-nitrosothiols and $NO^{\bullet}$. Only 1-2 μM cys-SNO were required to elicit Ca^{2+} release from skeletal SR vesicles. The release rate reached 83% relative of maximum with only 10 μM cys-SNO. Almost all the releasable Ca^{2+} from the vesicles was released with 50 μM of cys-SNO (data not shown). Another distinguishable aspect of cys-SNO induced SR Ca^{2+} release was that the rapid onset of Ca^{2+} release which was initiated within seconds after cys-SNO addition to the reaction medium. SR Ca^{2+} release induced by all NO donors used in this study were completely reversed by adding a sulfhydryl reducing agent, GSH or DTT. It has been reported that low pO_2 increased the potency of $NO^{\bullet}$. [83, 86] On the other hand, Stoyanovsky et al reported that the oxygenated and the deoxygenated solution didn't make the dramatic change in the potency of $NO^{\bullet}$ although $NO^{\bullet}$ was slightly more potent in deoxygenated solution and it remained too high to be of biological significance [15]. This project re-examined the effect of oxygen level on the potency of authentic $NO^{\bullet}$ gas and obtained similar results as reported by Stoyanovsky et al., that there was no dramatic increase in $NO^{\bullet}$'s potency to activate RyRs.

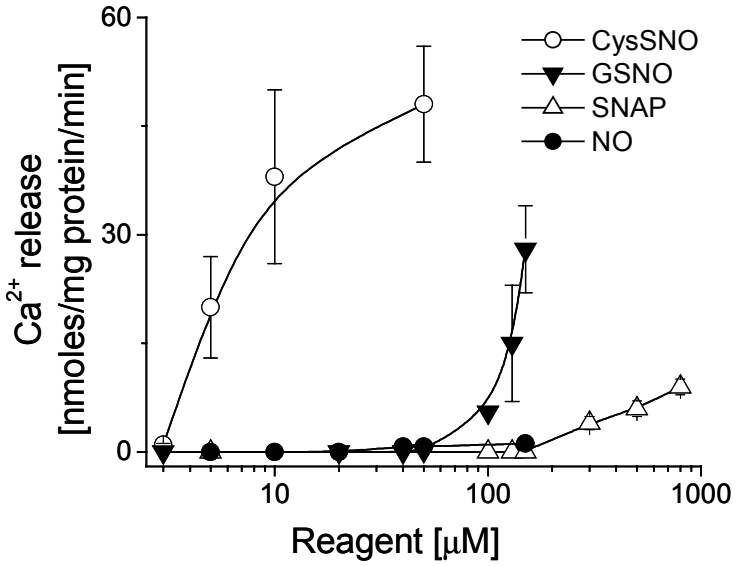

Figure 21. Rate of Ca^{2+} release as function of NO donor concentration.
The y-axis shows SR Ca^{2+} release rates (nmol Ca^{2+}/mg protein/min) induced by different NO donors, Cys-SNO, NO gas, GSNO and SNAP and x-axis is the concentration of the NO donors in log scale. Cys-SNO and GSNO were very potent compared to authentic $NO^{\cdot}$ and especially cys-SNO was uncompetitively potent compared to the other NO donors used in this study.

3.5 EFFECT OF CYS-SNO ON SINGLE CHANNEL ACTIVITY

The RyR1 proteins were purified from heavy SR vesicles solubilized by CHAPS and then separated on linear sucrose gradient. The RyR1 channel reconstituted in the planar lipid bilayer was tested for its response to Ca^{2+} concentration to confirm the functioning channel. The conductance of purified RyR1 channel was 781 ± 26 pS in a symmetric potassium buffer (250 mM KCl, 20 mM HEPES-Tris, pH 7.4). The single channel activities of purified RyR1s were recorded in the presence and absence of EGTA in the solution. Figure 22A represents one of 4 similar experiments done in the presence of 1 mM EGTA in the solution and figure 22B shows one of 4 experiments done in the absence of EGTA in the solution. RyR1 channel was activated by adding cys-SNO to the *cis* chamber in the presence or absence of EGTA in the solution (trace b), which agrees with the results showing that cys-SNO induced rapid Ca^{2+} efflux from SR vesicles even when $NO^{\bullet}$ liberation was blocked. Therefore, the single channel recordings provide the direct evidences to confirm our hypothesis that the release of $NO^{\bullet}$ is not required for S-nitrosothiols to activate RyR1. The effect of cys-SNO was reversed with the following addition of 1mM DTT (trace c), which shows that the activation of RyR1 was by S-nitrosylation of free thiols on RyR1. At the end of each experiment, addition of 5 μM ruthenium red, a RyR channel blocker, to the cis solution inhibited channel activity. Alternatively, an addition of 5 μM ryanodine to the cis solution locked up the channel activity in a subconductance state. The latter test was used to confirm that the channel in the bilayer was a ryanodine receptor (trace d).

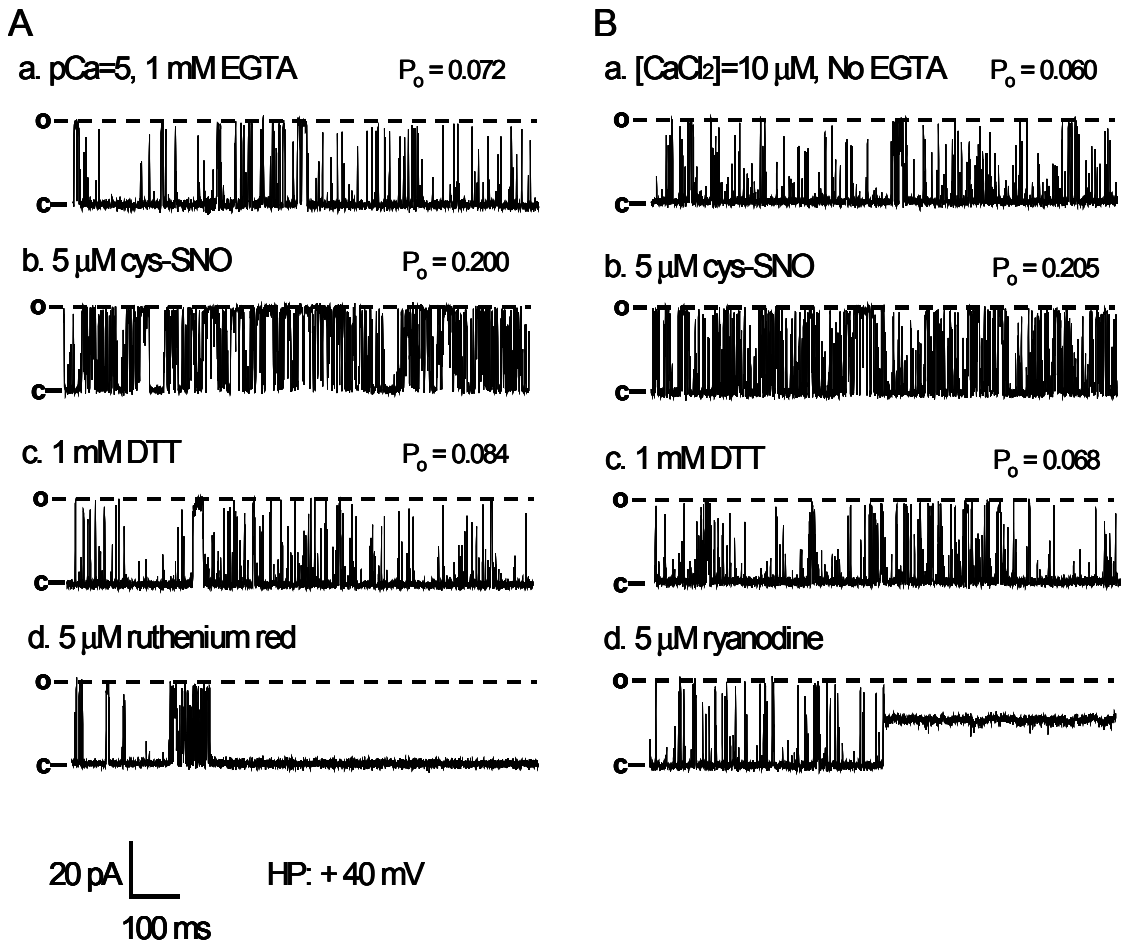

Figure 22. Cys-SNO activates RyR1via trans-nitrosation reaction.
RyR1 channels purified from rabbit skeletal muscle were reconstituted in the planar lipid bilayer. Single channel currents, shown as upward deflections from closed state (indicated as c) to open state (indicated as o), were recorded at +40mV holding potential with symmetric solutions: 250 mM KCl, 20 mM Tris-HEPES, pH 7.4 buffer in cis and trans chambers. Experimental conditions are a: control channel activity (at pCa=5 in figure A or at [$CaCl_2$]=10 µM in figure B) before adding cys-SNO, b: 5 µM cys-SNO in the cis solution, c: 1 mM DTT in the cis solution, d: addition of Ryanodine or ruthenium red confirms the RyR1 channels.
(A) represents one of 4 similar experiments done in the presence of 1 mM EGTA in the solution
(B) represents one of 4 similar experiments done in the absence of EGTA in the solution.
There was no difference in activation of RyR1 single channel induced by addition of cys-SNO to cytosolic side of the channel (*cis* chamber) in the presence and in the absence of EGTA in the solution.

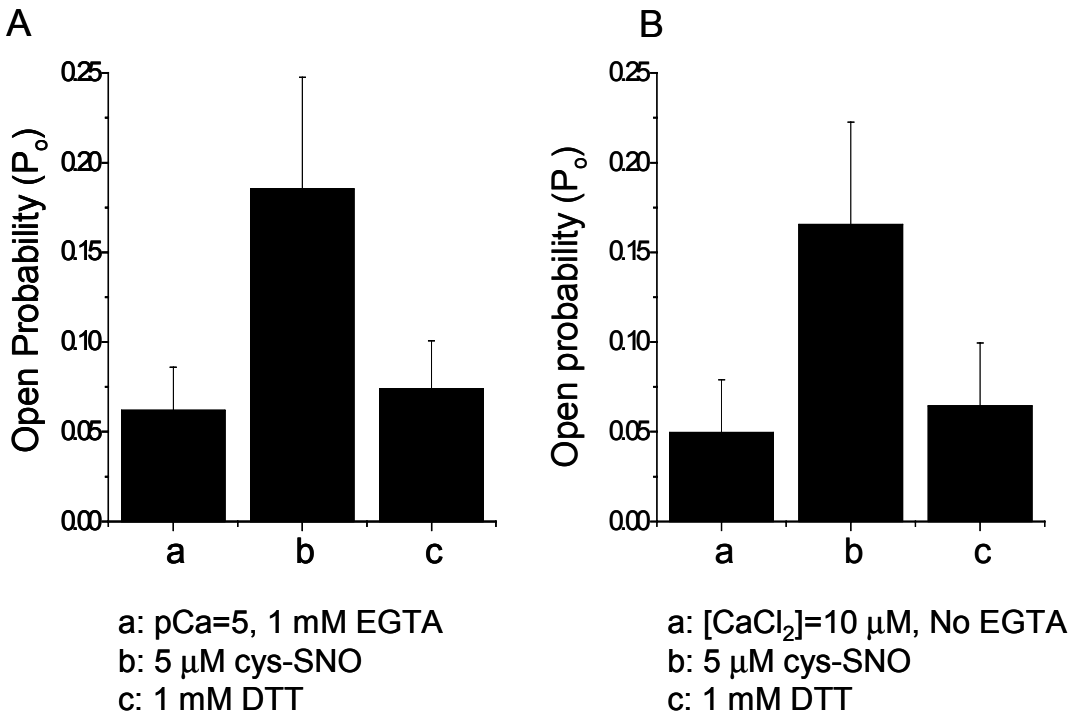

Figure 23. Open probability (P_o) calculated from single channel recording of purified RyR1.

The mean open probability of RyR1 channels purified from rabbit skeletal muscle were calculated from 4 similar experiments done in the presence or in the absence of EGTA in the buffer.

(A) The mean P_o was calculated from 4 similar experiments done with 1 mM EGTA in the solution: a: P_o=0.062±0.024, b: P_o=0.185±0.062 c: P_o=0.064±0.027.

(B) The mean P_o was calculated from 4 similar experiments done without EGTA in the solution: a: P_o=0.050±0.029, b: P_o=0.166±0.057, c: P_o=0.065±0.035.

Data are mean ± SEM of the 4 experiments. The P_o for each state was calculated from at least 3 min of continuous recordings.

In figure 23A, the mean values of open probabilities were calculated from 4 similar experiments done in the presence of 1 mM EGTA in the solution. Open probability increased from P_o=0.062±0.024 (a) at control condition to P_o=0.185±0.062 (b) significantly ($p<0.01$) when 5 μM cys- SNO was added to cis solution. Then, an addition of DTT decreased the open probability to P_o =0.064±0.027 (c) ($p<0.01$). In figure 23B, the average values of the open probabilities were calculated from 4 similar experiments, done in the absence of EGTA in the solution: a: P_o=0.050±0.029, b: P_o=0.166 ±0.057, c: P_o=0.065±0.035. The open probabilities of channels recorded with 5 μM cys-SNO in the cytosolic side of the channels were in the similar range with or without EGTA in the solution, which confirms that the activation of RyR1 channel by cys-SNO was not caused by $NO^{\bullet}$ generation.

3.6 EFFECT OF OXYGEN LEVEL ON $NO^{\bullet}$ AND S-NITROSOTHIOLS-INDUCED ACTIVATION OF RYR

It has been reported that low concentration of authentic $NO^{\bullet}$ activates RyR under low pO_2 conditions by reversing the inactivation of RyR induced by a previous addition of calmodulin. [83-86] On the other hand, Stoyanovsky et al reported that oxygenated and deoxygenated solution didn't make dramatic change in the potency of $NO^{\bullet}$ on RyR. [15] The effect of oxygen concentration on the activation of RyR1 by authentic $NO^{\bullet}$ and S-nitrosothiols was investigated in this study.

Ca^{2+} transport across the skeletal SR vesicles was investigated under tightly controlled O_2 concentrations in the reaction medium. We measured the actual O_2 concentration in the solution under ambient O_2 levels and how long it takes for the solution to be completely deoxygenated by

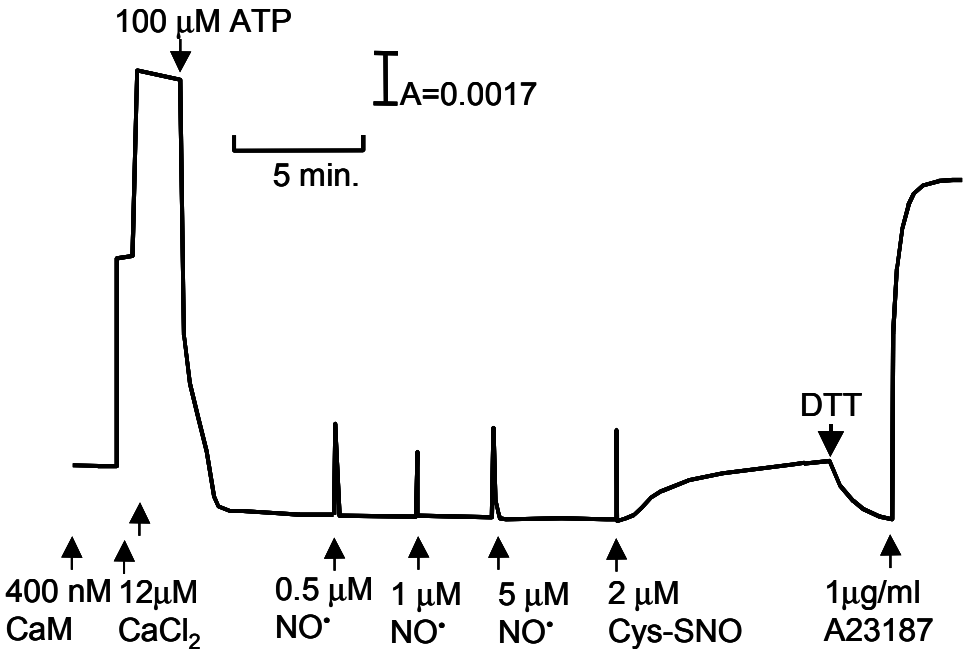

Figure 24. pO_2 level does not alter $NO^{\cdot}$ and cys-SNO induced Ca^{2+} release from SR vesicles.

Low O_2 concentration (10 mmHg O_2) did not affect the uptake of Ca^{2+} by SR vesicle. Addition of 0.5, 1 and 5 μM $NO^{\cdot}$ did not elicit Ca^{2+} release from SR vesicle, but addition of 2 μM of cys-SNO to the same reaction media induced Ca^{2+} release from SR vesicle, which was reversed by addition of DTT.

purging N_2 gas into the solution. The amount of ambient O_2 solutions needed to obtain the desired O_2 concentration was calculated and added to a deoxygenated reaction medium, in a sealed cuvette. Ca^{2+} transport across SR vesicles was measured in the deoxygenated solution and under the 5, 10 and 20 mmHg pO_2. As shown in figure 24, the low O_2 concentration (10 mmHg O_2) or addition of calmodulin (400 nM) did not affect the uptake of Ca^{2+} by SR vesicle. Addition of 0.5, 1 and 5 μM $NO^{\bullet}$ did not elicit Ca^{2+} release from SR vesicle. In contrast, an addition of 2 μM of cys-SNO to the same reaction medium induced Ca^{2+} release from SR vesicle, which was reversed by addition of DTT. No dramatic change in the potency of either of $NO^{\bullet}$ or S-nitrosothiols was observed in the experiments done under the low O_2 concentrations although $NO^{\bullet}$ was a little bit more potent in the deoxygenated solution.

Single channel activity was recorded under the low O_2 concentrations. The buffer was completely deoxygenated by gassing N_2 into the buffer for more than 20 min. RyR1 was purified from rabbit skeletal muscle and deoxygenated by putting the protein suspension under the vacuum for more than 10 min. The actual oxygen level was measured for the all the solutions used for these experiments. Continuous N_2 gas blown into the planar lipid bilayer cage excluded oxygen from the atmosphere in the cage to prevent the solution from being re-oxygenated. We measured the time for the deoxygenated solution to be re-oxygenated. The re-oxygenation of the solution was quite a slow process. We measured the oxygen concentration of the solution approximately 0.5 cm below the surface of the solution.

It took more than 2 min. for the deoxygenated solution to reach 10 mmHg O_2, 4 min. to reach 20 mmHg O_2, and more than 30 min. to equilibrate with air when completely exposed to the air with continuous stirring and without any purged N_2 gas. Therefore, the cage door remained open for less than 2 min with continuous N_2 gas flow to avoid re-oxygenation of the

medium. Nevertheless, the actual O_2 concentration in the solution was measured after each experiment to verify that it was kept between 5 and 10 mmHg pO_2.

Figure 25 illustrates one of 4 similar experiments done under the low O_2 concentration in the solution. After the reconstitution of a RyR channel (a), addition of 400 nM calmodulin (b) to *cis*-chamber (cytosolic side of the channel) decreased the open probability of RyR single channel ($p<0.05$). We could not observe the increase in P_o of RyR1 channel when 0.5 μM of authentic $NO^{\bullet}$ (c) was added into the cytosolic side of RyR1 channel under the low O_2 concentration. Further addition of $NO^{\bullet}$ (5 μM) (d) did not activate the RyR1 channel, but the addition of cys-SNO (5 μM) (e) to the same channel increased the P_o significantly ($p<0.05$), which agrees with the results from Ca^{2+} transport experiments. Figure 26 shows the mean P_o calculated from 4 experiments (a: $P_o=0.060\pm0.010$, b: $P_o=0.039\pm0.009$, c: $P_o=0.040\pm0.013$, d: $P_o=0.041\pm0.017$, e: $P_o=0.139\pm0.056$, f: $P_o=0.061\pm0.013$). It is worthy to notice that the open probabilities of the channel were obtained from continuous recordings of more than 7 min. in each condition.

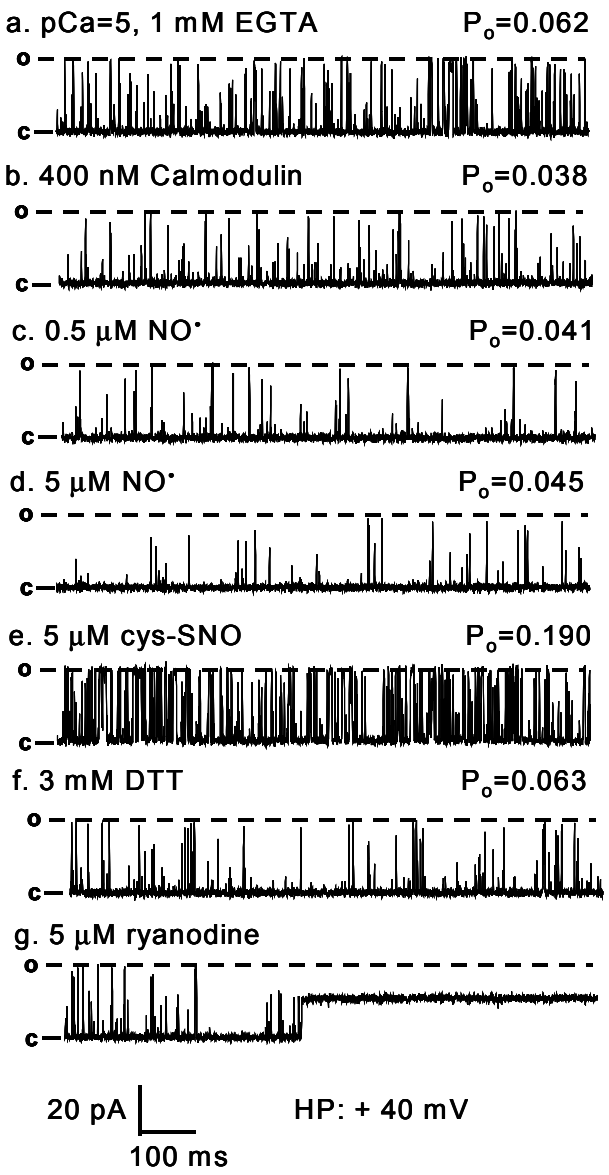

Figure 25. pO_2 does not alter RyR1 single channel activity triggered by NO• or cys-SNO. This is one of 4 similar experiments done under the low O_2 concentration (~10 mmHg) in the solution

a: control at pCa=5, b: 400 nM calmodulin to the *cis*-chamber c: addition of 0.5 μM $NO^{\cdot}$ to the *cis*-chamber, d: 5 μM $NO^{\cdot}$ to the *cis*-chamber, e: 5 μM cys-SNO to the cis-chamber, f: 1 mM DTT g: 5 μM ryanodine. After calibrating free Ca^{2+} concentration in the solution, calmodulin (400 nM) was added to the *cis* solution resulting in the reduced activity of RyR1 channel. The following addition of $NO^{\cdot}$ up to 5 μM into the *cis* solution didn't activate the purified RyR1 channel, but the following addition of 5 μM cys-SNO to the *cis*-side of the very same channel activated the RyR1 channel. The following addition of 3 mM DTT reversed the activation of channel and addition of 5 μM ryanodine to the *cis*-side at the end of each experiment confirmed that these channels were RyR.

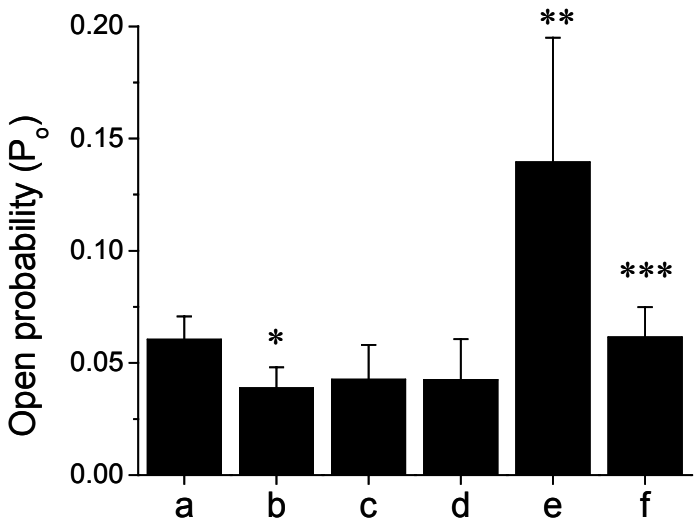

Figure 26. Open probability of purified RyR1 channel.
Open probability of purified RyR1 channel (P_o=mean±SEM) calculated from 4 experiments
a: control at pCa=5, b: 400 nM calmodulin to the *cis*-chamber c: addition of 0.5 µM $NO^{\cdot}$ to the *cis*-chamber, d: 5 µM $NO^{\cdot}$ to the *cis*-chamber, e: 5 µM cys-SNO to the cis-chamber, f: 1 mM DTT g: 5 µM ryanodine. P_o (mean±SEM) calculated from 5 experiments (a: P_o=0.060±0.010, b: P_o=0.039±0.009, c: P_o=0.040±0.013, d: P_o=0.041±0.017, e: P_o=0.139±0.056, f: P_o=0.061±0.013) Addition of calmodulin decrease the open probability of RyR1 channel (*:$p<0.05$). Addition of $NO^{\cdot}$ up to 5 µM into the *cis* solution didn't increase P_o of the purified RyR1 channel, but the following addition of 5 µM cys-SNO to the *cis*-side of the very same channel activated the RyR1 channel (**:$p<0.01$). The following addition of 3 mM DTT reversed the activation of channel resulting in the decrease of P_o (***:$p<0.05$).

When SR Ca^{2+} transport and the single channel activity were recorded without calmodulin in the solution under the low O_2 concentration, similar results were observed. We could not observe Ca^{2+} release from SR vesicles or an increase in P_o of RyR1 channel when 0.75 μM of authentic $NO^{\bullet}$ was added into the cytosolic side of RyR1 channel under low O_2 concentration. Further additions of $NO^{\bullet}$ (5 μM) still did not activate RyR1 channels, but an addition of cys-SNO (5 μM) to the same channel increased the P_o significantly ($p<0.01$), which agrees with the results from Ca^{2+} transport experiments.

The mean P_o calculated from 5 experiments are as follows: control: $P_o=0.052\pm0.019$, 0.75 μM $NO^{\bullet}$: $P_o=0.058\pm0.022$, 5 μM $NO^{\bullet}$: $P_o=0.067\pm0.06$ and 5 μM cys-SNO: $P_o=0.163\pm0.050$. When the single channel activity was recorded without EGTA in the solution under low O_2 concentrations, similar results were observed (data not shown). Therefore, we concluded that oxygen concentration affects neither the Ca^{2+} release from skeletal SR vesicles nor activation of RyR1 single channel induced by either of S-nitrosothiols or $NO^{\bullet}$ with or without calmodulin.

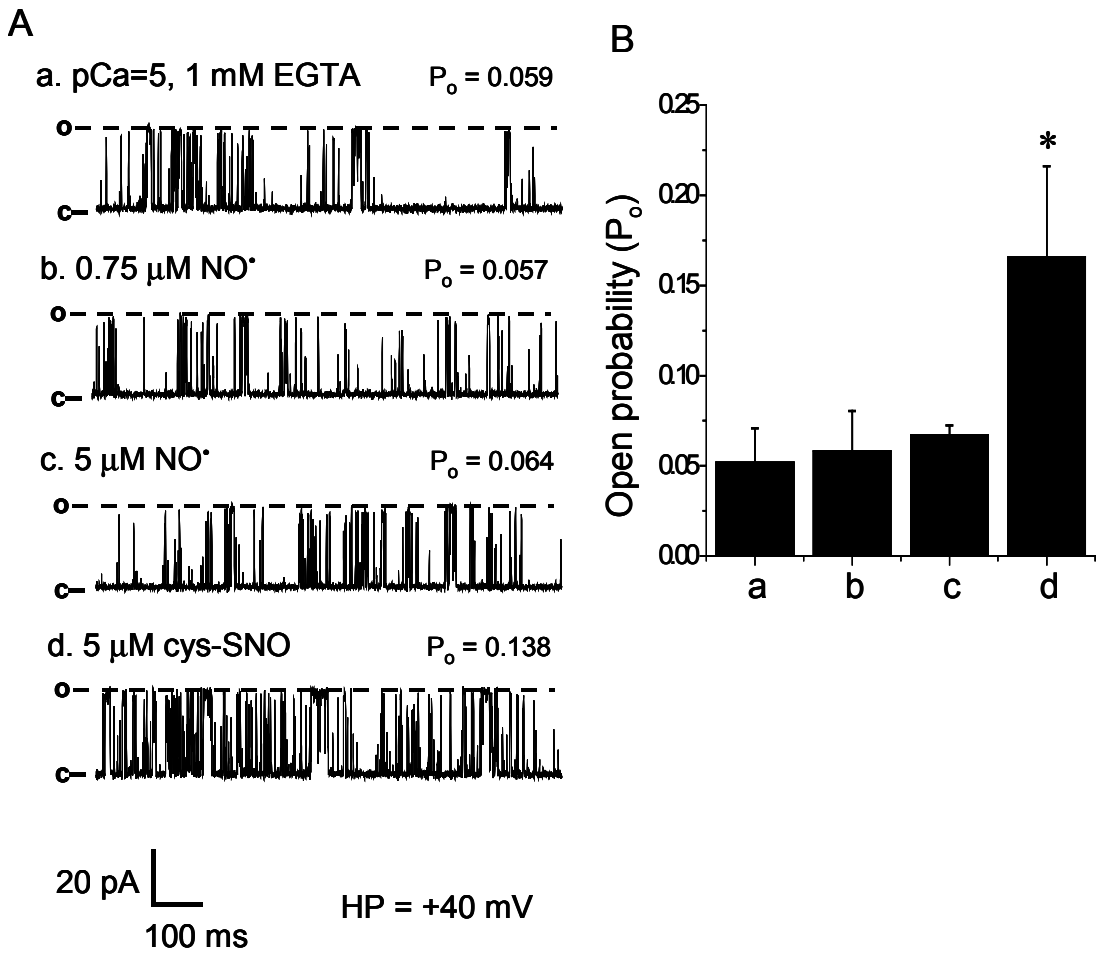

Figure 27. pO_2 does not alter activation of RyR1 channel induced by NO• and cys-SNO in the absence of calmodulin.

(A) One of 5 similar experiments done under the low pO_2 (~10 mmHg) Addition of NO• up to 5 μM into the *cis* solution (trace b and c) didn't activate the purified RyR1 channel, but the following addition of 5 μM cys-SNO to the *cis*-side of the very same channel activated the RyR1 channel (trace d).

(B) a: control at pCa=5, b: addition of 0.75 μM NO• to the *cis*-chamber, c: 5 μM NO• to the *cis*-chamber, d: 5 μM cys-SNO to the cis-chamber. P_o (mean±SEM) calculated from 5 experiments (a: P_o= 0.052±0.019, b: P_o= 0.058±0.022, c: P_o= 0.067±0.06 and d: P_o= 0.166±0.050). The addition of 5 μM cys-SNO to the *cis*-side increased P_o significantly (*:$p<0.01$)

3.7 GATING OF RYR

The measurement of open probability of the single channel is most commonly used tool to measure channel activity. It gives an overall picture about how long the channel stays in either the closed or open state, but doesn't provide detailed information regarding the possible states of the channel or its gating mechanisms.

Figure 28 shows the distribution of open and closed dwell times (lifetimes) of one RyR channel that was monitored in figure 22A, with 1mM EGTA in the solution. Under the control condition (pCa=5 with 1 mM EGTA), the RyR channel exhibits generally long closed dwell times and most of the open lifetimes were relatively short. After the channel became activated by cys-SNO, longer open dwell times that didn't exist under control conditions emerged and the overall open dwell times became longer. On the other hand, there was no dramatic change observed in the closed dwell time distribution before and after the addition of cys-SNO. After the effect of cys-SNO was reversed by the addition of DTT, the distribution of open and closed dwell times reversed to those under the control condition. This analysis gives us the general information about the change in the gating of RyR channel when it was activated by cys-SNO. This showed that the lifetime of open states of RyR got increased together with the increase of overall open probability. The mean open times and closed times in control were 0.874 ± 0.375 (ms) and 15.038 ± 9.624 (ms), respectively, and after the addition of cys-SNO, they were 8.252 ± 4.914 (ms) and 17.050 ± 10.891 (ms).

There are several ways to increase open probability of ion channels, increase dwell time in open state (decrease transition probability from open to closed state) and decrease the dwell time of closed state (increase transition probability from close to open state). In addition, if an

ion channel has several open and closed states, the transition probability of each state can be appropriately modified to increase the overall open probability.

To investigate how cys-SNO increased open probability, we applied Hidden Markov model analysis algorithm developed by Sachs' group in State University of New York at Buffalo (see method section). Figure 29 and 30 shows the distributions of open and closed interval durations using a log scale fitted with maximum likelihood method and the rate constants for the given model. The 30 sec-recordings which represent each condition were analyzed. Lifetime analysis demonstrated that at least two significant exponential components were required to fit the closed lifetime distributions with time constants of 1.285 ms and 24.853 ms and one component of with a time constant of 0.792 ms was required to fit the open lifetime distributions under the control condition (pCa=5). (Figure 29A) A number of Markovian kinetic models were examined. The model shown in figure 29B with two closed and one open component had the highest likelihood value (Figure 29C) among the candidate models. After the same channel was activated by the addition of cys-SNO to the cytosolic side of the channel, two significant components of the closed lifetime distribution with time constants of 0.872 ms and 62.344 ms and two component of the open lifetime distributions with time constant of 0.736 ms and 27.458 ms were detected (Figure 30A). The model shown in figure 30B had the highest likelihood value (figure 30C) among the candidate models with two closed components and two open components.

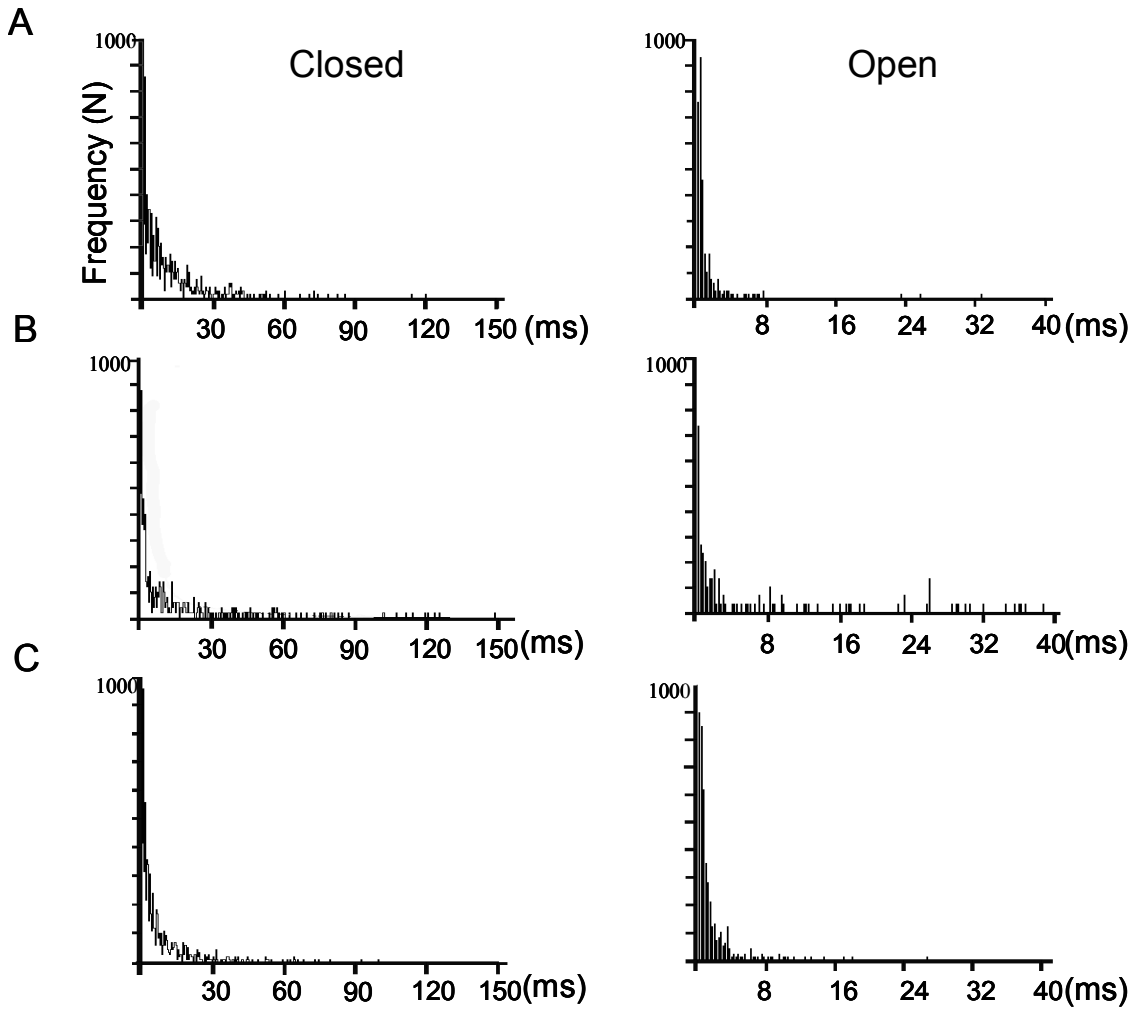

Figure 28. Open and closed dwell times of a RyR channel.
This is open and closed dwell time histograms obtained from the RyR channel shown in figure 21 recorded with 1mM EGTA in the solution.
A)Closed and open dwell times of RyR channel at pCa=5
B)Closed and open dwell times of RyR channel activated by 5 μM cys-SNO in cis side of the channel, which shows that overall open dwell times increased.
C)Addition of DTT (1 mM) reversed the effect of cys-SNO.

A

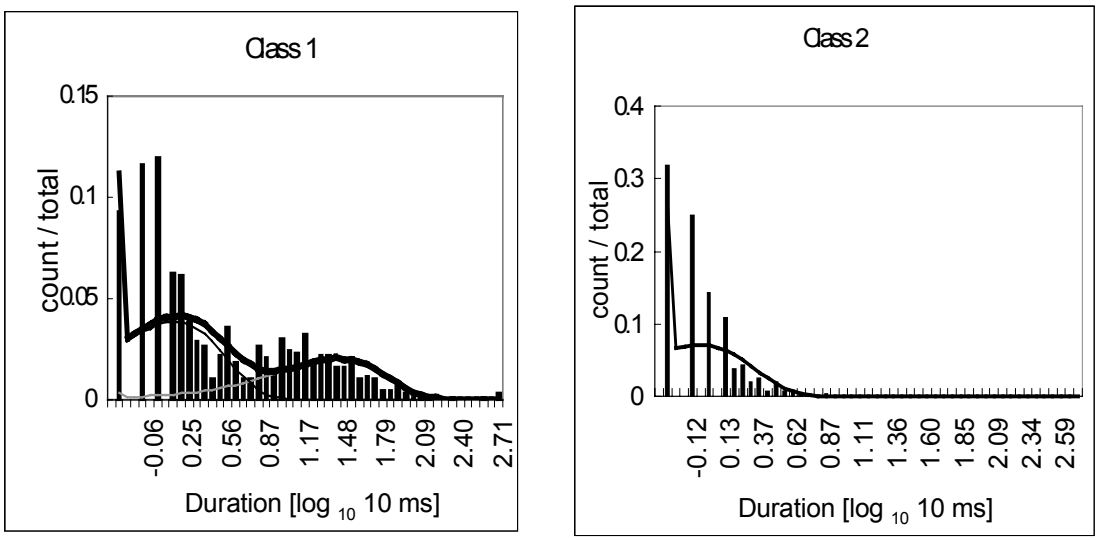

Time Constants (Tau, Amp):
(1.284758, 0.610067) (24.852614, 0.389933)

Time constant (Tau, Amp):
(0.792448, 1.000000)

B. Rate Constants for given Markov model calculated from Maximum-likelihood

$$C1 \underset{235.65}{\overset{59.87}{\rightleftharpoons}} C2 \underset{1518.8}{\overset{764.7}{\rightleftharpoons}} O1$$

C. Log likelihood score :6933.9

Figure 29. Markov Model for the purified RyR1 channel at pCa = 5.

A. The open and closed lifetime distributions were fitted using the maximum likelihood method. The two components of closed lifetime distribution and one component of the open lifetime distribution were detected. The time constants of the closed lifetime distributions are 1.285 ms and 24.853 ms and that of the open lifetime distributions is 0.792 ms.

B. A number of Markov kinetic model were examined and the likelihood values of them were compared to pick up the model with the highest score.The model shown in panel B has the highest likelihood score. The rate constants (s^{-1}) for the given Markov model based on the open and closed lifetime distribution data were calculated using maximum likelihood method.

C. The log likelihood score for the given model was shown.

A

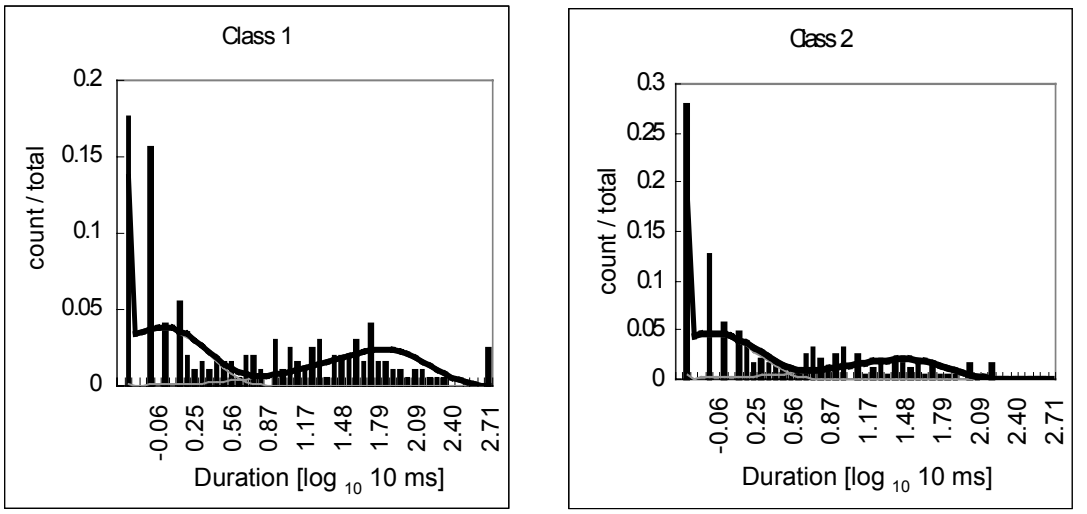

Time Constants (Tau, Amp):
(0.871712, 0.539492) (62.344198, 0.460508)

Time Constants (Tau, Amp):
(0.736206, 0.616059) (27.457553, 0.383941)

B. Rate Constants for given Markov model calculated from Maximum-likelihood

$$C1 \underset{430.66}{\overset{26.05}{\rightleftharpoons}} C2 \underset{1187.92}{\overset{936.1}{\rightleftharpoons}} O1 \underset{51.97}{\overset{390.93}{\rightleftharpoons}} O2$$

C. Log likelihood score :4498.7

Figure 30. Markov Model for purified RyR1 channels activated by cys-SNO.

A. The open and closed lifetime distributions were fitted using the maximum likelihood method. The two components of closed lifetime distributions and one component of the open lifetime distributions were detected. The time constants of the closed lifetime distributions are 0.872 ms and 62.344 ms and those of the open lifetime distributions are 0.736 ms and 27.458 ms.

B. A number of Markov kinetic model were examined and the likelihood values of them were compared to pick up the one with the highest score.The shown model is the one with the highest likelihood score. The rate constants (s^{-1}) for the given Markov model based on the open and closed lifetime distribution data were calculated using the maximum likelihood method.

C. The log likelihood score for the given model was shown.

The rate constants from hidden Markov model analysis suggests that the increase of open probability is mainly due to an increase in the dwell time of the long open state (O_2). The rate constants between C_1 and O_1 did not change before and after cys-SNO, indicating that rate constant of RyR channel opening from the closed state remains the same and is not the site of action cys-SNO. Therefore, our results support the hypothesis that cys-SNO locks the channel in the long open state (O_2). One may postulate the action of NO, as a ligand to the open state where NO may bind and stabilize preferentially the open state of RyR. It should be noted that cys-SNO results in the formation of nitrosothiols with thiols on RyR, which is a stable covalent reaction, broken only by the addition of sulfhydryl reducing agent. Therefore, the nitrosation of RyR thiols produces a stable continuous conformation of the receptor unlike the typical on/off stochastic behavior of an ionic ligand-receptor interaction.

3.8 EFFECT OF CYS-SNO ON CREATINE KINASE ACTIVITY

ATP-generating systems in muscle cells are direct phosphorylation, glycolysis and oxidative phosphorylation. Direct phosphorylation of ADP to generate ATP from creatine phosphate by creatine kinase (CK) is an extremely rapid reaction used to maintain constant ATP level in cells. Glycolysis is rapid and oxidative phosphorylation is a slow process. In the muscle cells, direct phosphorylation of ADP by CK and CP is important to supply ATP rapidly during cycles of high metabolic activity such as muscle contraction and relaxation.

Some reports indicate that creatine kinase (CK) is inhibited by S-nitrosylation by NO donors. [22, 151, 152] We examined the activity of CK in the presence of cys-SNO with the same concentrations of cys-SNO and creatine kinase that were used in Ca^{2+} transport experiment. Table 2 illustrates the CK activity with different concentrations of cys-SNO added to the medium.

CK activity was studied at 2.5 U CK/ml used in the Ca^{2+} transport measurement. CK activity was inhibited by cys-SNO, but the effect was gradual with a 15 % decrease in activity in 45 s using 10 μM cys-SNO. The rate of Ca^{2+} release from SR vesicles was considerably more sensitive of cys-SNO relative to CK since at 10 μM cys-SNO reached about 83% of the maximum value of Ca^{2+} release rate. The inhibition of CK activity by cys-SNO became significant within the first 1 min when the concentration of cys-SNO was higher than 20 μM. Most of Ca^{2+} release from SR induced by cys-SNO occurred within the first 1 min and it was most vigorous within the first 30 sec. This suggests that Ca^{2+} release from SR vesicles was initiated by activation of RyRs and in part due to a shortage of ATP due to the inhibition of CK. The inhibition of creatine kinase activity by cys-SNO was reversed by following the addition of sulfhydryl reducing agent, DTT, which indicated that the mechanism was an oxidation reaction of CK. Interestingly, bathocuproine disulfonic acid or myoglobin didn't stop the inhibition of creatine kinase activity, which suggests that this inhibition might be by the transnitrosation.

Table 2. CK activity in the presence of cys-SNO

CK activity: percent CK activity in the presence of cys-SNO relative to CK activity in the absence of cys-SNO.

Ratio of cys-SNO to CK: the ratios of cys-SNO to CK were kept through the experiment with the two different CK concentrations.

CK concentration: the experiments to investigate the CK activity in the presence of cys-SNO were done on two different CK concentrations. The ratio of cys-SNO relative to CK was maintained in both concentrations. CK activity was examined at 2.5 U CK/ ml that is used in the Ca^{2+} transport experiment.

Concentration of Cys-SNO (μM)	Ratio of cys-SNO to CK (pmoles/U)	CK activity (% of control)	
		45 sec after addition of cys-SNO	60 sec after addition of cys-SNO
2	0.8	100.0 ± 0.0	100.0 ± 0.0
5	2	100.0 ± 0.0	99.4 ± 0.3
10	4	97.5 ± 1.4	88.3 ± 5.0
20	8	86.0 ± 4.1	64.7 ± 3.8
30	12	68.6 ± 7.4	51.8 ± 4.1
40	16	56.3 ± 5.4	42.2 ± 4.5
50	20	35.2 ± 3.1	23.7 ± 6.2

3.9 SUMMARY AND CONCLUSION

S-Nitrosothiols Transnitrosate Thiols on RyRs

The copper (I) chelators, iron chelators, and Ca^{2+} chelators were found to stabilize S-nitrosothiols and arrest the liberation of $NO^{\bullet}$. Since S-nitrosothiols activate RyR channel equally well in the presence or absence of these chelators, one must deduce that S-nitrosothiols oxidize RyRs mainly by a mechanism other than the liberation of $NO^{\bullet}$. We propose that the most reasonable mechanism for S-nitrosothiols to impart its biological activity on RyR is the exchange of NO^{+} ion between hyperreactive thiol group on RyRs, through the direct 'transnitrosation' of NO from cys-SNO to RyR thiols. There was controversy about the role of pO_2 on the activation of RyR by $NO^{\bullet}$. This study showed that pO_2 doesn't have a significant effect on the potency of authentic $NO^{\bullet}$ or S-nitrosothiols.

Cys-SNO induced rapid Ca^{2+} release from isolated SR vesicles by activating ryanodine receptor and inhibiting CK activity that is the source of ATP for Ca^{2+}-ATPase through 'transnitrosation'. This suggests that NO requires low molecular weight thiol catalysis to interact with these proteins and transnitrosation by low molecular weight S-nitrosothiols may be a biologically relevant mechanism for NO to play its role to control the local Ca^{2+} transient in striated muscle.

4.0 HNO-INDUCED ACTIVATION OF RYR

4.1 GENERATION OF HNO

In model studies aimed at mimicking the biochemistry of HNO, ANGS is often used as a donor of HNO. Depending on the degree of protonation, the stability of ANGS in aqueous solution follows the sequence $N_2O_3^{2-} > HN_2O_3^- > H_2N_2O_3$ ($pK_1 = 3.0$ and $pK_2 = 9.35$. [153] ANGS is relatively stable in alkaline solutions (pH > 10) but its rate of decomposition in the pH range of 4 to 8 is rapid, $[H^+]$-independent, and leads to the formation of HNO ($k_{ANGS} = 6.9 \times 10^{-4}$ $M^{-1}s^{-1}$ [153]; Scheme 1). The latter species can dimerize to *cis*-hyponitrous acid ($H_2N_2O_2$; $k_{HNO} = 8 \times 10^6$ $M^{-1}s^{-1}$ [154], which is unstable and decomposes to N_2O and H_2O; the decomposition of this acid is especially fast in aqueous solutions with pH 7 –12. [155]

Scheme 1

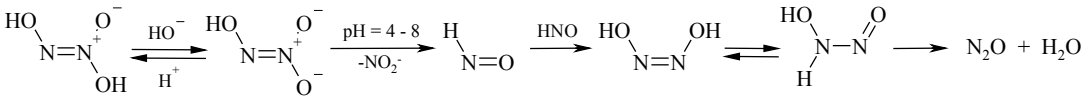

The hydrolysis of ANGS and the production of HNO were detected by UV and EPR spectroscopy. Figure 31A depicts the hydrolysis of ANGS in 0.1 M phosphate buffer (pH 7.4; 20 ^oC) where the decomposition of ANGS was followed by measuring a decrease in $N_20_3^{2-}$ absorption at 237 nm (↓; $\varepsilon_{ANGS} = 5460 \pm 240$ $M^{-1}cm^{-1}$). [156] It should be noted that the UV absorption spectrum of NO_2^- exhibits a maximum at 210 nm (↑), consistent with the increased

absorption of nitrates at 210 nm. [156] The formation of HNO from the hydrolysis of ANGS was monitored by EPR analysis. In the presence of Fe^{3+} and N-methyl-D-glucamine dithiocarbamate (MGD), the hydrolysis of ANGS was paralleled by the appearance of the characteristic EPR spectrum of $^{\bullet}$ON-Fe^{II}-MGD formed via the interaction of HNO and Fe^{III}-MGD (Figure 31B). [157] The formation of HNO was first order in $HN_2O_3^-$ at a rate that did not depend on $[H^+]$ variations within the pH range of 4 to 7.5 (data not shown), in agreement with previous studies. [153] If the hydrolysis of ANGS to HNO and the reaction of HNO dimerization are assumed to be irreversible processes, the steady-state concentration of HNO can be deduced from the equation $[HNO]_{ss}^2 = (k_{ANGS}/k_{HNO}) \times [ANGS]_{t=0\ min}$. Hence, in aqueous solutions of 0.01 mM ANGS (pH $\simeq$ 7.0; 20 ^{o}C) the steady-state concentration of HNO would be 29 nM; a values of 0.93 nM for $[HNO]_{ss}$ could be obtained if k_{HNO} is taken from reference [158] ($k_{HNO} = 8 \times 10^9\ M^{-1}\ s^{-1}$). Differences in k_{HNO} reflect the difficulties in analyzing the kinetics of HNO and HO-N=N-OH, because these species are highly reactive and short-lived.

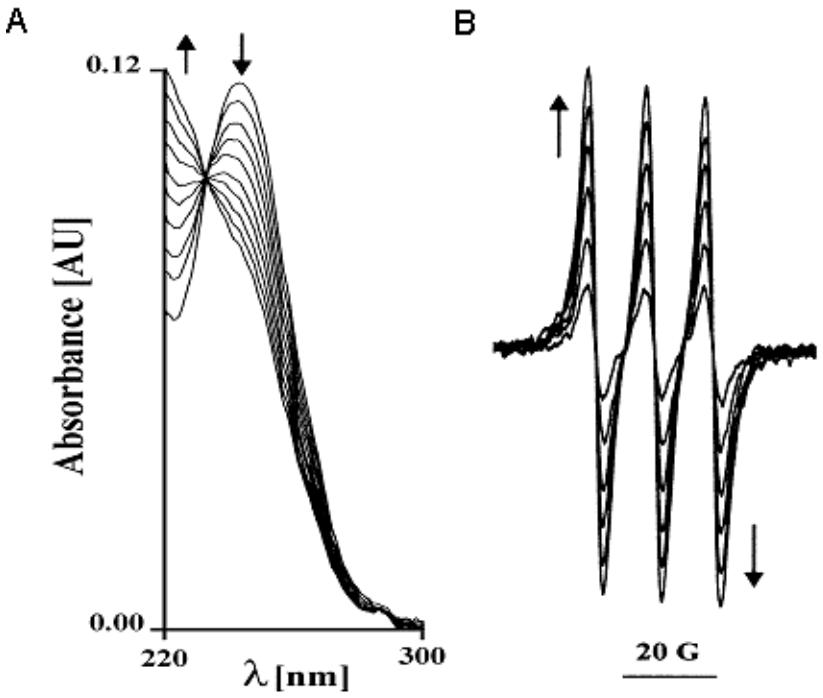

Figure 31 .UV- and EPR-spectra monitor the hydrolysis of ANGS.
A. Consecutive UV spectra of ANGS (0.01 mM) in 0.1 M phosphate buffer (pH 7.0; 20 °C). Spectral scans were carried out every 1 min. Arrows indicate the direction of time-dependent changes of the UV spectrum of ANGS.
B. EPR spectra of •ON-Fe^{II}-MGD formed in aqueous solution of ANGS and Fe^{III}-MGD. Reactions were carried out in 0.1 M TRIS buffer (pH = 7.0; 20 °C). $FeCl_3$, 0.3 mM; MGD, 1 mM; ANGS (0.1 mM). Consecutive spectra were recorded every 4 min. Arrows indicate the time-dependent increase of the EPR signal

4.2 HNO INDUCES Ca^{2+} RELEASE FROM SKELETAL SR

SR vesicles were suspended in a reaction medium to measure extravesicular Ca^{2+} concentrations. Two additions of $CaCl_2$ to SR suspension resulted in an increase in the differential absorption (790-720 nm) due to the formation of a Ca^{2+}-AP-III complex (figure 32A). Upon the addition of ATP in the presence of an ATP regenerating system, there was a time-dependent decrease of extravesicular Ca^{2+} due to ATP-driven Ca^{2+},Mg^{2+}-ATPase transport of Ca^{2+} into the lumen of SR. Once SR Ca^{2+} uptake was completed, an addition of ANGS caused a rapid release of Ca^{2+} from the vesicles. A subsequent addition of DTT reversed the effect of ANGS causing a re-uptake of Ca^{2+}, indicating that the Ca^{2+} release process was due to oxidation of sulfhydryl groups on RyRs. An addition of the Ca^{2+} ionophore A23187 (1 μg/ml) enhanced the Ca^{2+} permeability of the SR membrane resulting in the release of Ca^{2+} from the lumen of SR. The data indicated that ANGS elicited the translocation of Ca^{2+} through the SR membrane via a reversible oxidation reaction. ANGS increased the rate of Ca^{2+} release from SR in a concentration-dependent manner, reaching a maximum rate of release at 100-200 μM ANGS (figure 32B). It should be emphasized that the effective concentrations of HNO that caused release of Ca^{2+} were considerably lower. At concentrations of 3, 5, and 10 μM, ANGS caused release of Ca^{2+} after lag periods of 2.4, 1.1, and 0.47 min, respectively (n=4; SEM did not exceed 5% from the mean). At these lag periods, only a minor part of ANGS was hydrolyzed to HNO. Based on the results presented in figure 31A and published k_{HNO} and k_{ANGS} values, 10 μM ANGS generated HNO at a rate of 73 pmoles per minute (figure 31A) that established a steady-state concentration of HNO in the nM range.

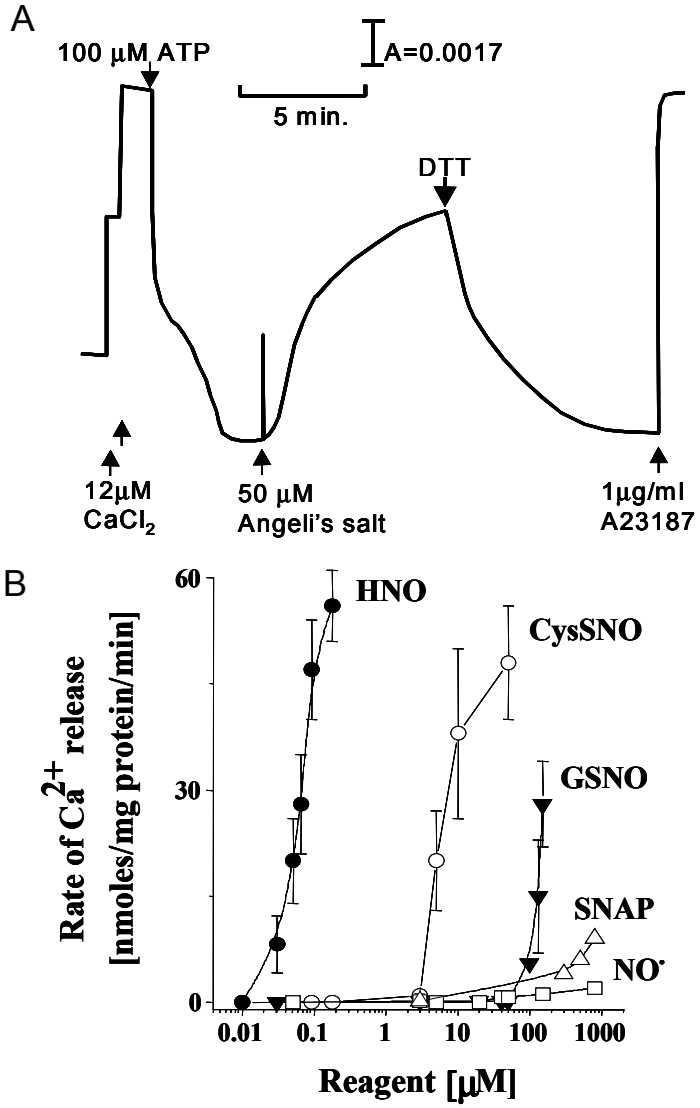

Figure 32. HNO induces Ca^{2+} release from Ca^{2+}-loaded SR vesicles.

A. HNO-induced Ca^{2+} release from SR vesicles. SR vesicles were incubated in a standard reaction medium (see Methods), Ca^{2+} was added in a step-wise manner to measure the changes in extra-vesicular Ca^{2+}, Mg-ATP was added in combination with an ATP-regenerating system to promote active accumulation of Ca^{2+} in the vesicles. The addition of 50 μM ANGS elicited a prompt and rapid release of Ca^{2+} from the vesicles, which was reversed upon the addition of DTT (1 mM). The amount of releasable Ca^{2+} that was accumulated in the vesicles was determined by permeabilizing the SR membranes with the ionophore A23187 (1 μM). The measurements were reproduced with five separate SR vesicle preparations.

B. Dose-dependences of HNO, S-nitrosothiols and $NO^{\bullet}$ on the rate of SR Ca^{2+} release. The concentrations of HNO were deduced from $[HNO]_{ss}^{2} = (6.9 \times 10^{-4} / 8 \times 10^{6}) \times [ANGS]_{t=0\ min}$. HNO (-●-); Cys-SNO (-○-); GSNO (-▼-); SNAP (-Δ-); $NO^{\bullet}$ (-□-). Each experimental point represents the mean of three experiments ± SEM.

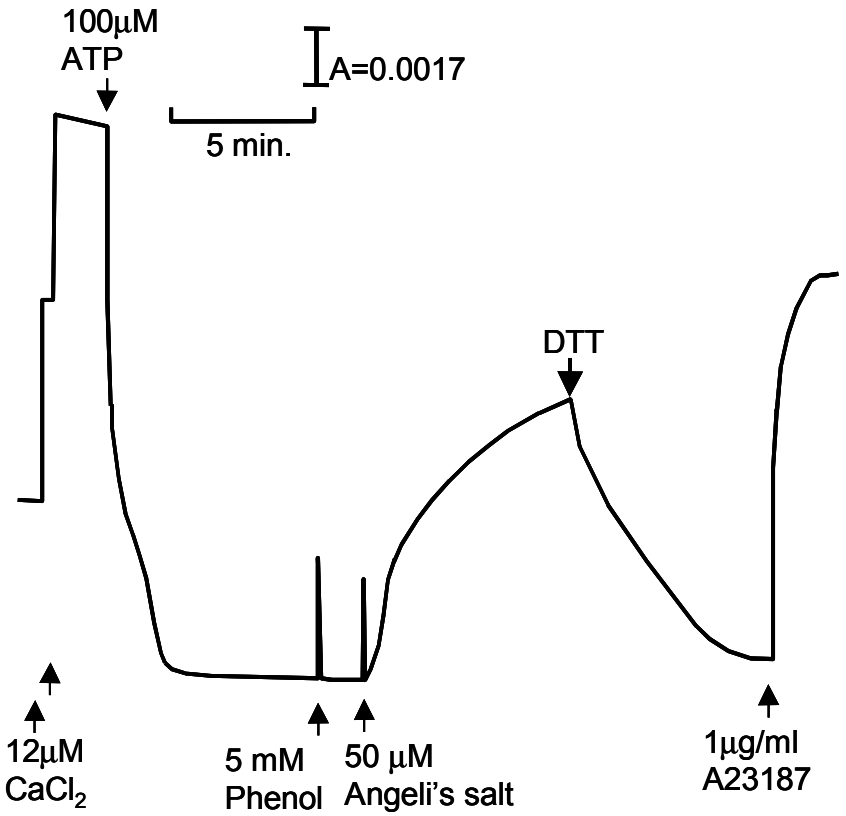

Figure 33. HNO-, not hydroxyl radical, released from ANGS induces Ca^{2+} release from Ca^{2+}-loaded SR vesicles.

SR vesicles were incubated in a standard reaction medium (see Methods), Ca^{2+} was added in a step-wise manner to measure the changes in extra-vesicular Ca^{2+}, Mg-ATP was added in combination with an ATP-regenerating system to promote active accumulation of Ca^{2+} in the vesicles. Phenol (5 mM) was added to arrest any hydroxyl radical that could be released from ANGS. The addition of 50 µM ANGS elicited a prompt and rapid release of Ca^{2+} from the vesicles, which was reversed upon the addition of DTT (1 mM). The amount of releasable Ca^{2+} that was accumulated in the vesicles was determined by permeabilizing the SR membranes with the ionophore A23187 (1 µM). The measurements were reproduced with five separate SR vesicle preparations. This confirms that Ca^{2+} release from SR vesicles induced by ANGS was caused by HNO- not by hydroxyl radical.

In aqueous solutions, ANGS can also generate hydroxyl radical that may oxidize the SR membrane resulting in a non-selective leak of Ca^{2+} from SR vesicles. [159] Such a process would not be reversed by sulfhydryl reducing agents. Nevertheless, we tested this possibility by adding a hydroxyl radical scavenger, phenol (5 mM) which when added to the reaction medium did not alter ANGS-induced SR Ca^{2+} release (figure 33). Phenol was chosen because it is known to interact with hydroxyl radical at an appreciable rate ($k_{PhOH} = 6.6 \times 10^9\ M^{-1}\ s^{-1}$. [160, 161] These control experiments affirm that the production of hydroxyl radicals did not contribute to ANGS- induced SR Ca^{2+} release and implicate HNO as the active reaction intermediate.

4.3 HNO ACTIVATES SINGLE RYR1 CHANNEL

HNO-induced Ca^{2+} release from SR vesicles suggests strongly that HNO activates RyRs because the effect is reversible and consistent with numerous studies on redox regulation of Ca^{2+} release channels. However, the possibility remained that HNO acted via Ca^{2+} pumps or indirectly via proteins associated with RyR1. Therefore, the actions of HNO were tested on the single channel properties of purified RyR1 reconstituted in a planar lipid bilayer. As shown in figure 31A (trace a and b), an addition of HNO to the *cis*-side of the channel caused a marked increase in the open probability of the channel and a subsequent addition of DTT reversed this effect (figure 34A, trace c). In all experiments, a final addition of ryanodine locked the channel in an open subconductance state to identify the reconstituted proteins as a RyR (figure 34A, trace d). HNO did not alter the K^+ conductance of RyR1 and elicited release of Ca^{2+} ions from SR through an increase in the open probability the release channel.

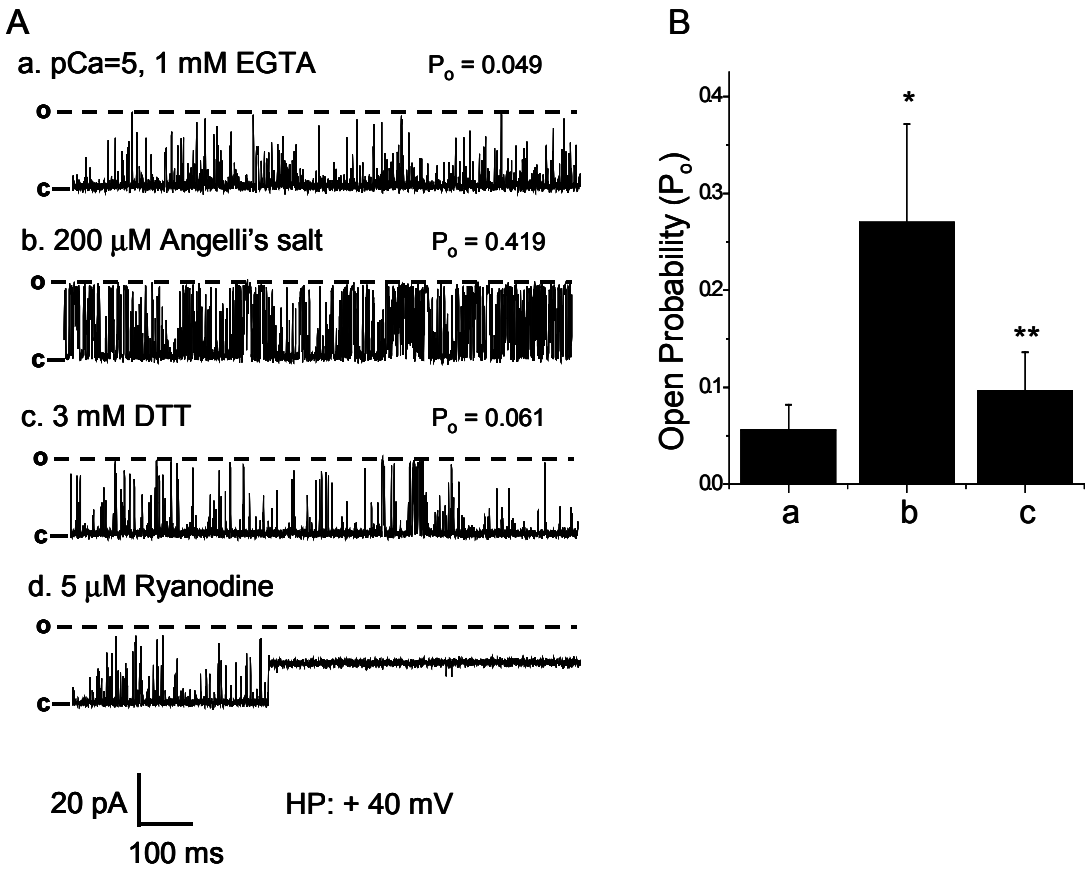

Figure 34. HNO increases P_o of purified RyR1 reconstituted in planar bilayers.
(A) *Trace a*: Single channel activity of RyR1 was recorded at +40 mV holding potential and at pCa = 5, P_o was 0.049. *Trace b*: The addition of HNO (200 µM ANGS) to the *cis*-side increased single channel fluctuation and a 10-fold increase in open probability of the channel to P_o = 0.419. *Trace c*: The addition of DTT (3 mM) reversed the effect of ANGS decreasing P_o to 0.061indicating that HNO most likely oxidized vicinal thiols on RyR1, which were reduced by DTT. It is important to emphasize that Po values were determined from continuous, uninterrupted recordings of traces a-c for > 10 min. *Traced d*: At the end of experiment, an addition of 5 µM ryanodine to the *cis*-side locked the channel in an open subconductance state typically used to affirm that the channel was a ryanodine receptor.
(B) The average open probability (P_o) (mean ± SEM) was calculated from single channel recordings (n = 4). Po was (a) 0.056 ± 0.026 under control condition (pCa = 5), increased to (b) 0.270 ± 0.102 (*: $p<0.005$) upon the addition of 200 µM ANGS then decreased to (c) 0.096±0.040 (**: $p<0.01$) upon the addition of 3 mM DTT to the *cis*-side. P_o was determined from ≥ 5 min of continuous single channel fluctuations

4.4 SUMMARY

The biological activity of nitric oxide ($NO^{\bullet}$) and NO-donors has been extensively investigated yet few studies have examined those of nitroxyl (HNO) species even though both exist in chemical equilibrium but oxidize thiols by different chemistries: S-nitrosation versus disulfide bond formation. Here, sodium trioxodinitrate ($Na_2N_2O_3$; Angeli's salt; ANGS) was used as an HNO donor to investigate its effects on skeletal ryanodine receptors (RyR1). HNO (10-200 μM ANGS) induced a rapid Ca^{2+} release from sarcoplasmic reticulum (SR) vesicles then the reducing agent, dithiothreitol (DTT = 1 mM) reversed the oxidation by HNO resulting in Ca^{2+} re-uptake by SR vesicles. With RyR1 channel proteins reconstituted in planar bilayers, HNO added to the *cis*-side increased the open probability (P_o) from 0.056 ± 0.026 to 0.270 ± 0.102 ($p<0.005$, n = 4) then DTT (3 mM) reduced P_o to 0.096 ± 0.040 ($p < 0.01$, n = 4). In parallel experiments, the time course of HNO production from ANGS (200 μM) was monitored by EPR and UV spectroscopy and compared with the rate of SR Ca^{2+} release indicating that picomolar concentrations of HNO triggered SR Ca^{2+} release. Controls showed that the hydroxyl radical scavenger, phenol (5 mM) did not alter ANGS-induced SR Ca^{2+} release, indicating that hydroxyl radical production from ANGS did not account for Ca^{2+} release from SR. The findings indicate that HNO is a more potent activator of RyR1 than $NO^{\bullet}$ and that HNO activation of RyRs may contribute to $NO^{\bullet}$'s activation of RyRs and to the therapeutic effects of HNO-releasing prodrugs in heart failure.

5.0 IDENTIFICATION OF REGULATORY CYSTEINES ON RYRS

Identification of regulatory cysteines on ryanodine receptors was hindered by the facts that there are about 100 cysteines per monomer and half of them are known to exist as free thiols. It is known that only 2-4 % of these thiols are involved in redox regulation of RyRs. The cysteines involved in redox regulation of RyRs have been referred to as 'critical' or 'hyper-reactive' thiols to distinguish them as a subset of thiols that are unique in their function, reactivity, and reversible modulation of channel properties. Despite extensive progress in our understanding of the chemistry of these thiols, there is still little information regarding the location of this subset of cysteines and the linkage between cysteines accessible from the cytosolic versus the luminal side of RyRs. The project tested the orientation of NO-induced activation of RyR channel to confirm the cysteine residues available for the sulfhydryl redox modification on each side of channel and the hypothesis that one or more of 'regulatory cysteine' found in a conserved amino acid motif modulate channel activity of RyRs through their changes in redox state. To test the hypothesis, truncated form of RyR1 that includes the most of conserved cysteine residues was studied to map functional cysteine domains that are involved in channel regulation.

5.1 CYTOSOLIC AND LUMINAL SIDE ACTIVATION OF RYR BY NO

Attempts to identify the 'regulatory cysteines' on each side of RyRs were made by incorporating RyR1 in planar bilayers and adding a membrane impermeable sulfhydryl reagent to the *cis* or

trans side of the receptor. The *cis*- and the *trans*-side are equivalent to the cytosolic and luminal face of the channel, respectively. It is very important to use membrane impermeable NO donors to discriminate the activation of RyR channel by S-nitrosylation of thiol(s) on cytosolic side of the channel from that on the luminal side.

As shown in figure 35, cys-SNO activates RyR channels from both cytosolic (*cis*) and luminal (*trans*) side of channels. RyR1 channel purified from rabbit skeletal muscle was reconstituted in the planar lipid bilayer and the single channel currents were recorded in the symmetrical solution in (*cis*/*trans* chamber) containing 250 mM potassium chloride, 10 mM HEPES-Tris, pCa=5, 1 mM EGTA and pH 7.4. RyR1 channel was activated by the addition of cys-SNO into the *cis* chamber (cytosolic side of channel) and further activated by the addition of cys-SNO to *trans* chamber (luminal side of channel). The following addition of DTT reversed the activation of RyR channel by cys-SNO, as expected for an activation caused by the S-nitrosation of cysteines on RyRs. More intriguing, when a membrane impermeable sulfhydryl oxidant was added to the trans-side, no changes in channel activity could be detected (n=4 out of 6 experiments), unless an oxidant had been first added to the cis-side which implies that there is a form of cross-talk between cysteine residues facing the cis and trans sides. At the end of the experiment, the addition of ruthenium red, a RyR channel blocker, to the *cis* chamber completely abolished the channel activity of RyR channel, which confirmed that the channel was the RyR. This result suggested that there might one or more thiols on luminal side of RyR available for the modification of RyR activity by nitric oxide. According to the 8 transmembrane domain model discussed in introduction, there are only two cysteines (C4876 and C4882 in RyR1) available from the luminal side of RyR channel. These two

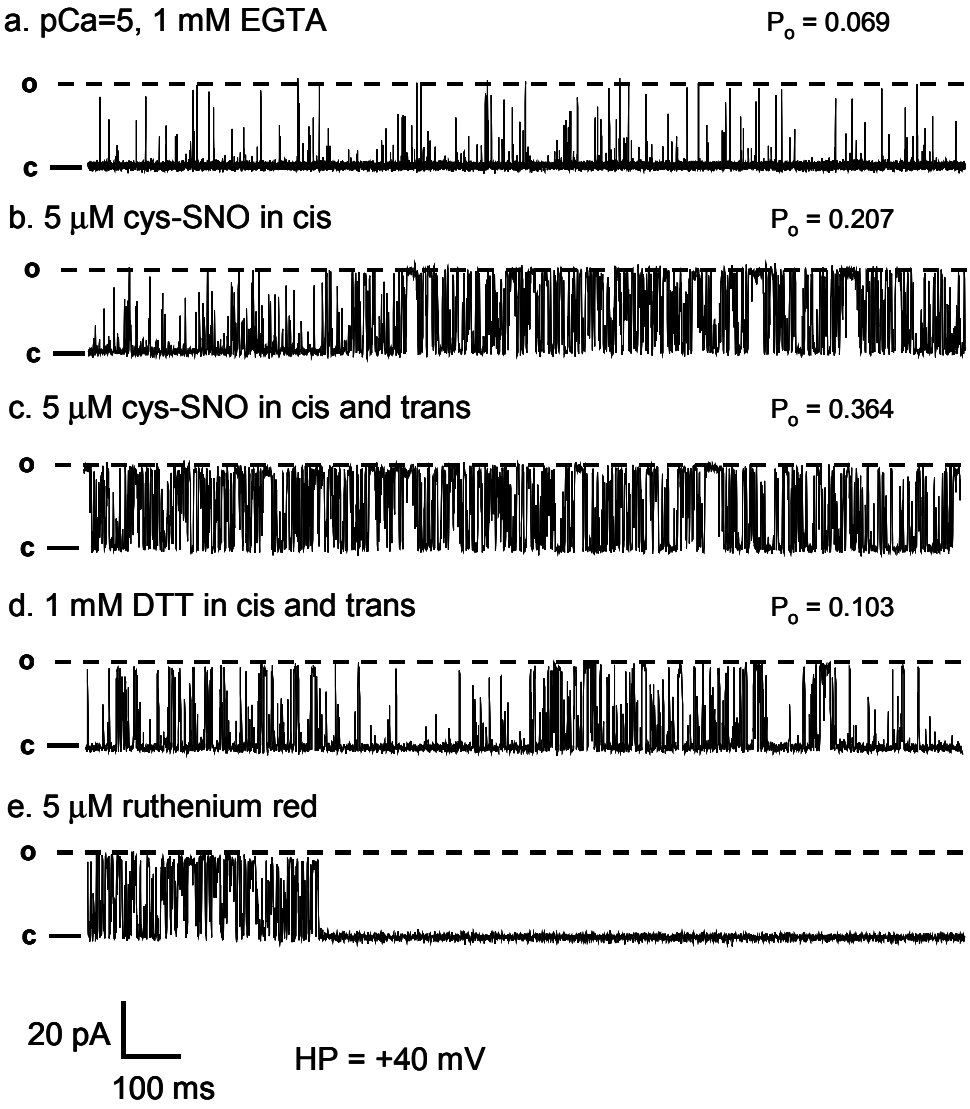

Figure 35. Cys-SNO activates RyR channel.

RyR1 purified from rabbit skeletal muscle was incorporated in the planar lipid bilayer. Single channel currents, shown as upward deflections (open state is indicated as o) from closed level(indicated as c) were recorded at +40mV holding potential with solutions: 250 mM (*cis/trans*) potassium chloride, 10 mM HEPES-Tris, pH 7.4 buffer containing pCa =5 with 1 mM EGTA. Trace a is the control channel activity before adding cys-SNO, a membrane impermeable nitric oxide donor. Ryanodine receptor showed the increased activities with addition of 5 μM cys-SNO to the *cis* solution (cytosolic side of channel) with increased open probability and more frequent opening event(trace b). The channel activity was further increased when 5 μM cys-SNO was added to *trans* solution (luminal side of channel) (trace c) and the effect of nitrosocysteine was reversed with the following addition of 1mM DTT into both of cis and trans solutions(trace e). Addition of 5 μM ruthenium red to the cis solution completely blocked the channel activity, which confirmed that the channel was ryanodine receptor(trace e).

cysteine residues are fully conserved among 8 mammalian RyRs and IP_3Rs isoforms and are located in the putative pore-forming region.

5.2 TRUNCATED RYR

The use of truncated RyR, especially the 75 kDa C-terminus RyR, could give us information about the topology of ryanodine receptor and a method to narrow down the location of the regulatory cysteines. If p75 RyR responds to the redox modification in the same way as p565 RyR, this will narrow down the number of candidate cysteines responsible for sulfhydryl redox regulation from 100 to 8. In that case, candidate cysteines that respond to the cytosolic redox state will be reduced to 2-4 cysteines: 2 fully conserved cysteines (C4958 and C4961) and 2 partially conserved cysteines (C5018 and C5027). Cysteines sensitive to the luminal redox state will be 2 fully conserved cysteines (C4876 and C4882) located in the pore-forming region.

If p75 RyR forms a functional channel and fails to respond to sulfhydryl oxidants, it would confirm that the domains M5-M10 are membrane associated as proposed by Du et al. [56], and suggest that the regulatory cytosolic cysteines are located near the N-terminal region that are missing in p75 channel protein. In tat case, fully conserved and partially conserved cysteines are found in the 'Foot' region (see Table 1) would likely be the sites of regulatory cysteines on RyR1. If p75 RyR fails to form a functional channel, we could deduce that the M5-M10 are insufficient to form a channel and that there might be more than 8 transmembrane domains. If there are more transmembrane domains, then additional luminal domains would have to be considered as well as additional regulatory cysteines that respond to sulfhydryl oxidation from the trans-side.

5.2.1 Transient Expression of Truncated Form of Ryanodine Receptors in CHO Cells

This is an alternative strategy to narrow down the location of critical thiols by characterizing the channel properties of truncated, 100% homologous forms of RyR1, testing the formation of a functional channel and the effects of NO and sulfhydryl oxidants to determine if the truncated receptors retain the sensitivity to sulfhydryl oxidation-reduction. The ultimate goal is to reduce the number of candidate cysteine residues that might be involved in gating the opening and closure of RyRs and to apply site-directed mutations to identify the molecular site of interaction between NO and RyRs.

CHO cells were maintained in a 1:1 mixture of Dulbecco's modified Eagles medium and Ham's F-12 medium (GIBCO BRL) containing 5% heat-inactivated fetal calf serum (Hy-Clone) in a water-saturated 5% CO_2 incubator at 37^{o}C. The cells were grown to confluence in 75-cm^2 tissue culture flasks, passed at 1:5 dilution. An avian host-range-restricted vaccinia virus encoding bacteriophage T7 RNA polymerase, MVA/T7 pol (kindly provided by Dr. Bernard Moss) was used for the transient expression in CHO cells. [137, 138] Because it is replication-deficient in mammalian cells, MVA/T7 pol has low cytopathic effects while providing a high level of gene expression. For immunofluorescence staining and Ca^{2+} release assay, 1x10^4 cells were seeded on a coverslip that was placed in a 35-mm plate where they were grown to 40-50% confluence for transfection the next day. After removal of the medium, 5x10^5 MVA/T7 pol virus in 1 ml of DMEM/F12 was added to each plate and incubated at 37^{o}C in a 5% CO_2 incubator for 60 minutes. The virus-containing medium was then replaced with a 0.8-ml mixture of pBS/RyR DNA and lipofectamine (BRL GIBCO) according to the manufacturer. Cells were used 20-24 hours post transfection when no severe cytopathic effects were observed.

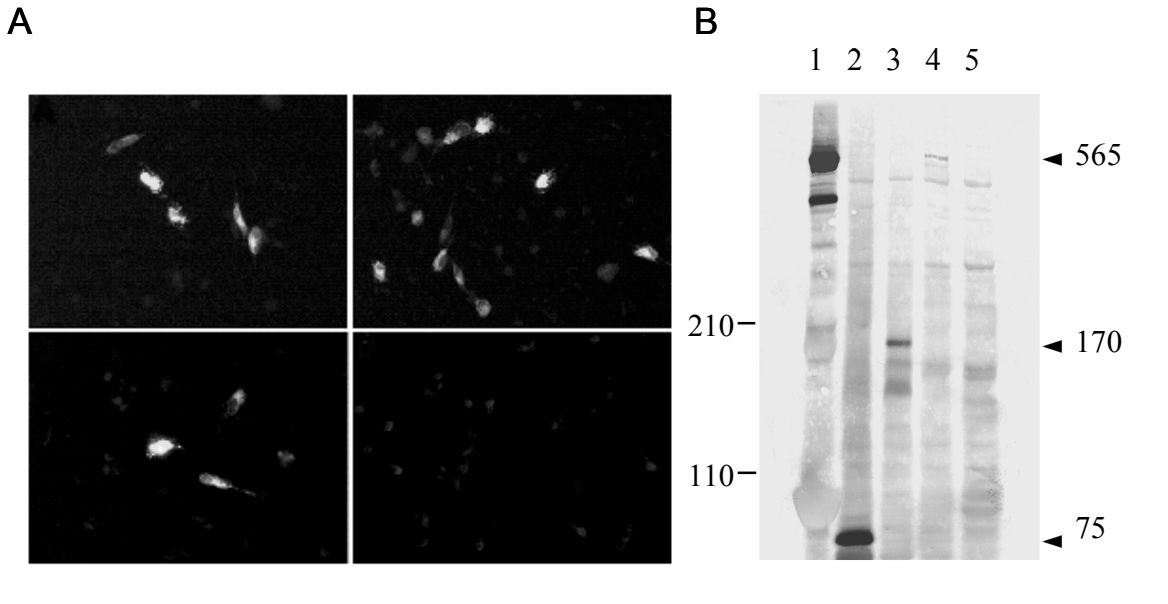

Figure 36. Immuno-analysis of full-length and truncated RyR1 expressed in CHO cells.
A. Immuno-fluorescence of CHO cells transfected with p565, p170 or p75 versus control CHO cells. CHO cells expressing p565 or truncated RyRs1 were cross-reacted with RR2 monoclonal antibody raised against rabbit RyR1. Cells transfected with p565 (*top left*), p170 (*top right*), p75 (*bottom left*), virus without plasmid (*bottom right*).
B. Western blots of cell homogenates from control and transfected CHO cells (50 µg protein/lane) expressing p75, p170, or p565 compared to control cells infected with *vaccinia* virus in lanes 2 to 5, respectively. Lane 1: SR vesicles. The relative immuno response was p75 > p170 >p565 which reflects the relative level of expression; the smaller the molecular weight the greater level of expression since the same amount of protein was loaded in each lane

Full length and truncated RyR expression levels were monitored by immunofluorescence staining and western blot analysis (figure 36).

Intracellular Ca^{2+} Assay of the CHO Transiently Expressing RyRs Figure 34 illustrates the response of various CHO cells to ryanodine (10 μM). Control or virus infected cells did not exhibit a change in Cai upon the addition of ryanodine (figure 37A). CHO Cells expressing either p565 (figure 37B), p170 (figure 37C) or p75 (figure 37D) exhibited a ryanodine-dependent increase in Ca_i.

When the reactive disulfide, or NO donor were added to control CHO cells, we observed a rise in Cai in control CHO cells most likely through its oxidation of IP_3 receptors which are also activated by sulfhydryl oxidizing agents and NO. [162] Heparin, an antagonist of IP_3 receptors was tested in attempts to block NO and DTDP-induced Ca_i elevation. In CHO cells bathed for 5-10 min with low molecular weight heparin, the Ca_i elevation elicited by cys-SNO was markedly inhibited. Several controls indicated that low molecular weight heparin was internalized in CHO cells and blocked IP_3 receptors in CHO cells. For instance, the degree of block by heparin was dependent on the molecular weight of heparin and the time of incubation. Low molecular weight heparin required a 5 min of incubation to block IP_3 whereas higher molecular weight heparin required longer incubation times or were ineffective at blocking Ca_i mobilization induced by cys-SNO. Incubation of control CHO cells with low molecular weight heparin inhibited the effects of cys-SNO, which suggested that NO elicited Ca^{2+} release through the S-nitrosylation of IP_3Rs. As shown in figure 38, cys-SNO elicited the elevation of Ca_i in the CHO cells expressing p565, p170 and p75 RyR1 even after incubating the cells with low molecular weight heparin, which indicate the elevation of Ca_i in these CHO cells is not through IP_3Rs.

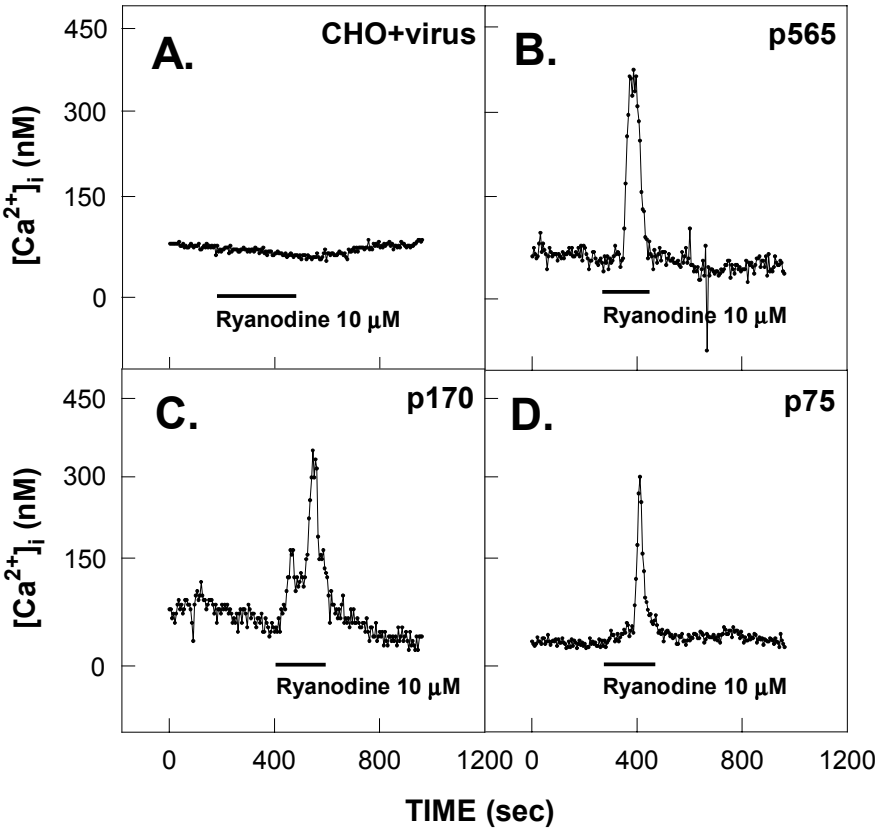

Figure 37. Effect of ryanodine (10 µM) on control and transfected CHO cells.
CHO cells were loaded with Fura 2/AM and Cai was monitored continuously before during and after an exposure to ryanodine. Cells transfected with virus did not respond to ryanodine (A), whereas ryanodine elicited an increase in Cai in cells expressing p565 (B), p170 (C), or p75 (D).

To verify that the elevation of Cai elicited by cys-SNO was due to Ca^{2+} release from internal stores, these measurements were done in zero Ca^{2+} medium.

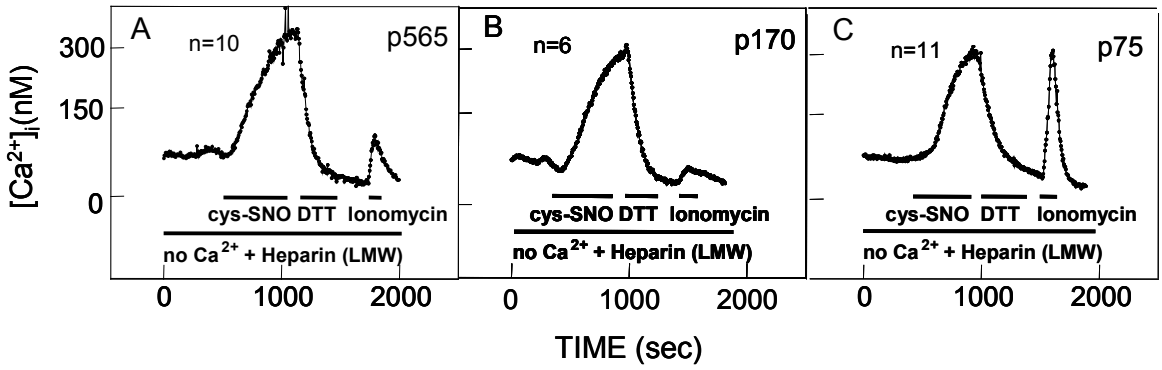

Figure 38. Cai elevation induced by cys-SNO in CHO cells expressing ryanodine receptor in the absence of external Ca^{2+}.
In heparin treated CHO cells, cys-SNO elicited Ca^{2+} release from cells transfected with p565 (A), p170 (B), and p75 (C). Bars indicate periods of drug application.

Even though heparin inhibited Ca^{2+} release from control cells via IP_3Rs, the possibility remained that Ca^{2+} release elicited by NO in transfected cells occurred in part via IP_3Rs. To ascertain that Ca^{2+} release occurred via the expressed RyRs, cells were treated with heparin and one of 3 possible blockers of RyRs, high concentrations of ryanodine (100 μM), tetracaine (200 μM) or ruthenium red (5 μM). These blockers inhibited Ca^{2+} release elicited by NO donors indicating that the elevation of Cai was due to the activation of the expressed p565, p170 or p75 RyRs.

As shown in figure 38, the data showed that cys-SNO caused almost the same levels of Cai elevation in CHO cells that express p75, p170 or p565. Thus, the cysteine residues that cys-SNO acts on must reside in the small p75 truncation of the receptor. These data are statistically significant because each measurement of Cai mobilization in a single CHO cell requires that a

large population of receptors respond simultaneously and in the same way to a particular pharmacological intervention.

The intracellular Ca^{2+} assay in CHO cells transiently expressing RyR proteins provided a quick and strong tool to test if the truncated RyR can form a functional channel when they were expressed in the intracellular membrane and if they can respond to the channel modulators. But, this method has a limitation to study the single channel activity of RyRs with the interference by other channels existing in the cells such as IP_3Rs. Therefore, the reconstitution of single channel was essential to study the channel activity of these truncated RyRs.

5.2.2 Permanent Expression of Truncated RyRs in HEK Cells

Transient expression of truncated RyRs in CHO cells made it possible to test a various constructs in a relatively short time, but it was necessary to produce large amount of protein to purify and incorporate RyR channel into planar lipid bilayer. Therefore, it was attempted to generate the permanent cell line stably expressing the truncated RyRs.

Figure 39 shows immunoanalysis of truncated RyR1s stably expressed in Flpin HEK cells. In figure 39A, the immunofluorescence images of Flpin HEK 293 cells expressing p75/wild type (a) and p75/c4961a (b) show that the proteins expressed in the cytosol were labeled with green fluorescence while control HEK 293 cells (c) don't show any labeled protein. Rat polyclonal antibody to recognize the C-terminus of rabbit RyR1was used to label the RyR protein. Western blots of microsomal membrane vesicles consisting of intracellular membrane fraction purified from Flpin HEK cells and SR vesicles confirmed the expression of truncated RyRs compared to the microsomal vesicles from control Flpin HEK cells.

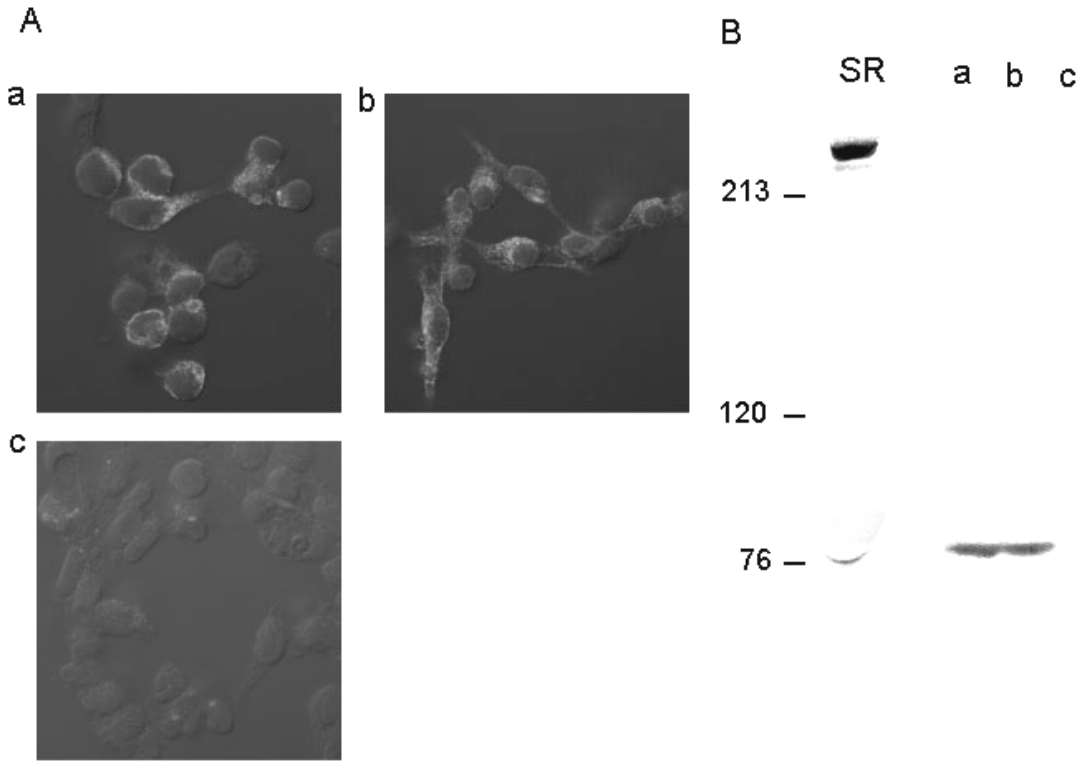

Figure 39. Immuno-analysis of truncated RyR1s expressed in Flpin-HEK293 cells.
A: Confocal microscopic images overlapping DIC (differential interference contrast) and immunofluorescence of HEK 293 cells stably expressing p75 RyR1 wild type and mutated p75 RyR1/C4961A versus control HEK 293 cells. p75 RyR1 was labeled with green fluorescence (shown as light gray in grayscale). Images from HEK 293 cells expressing p75/wild type (a) and p75/c4961a (b) show that the proteins were expressed in the cytosol while control HEK 293 cells (a) don't show any labeled protein. HEK 293 cells were cross-reacted with Rat polyclonal antibody raised against C-terminus of rabbit RyR1 and Alexa 488 (green) conjugated goat anti-rat serum.
B: Western blots of microsomal membrane vesicles prepared from control and transfected HEK 293 cells (25 µg protein/lane) expressing wild type p75 RyR1 (lane a) and a mutated p75 RyR1 (C4961A) (lane b), compared to control HEK 293 cells (lane c). Lane SR: SR vesicles.

This commercial Flpin HEK cells didn't require subculturing to get the optimum and stable expression level of protein. Western blotting on the microsomal membrane vesicles prepared from HEK cells at different stages (6, 16 and 31 weeks after transfection) showed that very stable expression levels were maintained in the transfected cells.

5.2.3 p75 RyR1 Forms a Functional Channel

The intracellular membrane vesicles were isolated from the HEK cells as described in method part and incorporated into planar lipid bilayer. The unsymmetrical solution in *cis/trans* (200 mM/50 mM Cs-gluconate, 10 mM HEPES-Tris, pCa=5, 1 mM EGTA and pH 7.4) chambers was used to promote vesicles fusion with the bilayer. Truncated p75 wild type RyR1 channel reconstituted in planar lipid bilayer showed that it forms a functional channel and it responded to conventional RyR modulators including ryanodine and NO donors, which provides staunch evidence that the 4 transmembrane model suggested by Dr. Takeshima and M5-M10 transmembrane domains confirmed by Du et al. are valid. The channel showed a slight inward rectification. The conductance of this channel was 390.3 ± 33.4 (pS) with inward currents (luminal to cytosolic) and 294.2 ± 37.1 (pS) with outward currents (cytosolic to luminal). Activation of p75 wild type RyR channel by NO donor from the cytosolic side of the channel suggested that at least one or more cytosolic cysteines residing in the truncated form of RyR is involved in nitric oxide-mediated regulation of RyRs. The addition of cys-SNO increased the open probability of p75 RyR1 channel without changing the conductance of the channel. As described in introduction, there are only 4 cysteines (C4958, C4961, C5018 and C5027) available from the cytosolic side of channel in p75 RyR1. All of them are located in the C-terminal tail of the RyR1. This narrows down the number of candidate for the regulatory cysteines for the modification by nitric oxide.

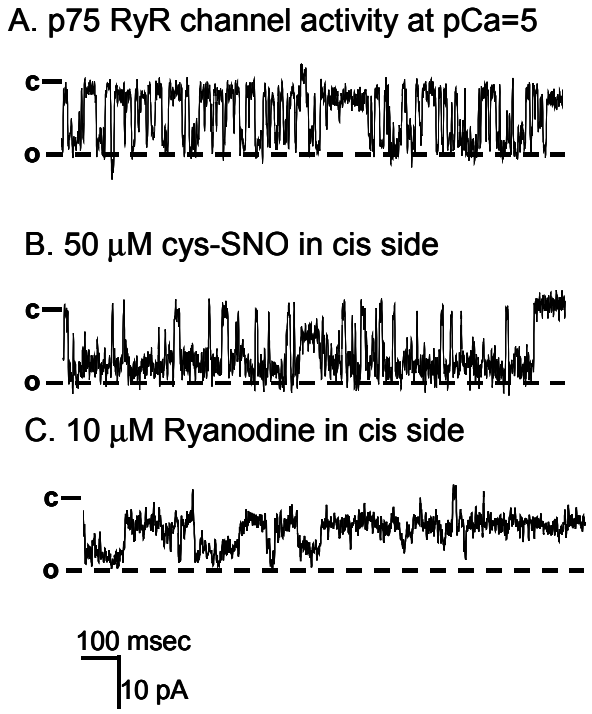

Figure 40. Cys-SNO increases P_o of truncated (p75) RyR1 reconstituted in planar bilayer.

p75 RyR stably expressed in Flpin HEK 293 cells were incorporated in planar lipid bilayer. Single channel currents, shown as downward deflections from closed level (indicated as c) were recorded at –30mV holding potential with solutions: 200 mM/50 mM (cis/trans) cesium gluconate, 10 mM Tris-HEPES, pH 7.4 buffer. Trace a shows the channel activity at pCa=5 (P_o: 0.332). Trace b,shows that addition of 50 μM cys-SNO into cis chamber activated p75 RyR1 (P_o: 0.673). Addition of 10 μM ryanodine to cis chamber confirmed that this is ryanodine receptor (trace c). Addition of cys-SNO didn't change the conductance of the channel.

5.3 SUMMARY

The single channel study of purified RyR1 reconstituted in planar lipid bilayer suggested the existence of 'critical' cysteine residues on both cytosolic and luminal side of the channel and possible cross talk between them.

The intracellular Ca^{2+} assay in CHO cells transiently expressing RyR proteins provided a powerful tool to show that the truncated RyR can form a functional channel when they were expressed in the intracellular membrane of subcellular organelles like the endoplasmic reticulum. Moreover, the expressed channels responded to the conventional RyR channel modulators including nitric oxide donors. But, this method has a limitation in that other associated proteins might modify the properties of RyRs and interfere with agents that modify channel activity Therefore, the reconstitution of cloned truncated channel was crucial to fully characterize the gating properties of truncated vs. full-length RyRs. The p75 RyR single channel reconstituted in planar bilayer responded to the conventional RyR channel modulators such as Ca^{2+}, ryanodine. It was also activated by cys-SNO, which confirms the existence of regulatory cysteine residue(s) in the C-terminus of RyR1 where most of cysteine residues are highly conserved among mammalian RyRs and IP_3Rs.

This study supports that M5-M10 domains in the previous study [56] are all the transmembrane domains required to form a functioning Ca^{2+} channel since the truncated p75 RyRs form functional channels with normal regulation, including redox-mediated gating from the cytosolic side. NO-donors activated the p75 receptor like the p565 RyR1 indicating that the 'critical' regulatory thiols are located closer to the C-terminus of the protein. Therefore, candidate cysteines sensing the cytosolic redox state will be reduced to 2-4 cysteines: 2 fully conserved cysteines (C4958 and C4961) and 3 partially conserved cysteines (C4663, C5018 and

C5027). Based on the model suggested [56], cysteines sensitive to the luminal redox state will be 2 fully conserved cysteines (C4876 and C4882) located in the pore-forming region.

6.0 DISCUSSION

The modification of the redox state of critical or hyperreactive thiols on RyRs by NO-related molecules has been implicated as a mechanism to regulate RyRs in physiological and pathological phenomena in the striated muscles. However, a detailed mechanism of the modulation of RyR activity by these NO-related molecules is currently not well known. This study highlights the importance of nitric oxide modification of the critical thiols of the RyR on the regulation of RyR activity.

6.1 MEASUREMENT OF RYR ACTIVITY

6.1.1 Single Channel Recording

We used Ca^{2+} transport across the SR vesicle membrane and single channel recording after reconstituting the RyR channel in the planar lipid bilayer to measure RyR channel activity modulated by nitric oxide donors. The first reason to use single channel activity in the planar lipid bilayer is that it allows us complete control over the solution condition on both side of a channel. Second, the single channel recordings show the changes in RyR channel activity directly resulting from the reaction between the RyR molecule and modulators added into the system. It is worth noticing that some of the reactions between the RyR protein and reagents wouldn't necessarily result in a change in RyR channel activity. In some studies, the measurement of [^{3}H] ryanodine-binding or S-nitrosylation of the RyR channel was considered to

represent channel activity [83-86]. But, the correlation between ryanodine binding and channel activity has been challenged changes particularly with respect to channel oxidation which activates the channel and inhibits ryanodine binding. The conditions that these measurements can be used to represent channel activity might be very limited. Therefore, it is quite risky to use [^{3}H] ryanodine binding as a method to measure RyR channel activity.

6.1.2 Use of Purified RyR

We used purified RyR to reconstitute single channels in the membrane instead of fusing SR vesicles into the membrane. There are advantages and disadvantages in both methods. When SR vesicles are used to reconstitute a RyR channel, most of the endogenous accessory proteins linked to RyRs on the SR will be intact and RyR channel activity in concert with these endogenous RyR modulators can be recorded, which is probably closer to what happens in intact cells. But, it is hard to tell if nitric oxide affects RyR channel activity through a direct interaction with RyRs or through indirect interaction by acting on other proteins or endogenous modulators linked to RyRs. On the other hand, the RyR channel purified in sucrose gradient will exclude any of these linked proteins on its activity, which could be a little far from what happens in intact cells. However, it will show the direct action of nitric oxide donors on the RyR molecule itself and its activity without any interference of other proteins or linked endogenous modulators of RyR. Therefore, the purified RyR proteins were incorporated to reconstitute RyR channels to study direct NO actions on the RyR molecule.

6.2 REDOX REGULATION OF THE RYANODINE RECEPTOR

Extensive studies have shown that sulfhydryl oxidation-reduction activated and inactivated RyRs in isolated SR vesicles [68, 69, 72, 89, 93] and in RyRs incorporated in planar bilayers [70, 140].

These measurements showed that RyRs contained critical or regulatory thiols, which could control the opening and closing of the RyR channel. Because these sulfhydryl reagents were not related to a physiological signaling pathway, it was suggested that oxidation of RyRs would most likely occur under pathological conditions [90, 101, 163]. But, nitrosation by nitric oxide donors, a chemical reaction analogous to oxidation of free thiols on the RyR, also activates RyR. It was found that nitric oxide is produced by the enzymes endogenously [4, 8, 103, 114]. Moreover, it was reported that the redox state of critical thiols on the RyR modulates its response to the conventional endogenous modulators such as Ca^{2+} and ATP [96, 164]. When a RyR molecule is in a highly reduced state, its response to Ca^{2+} was negligible. This observation emphasized the importance of redox regulation of RyR activity under physiological phenomena.

Therefore, this study aimed to investigate the chemical reaction underlying the thiol-oxidation and activation of the RyR by different type of NO donors, including authentic $NO^{\bullet}$, S-nitrosothiols and HNO, to better evaluate the physiological significance of RyR activation by biologically relevant forms of NO.

Sulfhydryl Oxidation Activates RyRs There is little doubt that sulfhydryl oxidation-reduction reactions regulate the gating of RyRs under physiological and pathological conditions but the exact role of this process is controversial. For instance, there is general agreement that sulfhydryl oxidation activates RyRs but NO has been reported to activate [13, 15, 83], inhibit [116] or first inhibit then activate, as a function of concentration [165]. The present data on measurements of Ca^{2+} transport across the SR vesicle membrane and RyR single channel activity showing the RyR is activated by S-nitrosylation is consistent with a large body of evidence on numerous preparations from purified reconstituted channels, SR vesicles, skinned fibers and intact muscle cells [14, 15, 68, 69, 71, 72, 92-94, 166]. All these studies show that oxidation opens the channel

and reduction closes the channel, and they contradict the findings of Mészáros et al. [116], that NO inhibits and sulfhydryl reducing agents activate the channel. Aghdasi et al. [165] attempted to reconcile these opposite findings by proposing that NO inhibits RyRs at low concentrations but activates them at high concentrations. Low NO concentrations inhibited Ca^{2+} release induced by maleimide, a non-selective thiol alkylating reagent that requires high substrate concentrations, that interacts equally well with non-thiol moieties, and is not a physiological activator of RyRs [120]. The inhibitory effect of low [NO] shown in this study could be due to a direct interaction between NO and maleimide rather than a sulfhydryl mediated mechanism. Maleimides are thought to elicit Ca^{2+} release from RyRs by cross-linking neighboring proteins with the receptor or different moieties of the receptor to itself [120]. However, the relationship between alkylation and enhanced channel activity remains unclear because maleimides could be acting at non-thiol moieties and are likely to be different from the NO and DTDP sites of action because maleimides are non-selective and react with high and low pK_a thiols [91, 167]. Nevertheless, other findings strongly support the notion that the oxidation of RyRs by NO-related molecules gates the opening of RyRs [15, 135].

6.3 ACTIVATION OF THE RYR BY S-NITROSOTHIOLS

Although nitric oxide has been implicated in activation of the RyR by nitrosylating regulatory thiols on it, it was observed that it has low potency to activate RyRs. The concentration required to activate the RyR was too high to be physiologically obtainable (over 100 μM). Eu et al. suggested that that authentic $NO^{\bullet}$ could activate the RyR only at low pO_2 (~10 mmHg) and this is the reason that most studies done under the ambient oxygen level failed to observe the activation of the RyR by authentic $NO^{\bullet}$ [83]. On the other hand, the addition of L-cysteine to the

reaction buffer potentiates $NO^{\bullet}$ to elicit Ca^{2+} release from SR vesicles and suggested that LMW S-nitrosothiols are more potent NO donors to activate RyRs than $NO^{\bullet}$ itself [15]. In this study, $NO^{\bullet}$-, *trans*-S-nitrosation- and disulfide formation-dependent activation of RyRs were investigated to evaluate biologically relevant forms of NO.

6.3.1 S-nitrosothiols Activate the RyR by Transnitrosation

The biological activity of S-nitrosothiols has been often related to their release of $NO^{\bullet}$. Then substantial evidence has established that the liberation of $NO^{\bullet}$ from S-nitrosothiols requires catalytic concentrations of copper [125, 127-129, 131]. However, it was not clear that these potential NO-donors liberated $NO^{\bullet}$ or served as stable carriers of $NO^{\bullet}$ in cells, because the cellular levels of Cu^{+} available to catalyze the reaction are difficult to evaluate, as Cu^{+} may be bound to metallo-proteins. NO donors such as S-nitrosothiols exhibit a higher potency to activate RyR than authentic $NO^{\bullet}$, which cannot be explained by a mechanism whereby S-nitrosothiols release $NO^{\bullet}$ which then acts by nitrosating RyRs. Therefore, S-nitrosothiols most likely impart their biological actions differently from those of $NO^{\bullet}$. The trans-S-nitrosation by delivering NO^{+} directly from S-nitrosothiols to hyper-reactive thiols on the target was suggested as a feasible model [15, 100, 128, 168-173], but the evidence supporting this was mechanism was indirect. Therefore, we investigated the activation of the RyR1 channel and Ca^{2+} release from SR vesicles induced by S-nitrosothiols in the presence and absence of the liberation of $NO^{\bullet}$ from S-nitrosothiols to determine the predominant mechanism for S-nitrosothiols to deliver its NO-function to the regulatory thiols on the RyR between the $NO^{\bullet}$-dependent and trans-S-nitrosation pathways.

We showed that S-nitrosothiols induced rapid Ca^{2+} release from SR vesicles while metal ion chelators blocked the liberation of $NO^{\bullet}$ from them. GSNO and Cys-SNO were highly potent

to elicit Ca^{2+} release from SR vesicles compared to authentic $NO^{\bullet}$, which implies that Ca^{2+} release from the SR induced by them was not caused by $NO^{\bullet}$ released from them. An intriguing finding in this study was that EGTA was found to arrest the liberation of $NO^{\bullet}$ from S-nitrosothiols. EGTA is commonly used in the single channel activity studies in the planar lipid bilayer to calibrate the free Ca^{2+} in the solution. Therefore, it was attempted to investigate the single channel activities of purified RyRs activated by cys-SNO in the presence and absence of EGTA in the solution to compare the activation of the RyR channel in the presence and absence of $NO^{\bullet}$ release in the solution. As shown in figure 22, the presence of EGTA in the solutions didn't alter the cys-SNO-induced-activation of RyR1 channels reconstituted in the planar lipid bilayer, which agrees with Ca^{2+} transport measurement on isolated SR vesicles.

These results provide convincing evidence of two facts: first, activation of RyR1 was not by $NO^{\bullet}$ released from S-nitrosothiols, which suggests that the trans-S-nitrosation must be the prevailing mechanism for S-nitrosothiols to deliver NO-function to RyR1; second, Ca^{2+} release from SR vesicles by S-nitrosothiols was caused by activating RyR1, not other proteins in SR vesicles.

6.3.2 Cys-SNO versus GSNO

Although there is increasing agreement that low molecular weight S-nitrosothiols may be the physiological form of NO, most attention has been paid to GSNO that could be formed from $NO^{\bullet}$ and glutathione that is the most abundant low molecular thiol compound in cells [98, 122]. According to the recent studies showing that S-nitrosothiols could exchange NO^{+} by transnitrosation with the other thiol compounds according to the relative pK_a values of these two thiol compounds [169-171], pK_a value of each S-nitrosothiol determines how good a NO^{+} donor it is. Based on this, cys-SNO has great potential as a potent NO^{+} donor. Also, cys-SNO can be

readily generated in the presence of $NO^{\bullet}$ and L-cysteine at physiological pH (7.0). Indeed, we found that cys-SNO was noncompetitively potent compared to authentic $NO^{\bullet}$ and the other S-nitrosothiols, including GSNO, in this study. It could elicit rapid SR Ca^{2+} release at a submicromolar level (1-2 μM) with little delay. These features made cys-SNO the most prominent candidate for a physiological NO donor that stabilizes the $NO^{\bullet}$ and delivers NO-function to hyper-reactive thiols on RyR1 selectively and efficiently. In this study, we suggest that cys-SNO would be a more promising likely for the physiological NO donor rather than GSNO.

6.3.3 NO-function and Oxygen

It was reported that authentic $NO^{\bullet}$ could activate the RyR only at low pO_2 (~10 mmHg) and its effect on the channel is calmodulin dependent. [83-86] These studies reported that pO_2 controls the redox state of 6-8 out of the 50 free thiols in each RyR1 subunit and thereby tunes the response to $NO^{\bullet}$. They suggested that 1 thiol out of those 6-8 thiols was nitrosylated only at low $NO^{\bullet}$ (0.5-1 μM) and low pO_2 (~10 mmHg). They tried to explain the reason that activation of the RyR by authentic $NO^{\bullet}$ at physiologically attainable concentration (submicromolar range) couldn't be observed in other studies by suggesting that the thiol to be nitrosylated by $NO^{\bullet}$ has been already oxidized at the ambient pO_2. In another respect, cysteine 3635 residing in a calmodulin-binding domain was proposed as the free thiol nitrosylated by authentic $NO^{\bullet}$, leading to the activation of the RyR [84]. They recorded the single channel activity of RyR1 in a bilayer system and correlated it with [^{3}H] ryanodine-binding assay, although it is controversial if [^{3}H] ryanodine-binding correlates directly to the channel activity when nitrosylated.

The effect of pO_2 on the activation of RyRs by $NO^{\bullet}$ and S-nitrosothiols was investigated in this study to resolve the debate on the role of oxygen in the activation of RyRs by authentic

$NO^{\bullet}$. The modulation of the channel activity of RyRs by authentic $NO^{\bullet}$ and S-nitrosothiols under the tightly controlled oxygen levels was studied. We couldn't reproduce their results showing that $NO^{\bullet}$ activates the RyR at low pO_2. We measured Ca^{2+} transport across SR vesicles and the single channel activity of RyR1 reconstituted in the planar lipid bilayer at low pO_2, but we did not observe a dramatic increase in the potency of $NO^{\bullet}$ to activate the RyR1 channel in the absence or presence of calmodulin. The potency of $NO^{\bullet}$ to induce Ca^{2+} release from SR vesicles was not significantly improved in a deoxygenated or low pO_2 medium, but a minimum 50 μM $NO^{\bullet}$ was required to observe a weak release of Ca^{2+} from SR vesicles. Eu et al. showed that the addition of 0.75 μM $NO^{\bullet}$ to RyR1 antagonized calmodulin's inhibitory effect on RyR1 at low pO_2 (~10 mmHg). But, RyR1 channels were observed to show little increase in P_o with the addition of $NO^{\bullet}$ (0.5-5 μM) in either the presence or absence of calmodulin, and the very same channel was activated by the subsequent addition of 5 μM cys-SNO (figure 25-27).

What causes the discrepancy in these observations is not clear. Endogenous modulator or proteins associated with the RyR might be involved in the activation of the RyR by authentic $NO^{\bullet}$. These studies recorded single channel activity of RyR1 reconstituted from incorporating SR vesicles based on the importance of keeping the lipid environment, endogenous modulators and other associated proteins [83]. Therefore, the activation of the RyR1 channel by $NO^{\bullet}$ observed in that study might be mediated by nitrosylating thiols on one or more of these associated proteins because we observed that the purified RyR was not activated by $NO^{\bullet}$ (0.5 –5 μM) even at low pO_2. Our observation that the purified RyR1 channel without the associated proteins was activated by sub-micromolar cys-SNO confirmed that the target thiols of S-nitrosothiols were right on RyR1. However, measurement of RyR1 activity on SR vesicles at low pO_2 (0, 5, 10 and 20 mmHg) did not show the activation of RyR1 with low $NO^{\bullet}$ (0.5 to 5 μM),

which leaves us to question why we couldn't observe the activation of the RyR by $NO^{\bullet}$ in the presence of associated proteins on the SR at low pO_2.

They reported that 6-8 thiols were reduced at low pO_2 compared to ambient pO_2 and one of them was nitrosylated by 0.75 μM $NO^{\bullet}$ [83]. They also suggested that pO_2 tunes the RyR's response to $NO^{\bullet}$. But our observation that cys-SNO activates RyR1 channels that were not activated by the addition of $NO^{\bullet}$ (0.5-5 μM) at low or ambient pO_2 suggested to us that the critical, hyper-reactive thiols to be nitrosylated by S-nitrosothiols might not be the thiols observed to be reduced when SR vesicles were placed at low pO_2 and nitrosylated by $NO^{\bullet}$ at low pO_2.

Could It Be An Allosteric Effect by O_2? Recently, Sun et al. tried to explain how pO_2 affects the nitrosation of RyRs by suggesting that the pO_2 has an allosteric effect on the conformation of the RyR molecule. [86] That is, the conformation of the RyR molecule is changed to favor the nitrosylation by authentic $NO^{\bullet}$ only when it is at low pO_2 (5-10 mmHg). On the other hand, the conformation of the RyR under ambient pO_2 doesn't allow $NO^{\bullet}$ to nitrosylate the critical thiol because the thiol is not exposed at ambient pO_2. The O_2-dependent change in conformation could result in a change in channel activity. However, we did not observe a distinguishable difference in the P_o of purified RyR1 channels; P_o=0.062±0.024 at ambient pO_2 (~150 mmHg) and P_o=0.055±0.019 at low pO_2 (~10 mmHg) at pCa=5 with 1 mM EGTA in the solution. This might be because O_2 acts indirectly via a more associated proteins but not directly on RyR1. We did observe a slight difference in RyR1 activity measured from SR vesicles at ambient versus low pO_2. Again, there is not yet a mechanistic explanation about how the thiols became reduced when RyR1 is placed in a deoxygenated environment for 40-60 min.

Is $NO^{\bullet}$ Selective? Another controversial issue is that several NO donors such as GSNO and nitrosoamines (NOC-12) activate RyR1 through the release of $NO^{\bullet}$ in pO_2 independent chemical reaction [86]. The later study claimed that $NO^{\bullet}$ released from NOC-12 activates the channel by S-nitrosylation of C3635 within a calmodulin-binding domain which is the same site of action as authentic $NO^{\bullet}$. But paradoxically NOC-12 acts at C3635 independently of pO_2 following the liberation of $NO^{\bullet}$ yet $NO^{\bullet}$ when added as gas activates RyR1 only at low pO_2 (~10 mmHg). It was reported that $NO^{\bullet}$ released from GSNO activates RyR1 by S-nitrosylation of thiols other than C3635 and calmodulin is not involved in GSNO-mediated activation. However, no explanation has been offered as to how $NO^{\bullet}$ released from NO donors could act with a different chemistry compared to the addition authentic $NO^{\bullet}$. It is reasonable to propose that $NO^{\bullet}$ was released from a NO donor will be identical as added authentic $NO^{\bullet}$. Also, it is hard to rationalize the fact that $NO^{\bullet}$ released from NOC-12 would act on C3635 with high selectivity while $NO^{\bullet}$ released from GSNO would only act on other thiols. Here, we showed that a mechanism other than the release of $NO^{\bullet}$ explains the actions of NO donors and accounts for the different responses obtained with authentic $NO^{\bullet}$ and No donors. One such mechanism is the trans-S-nitrosation depending on the relative pK_a values as suggested in this work.

6.3.4 Gating of the RyR

It was attempted to analyze the gating of the RyR channel before and after the channel was activated by cys-SNO. There are several mechanisms that lead to the overall increase of open probability: the increase of open dwell times (decrease in rate constant going from open state to closed state); decrease of closed dwell times (increase in rate constant going from closed state to open state). If there are several closed states and the channel can only reach the open states from one of the closed states, an increase in rate constant from one closed to another closed state will

increase the probability for the channel to go to the open state. Thus, the probability for the channel to go to the open state will increase, increasing the open probability. Therefore, Markovian modeling of rate constant for each model and state of the channel gave us insight into the mechanism and how the open probability of a channel increased when it is activated by NO donors.

The analysis using a maximum likelihood method to fit the dwell time distributions showed that there are a number of components of closed and open states and the relative contribution of each component. The increase in the overall open probability of the RyR channel after the activation by cys-SNO was due to the introduction of a new opening state with a longer dwell time that didn't exist before cys-SNO. The analysis was based on typical traces with the RyR in each condition, but RyRs are known to go through different modes of gating, with high activity, low activity, and an inactivated state (so called modal gating) [174, 175]. Therefore, more extensive analysis on the data from each condition throughout the whole recording is needed to understand changes in RyR channel gating, before and after the activation of the channel by nitric oxide donors. The open and closed dwell time distributions showed that there are many zero points at a high frequency region (>2 kHz), for it couldn't detect the opening and closing occurring in a very short time because of the limitation in the sampling rate. (figure 29 A and figure 30 A) This caused the poor fitting in the maximum likelihood method to fit the open and closed dwell time distribution.

Despite the limitations mentioned above, the analysis showed that a Markovian kinetic model may explain channel behavior, and provides insight on RyR gating elicited by channel oxidation.

6.3.5 NO Inhibits CK

CK was chosen as the ATP regeneration system because the CK system is known as a predominant pathway for a rapid replenishment of intracellular ATP content when metabolic demand is increased in muscle cells. Several reports showed that CK activity is inhibited by S-nitrosylation by nitric oxide donors. [22, 151, 152] We examined the activity of CK in the presence of cys-SNO with the same concentrations used in the Ca^{2+} transport experiment and observed an inhibition of CK activity. However, the inhibition wasn't significant within the first 60 sec after a cys-SNO addition of 10 μM, while Ca^{2+} release was vigorous within 60 sec. This suggests that the Ca^{2+} release from SR vesicles was initiated by the activation of RyRs and may have been enhanced by a shortage of ATP due to CK inhibition.

We measured Ca^{2+} transport of isolated SR vesicles using only high ATP without an ATP regenerating system (data not shown) in order to isolate the effect of S-nitrosothiols on RyR1 from the effect on CK. Caution had to be used to avoid the activation of RyRs by a high ATP level in the solution. We could elicit Ca^{2+} release from the SR vesicle by adding cys-SNO while Ca^{2+}-ATPase vigorously pumped extravesicular Ca^{2+} into the vesicle, but Ca^{2+} release was not fully reversed by adding a sulfhydryl reducing agent, DTT, due to a decrease in ATP/ADP ratio. It was not obvious if the system ran out of ATP enough to pump Ca^{2+} released from SR vesicles or if NO affected any other factors on the SR vesicle. This question was addressed by showing that high level of ADP high Ca^{2+}-ATPase pumping rate. [176] The reduction in the SR Ca^{2+} pump rate was observed when [ADP] was 100 μM. Therefore, we concluded that the amount of ADP in the reaction medium increased to the level that decreases the Ca^{2+}-ATPase pumping as the ATP was hydrolyzed to ADP in these experiments.

Neither BCS nor EGTA affected the inhibition of CK by S-nitrosothiols, which suggested that this is via trans-S-nitrosation between LMW S-nitrosothiols and free thiols on CK. The finding that S-nitrosothiols activate the RyR and inhibit CK by S-nitrosation in the same mechanism may indicate that this is a mechanism by which S-nitrosothiols cause a massive release of Ca^{2+} from the SR via activating the RyR and inhibiting Ca^{2+}-ATPase indirectly via inhibiting CK locally.

6.4 HNO-INDUCED ACTIVATION OF THE RYR

One of the main findings of the present work is that HNO produced from ANGS elicits a prompt release of Ca^{2+} from Ca^{2+}-loaded skeletal SR vesicles and that the addition of a sulfhydryl reducing agent, DTT, reversed the effect, resulting in an active re-uptake of Ca^{2+} by SR vesicles. The release of Ca^{2+} from vesicles occurred via an activation of SR Ca^{2+} release channels or the ryanodine receptor since HNO increased the single channel open probability of purified RyR1 reconstituted in the planar bilayers when added to the *cis*-side of the channel. The subsequent addition of DTT reversed the open probability of RyR1 that was treated with HNO, while ryanodine locked the channel in an open subconductance state.

The distinct biological actions of HNO have made this species the subject of intense research. The biosynthesis of HNO is believed to proceed via reduction of $NO^{\bullet}$ by SOD [177], cytochrome c [178] or the reduction of S-nitrosoglutathione by low molecular weight and protein thiols [98, 134, 179]. HNO is a weak acid whose pKa value and redox potential have been recently re-examined and corrected from 4.5 and -0.3V to 11.4 and -0.8V, respectively [154, 180, 181]. Hence, in biological systems, HNO will exist in a protonated form (as opposed to NO^-), which readily interacts with O_2 to form peroxynitrite [133] and will possess a remarkable redox

potential. At the molecular level, there are several differences between the reactivity of $NO^{\bullet}$ and HNO that may account for the biological effects of the latter species. In contrast to $NO^{\bullet}$, HNO directly interacts with thiols [20, 134]. It preferentially binds to Fe^{III}-complexes [157, 182] and can act as a hydroxylating agent [159, 183, 184]. Although HNO is a strong reductant, it readily oxidizes thiols. Mechanistically, the latter reactions proceed via the intermediate formation of S-derived hydroxylamines that can interact, intra- or inter-molecularly, with a second thiol function to form dithiols and hydroxylamine (Scheme 2 reactions ***a*** and ***b***, respectively):

Scheme 2

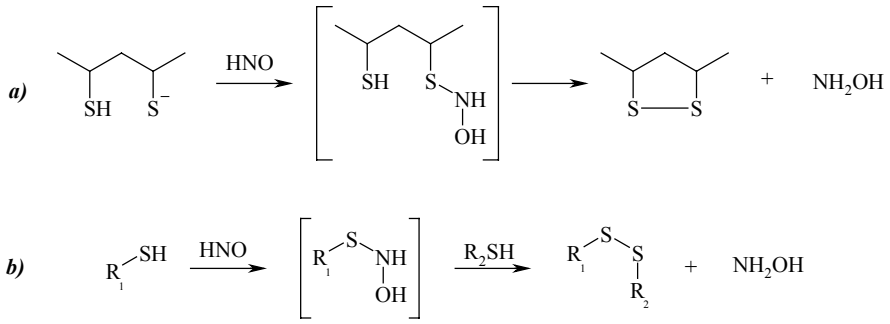

Since the formation of S-derived hydroxylamines reflects a nucleophilic addition of thiol function to HN=O (or HN^{+}-O^{-}), it is likely that low pK_a thiols that are deprotonated at physiological pH will interact at a higher rate with this species than protonated thiols ($v_{[RS^-]} > v_{[RSH]}$).

RyRs are channel proteins thought to contain multiple thiols with different redox states and functional responses to oxidation-reduction reactions [85, 95]. The HNO-induced activation of RyRs most likely occurs according to the reaction mechanism presented in Scheme 2a. The latter mechanism differs from the activation of RyRs with S-nitrosothiols [15] and $NO^{\bullet}$ plus low oxygen [83], which are believed to change the conformation of these proteins via the formation

of stable S-nitrosothiols. It is important to emphasize that RyR1 was activated by nM concentrations of HNO whereas $NO^{\bullet}$ required 10^{-6} to 10^{-4} M [15, 83]. These results suggest that shifts in the equilibrium among $NO^{\bullet}$, S-nitrosothiols, and HNO will promote low levels of the latter species that will affect calcium homeostasis via activation of RyRs. Further studies are needed to assess the effects of HNO on RyRs in intact cells and muscle under physiological and pathological states.

6.5 TRUNCATED RYR (P75) FORMS A FUNCTIONING CHANNEL

6.5.1 Transient Expression of RyRs in CHO Cells

It was observed that transfected CHO cells express functional RyRs at high efficiency from full-length and truncated cDNA encoding the skeletal muscle isoform of RyR since they retain ryanodine sensitivity, NO and sulfhydryl regulation of the channel. The data confirms that the pore of the channel resides in the carboxyl-terminal end of the protein. It also supports earlier predictions that the pore consists of 4 transmembrane domains, suggested by Takeshima et al. [45], because p75 RyR forms functional channels, yet is too small a fragment to contain 10 transmembrane domains as proposed by Zorzato et al. [44]. Recent work to test the Zorzato model supported that transmembrane domains are at the further C-terminal end, similar to Takeshima's model [56]. The truncated p75 RyR produced similar responses to ryanodine and NO as the full-length expressed RyR1. These findings indicate, as a first approximation, that the molecular interaction of NO with RyRs occurs at cysteine residues located in the p75 fragment of the channel. The p75 protein does not include C3635, which is located at the calmodulin binding site and was proposed to be the NO binding site; yet NO-donors activated the p75 receptor, like the p565 RyR1, indicating that the 'critical' regulatory thiols are located closer to

the C-terminus of the protein. The p75 RyR contains 9 cysteine residues; two of these cysteines are found in a 13 amino acid segment 4952 to 4964 which is conserved in the skeletal, cardiac, and brain isoforms of RyRs, RyR1, RyR2 and RyR3. Hydrophobicity analysis of the RyR amino acid sequence predicts that this domain is located at the vestibule of the channel facing the cytosolic milieu near the last membrane-spanning segment of the channel. The small size of the truncated p75 RyR makes it possible to apply site directed mutations at cysteine residues residing in a conserved domain of the receptor, thus making them candidates for the site of action of sulfhydryl reagents and NO.

In control CHO cells, NO donors elicited a rise in Cai most likely through the oxidation of IP_3 receptors. IP_3 receptors are Ca^{2+} channels activated by inositol (1,4,5)-trisphosphate resulting in Ca^{2+} release from intracellular stores, and have been found in many cell types [185]. Heparin is one of the best-characterized antagonists of IP_3 receptors and is generally thought to be membrane impermeable. Heparin inhibits IP_3 binding to its purified receptor, blocks Ca^{2+} release from IP_3-sensitive intracellular stores, and hinders IP_3-gated channel activity [185, 186]. Single channel recordings using a patch clamp revealed that heparin inhibits IP_3 receptors [187]. IP_3 receptors are routinely purified by a procedure that includes a heparin-affinity step, and heparin has been successfully used to distinguish Ca^{2+} release from IP_3 sensitive stores from that evoked by other signaling pathways [185, 186]. Numerous studies have used heparin to block IP_3-receptors in intact cells, but blockade was achieved by microinjection of heparin in single cells. We pursued tests of heparin added externally to intact cells to block IP_3 receptors because microinjection is impractical and because of a lack of characterized membrane permeable inhibitors of IP_3 receptors. We found that low molecular weight heparin blocked IP_3 receptors and inhibited the Cai elevation elicited by DTDP and NO donors in control CHO cells. Heparin

treated CHO cells allowed us to obtain direct evidence of RyRs' regulation by sulfhydryl oxidation-reduction in transfected CHO cells. We confirmed our interpretation that NO and thiol reagents acted on the cloned RyRs by verifying that blockers of RyRs blocked the actions of sulfhydryl reagents and NO donors only in CHO cells expressing various isoforms of RyRs. Furthermore, heparin often elicited an elevation of Cai in CHO cells expressing p565, p170 or p75, but not in control cells. The latter is consistent with the known actions of heparin as an activator of RyRs and with the interpretation that low molecular weight heparin was internalized CHO cells.

The activation of p75 RyRs by sulfhydryl oxidants and NO implies that one or more of the nine cysteine residues in the p75 protein are the primary site of action of NO since the p75 truncated channel exhibits similar properties as the full-length receptor with respect to NO. The p75 protein does not include C3635, which is located at the calmodulin binding site and was proposed to be the NO binding site; yet NO-donors activated the p75 receptor, like the p565 RyR1, indicating that the 'critical' regulatory thiols are located closer to the C-terminus of the protein, where a total of 9 cysteine residues reside. Moreover, two of the 9 cysteine residues, C4958 and C4961, are the most likely candidates because they reside in a conserved domain for RyR1, RyR2 and RyR3, as well as IP3 receptors. However, the possibility remains that additional thiols are involved in the interaction with NO, as suggested by the various RyR1 fragments that can be cross-linked by maleimides [120] and because of the graded levels of RyR2 S-nitrosylation that can be obtained as a function of NO concentration [14]. Nevertheless, the strategy of testing truncated RyRs shows immense promise to help us resolve the structure function relationship by site directed mutations in an otherwise large and unmanageable protein.

6.5.2 Permanent Expression of p75 RyR1

The data from intracellular Ca^{2+} assay in transfected CHO cells expressing truncated RyRs suggested p75 RyR1 forms a functioning channel since they retain ryanodine sensitivity, NO and sulfhydryl regulation of the channel. The cells expressing p75 RyR1 lost the response to caffeine, but the responses to the other conventional RyR modulators were retained, suggesting that this mini version of RyR might be able to work as a functioning Ca^{2+} channel.

p75 RyR was particularly interesting to study because: 1) cDNA encoding this 75 kDa RyR1 was cloned in the brain by Takeshima et al. [45]; 2) it contains only putative transmembrane domains and a carboxylic terminus excluding the large cytoplasmic region of RyR; 3) the formation of a functioning Ca^{2+} channel from p75 RyR will verify that the transmembrane domains required to form a functioning channel suggested by Takeshima et al. and Du et al.; 4) there are only 9 cysteine residues in p75 RyR1 and most of them are highly conserved among the mammalian RyRs and IP_3Rs. Therefore, we can test our hypothesis that the regulatory cysteine residues involved in the nitric oxide-mediated regulation of RyRs are in a highly conserved domain. Therefore, it was attempted to express p75 RyR1 and record its single channel activity.

The transient expression method allowed us to obtain proteins in a short time after the transfection, but one needs to transfect cells every time proteins are needed and the concentration of the expressed protein in the membrane fraction is often not high enough because of the limited efficiency of transfection. To obtain an ample supply of protein to study single channel activity, we developed a perpetual cell line expressing p75 RyR. The use of FlpIn system (Invitrogen, CA) make it possible to obtain perpetual cell lines to express various truncated and mutated RyRs in a relatively short time.

6.5.3 Single Channel Study of p75 RyR1

To test the hypothesis that cysteines involved in redox regulation of RyRs are located in the C-terminal region of RyRs, truncated p75 RyR1 clones were expressed in mammalian cells, purified and reconstituted in planar bilayers. The properties of truncated RyR1 were then compared to the full-length RyR1 in terms of conductance, their responses to ryanodine, redox state and NO.

p75 RyR1 forms functional channel. The reconstituted channel showed a slight inward rectification showing that the current from the luminal to cytosolic side was bigger (390.3 ± 33.4 (pS)) than the current from the cytosolic to luminal side (294.2 ± 37.1 (pS)). The conductance of full length RyR with the solution condition employing Cs^+ as a current carrier is around 450 pS. Therefore, the conductance of the p75 RyR1 channel was slightly lower than that of native RyR1. p75 channels responded to ryanodine resulting in a channel locked in a subconductance state. Moreover, the truncated channel was activated by cys-SNO added to the cytosolic side of the channel. This provides staunch evidence that the M5-M10 transmembrane domains confirmed as membrane associated domains in the previous study [56] were the entire transmembrane domains necessary to form a functioning channel, and at least one or more cytosolic cysteine residues in p75 RyR1 is involved in the nitric oxide-mediated activation of RyR1. It is important to note that cysteine residues available from the cytosolic side are highly conserved among mammalian RyRs.

6.6 REVISITING NO-INDUCED RELAXATION OF SMOOTH MUSCLE

Nitric oxide got its fame from its function on smooth muscle relaxation through the cGMP-dependent pathway. Our findings that more stable NO-molecules that can carry NO-

function to regions far from where NO was synthesized and that NO acts on the conserved moiety of RyR have immense meaning in that the NO-mediated regulation of RyR would be a universal mechanism to regulate all isoforms of RyRs.

Smooth muscle cells could be relaxed by lowering cytoplasmic Ca^{2+} or desensitizing the contractile apparatus to Ca^{2+}. A major pathway to relax smooth muscle cells is known to be cGMP-dependent. Several mechanisms have been proposed to explain how cGMP mediates the relaxation of smooth muscle. cGMP stimulates cGMP-dependent protein kinase (PKG), which phosphorylates several proteins to cause the relaxation of smooth muscle. It was proposed that PKG phosphorylates phospholamban resulting in the activation of Ca^{2+}-ATPase on the SR membrane, which increases SR Ca^{2+} load, and increases Ca^{2+} sparks frequency [107, 188, 189]. PKG phosphorylates the BK_{Ca} channel [108], but the direct effect of PKG and PKA on BK_{Ca} channel activity in intact cells appears to be weak compared to the activation caused by increased Ca^{2+} spark frequency [107]. cGMP were shown to activate myosin light chain phophatase (MLCP), resulting in decreased Ca^{2+} sensitivity of the contractile apparatus. This study used ODQ to selectively inhibit the soluble guanylate cyclase and confirmed that this desensitization effect by NO was through the cGMP-dependent pathway [190]. But, they did not separate the effect of cGMP on the myosin light chain phophatase (MLCP) from that on the other factors that might contribute to the muscle relaxation. In another report, GSNO was shown to reduce the phosphorylation of myosin light chain resulting in the decreased Ca^{2+} sensitivity of myofilament, but the mechanism behind this observation was not elucidated [191].

Inhibition of cGMP production by ODQ did not completely abolish the NO-derived relaxation of smooth muscle [110], which indicates that NO relaxes smooth muscle cells by cGMP independent mechanism. For instance, repolarization can relax smooth muscle cell by a

cGMP-independent mechanism [110]. NO could act by a direct activation of the BK_{Ca} channel, but support for the mechanism is sparse. Most studies have overlooked that NO can activate the RyR directly to impart relaxation without involving cGMP. Single channel activity of RyRs from smooth muscle cell has not been extensively studied due to technical difficulties such as isolation of SR and reconstitution of channels.

Here, we propose that cGMP-independent relaxation of smooth muscle cells are mediated via the activation of the RyR on the SR by NO or more precisely a physiological form of NO, such as LMW S-nitrosothiols, resulting in increased Ca^{2+} sparks from the SR, enhanced outward currents through the BK_{Ca} channels, hyperpolarization of the membrane potential, which leads to the relaxation of smooth muscle.

6.7 LIMITATION OF THE CURRENT STUDY AND FUTURE WORK

This study excluded the action of NO on the accessory proteins associated with the RyR channel or any other proteins related to Ca^{2+} homeostasis. LMW S-nitrosothiols, especially cys-SNO and HNO, were shown to be highly potent in activating the purified RyR1 channel via trans-S-nitrosation and the formation of a disulfide bond respectively. However, the experimental methods are simplifications of intact cells which contain reactive oxygen species and antioxidant systems (NADPH, glutathione); thiol compounds that protect cells, the thioredoxin system, superoxide dismutase (SOD), catalase, and various molecules containing free thiols that might work as a sulfhydryl reductant, such as L-cysteine; several proteins containing heme moiety that reacts with $NO^{\bullet}$; and many more factors.

Further studies are needed to elucidate the interplay of oxidizing and reducing agents formed in the cytosolic milieu of all cells and how these activators and inhibitors act to regulate

the opening and closure of Ca^{2+} release channels while all endogenous RyR modulators and accessory proteins are intact in order to understand the regulation of Ca^{2+} homeostasis in intact cells.

7.0 SUMMARY AND CONCLUSIONS

This study showed that S-nitrosothiols activate the SR Ca^{2+} channel equally well in the presence or absence of $NO^{\bullet}$ liberation from them, and one must deduce that S-nitrosothiols oxidize RyRs predominantly by an exchange of NO^{+} ions between the hyperreactive thiol group on RyRs and S-nitrosothiols through 'transnitrosation'. LMW S-nitrosothiols, especially cys-SNO, induced rapid Ca^{2+} release from isolated SR vesicles by activating RyR1 and inhibiting CK activity that is the source of ATP for Ca^{2+}-ATPase through 'transnitrosation'. This suggests that NO requires low molecular weight thiol catalysis to interact with these proteins and the transnitrosation of free thiols on these proteins by low molecular weight S-nitrosothiols may be a biologically relevant mechanism for NO to control local Ca^{2+} concentration in muscle cells. The study proposes that cys-SNO is the biologically significant NO compound that modulates muscle force. There was a controversy about the role of oxygen on the nitrosation of the RyR. This study showed that pO_2 did not alter the activation of RyR1 by NO-dependent or NO-independent (trans-nitrosation) nitrosation.

HNO produced from ANGS was found to elicit a prompt release of Ca^{2+} from Ca^{2+}-loaded skeletal SR vesicles and that the addition of a sulfhydryl reducing agent, DTT, reversed the effect, resulting in the active re-uptake of Ca^{2+} by SR vesicles. These results suggest that shifts in the equilibrium between $NO^{\bullet}$, S-nitrosothiols, and HNO will promote low levels of the latter species that will affect calcium homeostasis via activation of RyRs.

Truncated RyR (p75 RyR) forms a functional channel responding to ryanodine resulting in the channel locked up at subconductance level. Moreover, it was activated by cys-SNO added to the cytosolic side of the channel. This gives staunch evidence that all the transmembrane domains necessary to form a functioning channel are located within p75 kDa RyR, and at least one or more cytosolic cysteine residue(s) among cysteine residues residing in p75 RyR1 is (are) involved in the nitric oxide-mediated activation of the RyR.

Although the nitric oxide-mediated regulation of the RyR shown here is certainly a simplification of the true nature of regulation of Ca^{2+} homeostasis in striated muscles, it has given useful insight into the direct action of NO-related molecules on RyR molecule.

In conclusion, we investigated the chemical reaction underlying the nitric oxide-mediated regulation of the ryanodine receptor and identification of cysteine residues involved in nitric oxide regulation of the RyR and found that the trans-S-nitrosation by LMW S-nitrosothiols or the disulfide formation by HNO might be more realistic mechanism for nitric oxide to regulate Ca^{2+} handling via RyRs. At least one or more 'critical' regulatory thiol(s) involved in the activation of the RyR by S-nitrosothiols must be part of the cysteine residues located close to the C-terminus of the RyR molecule where most cysteine residues are highly conserved.

BIBLIOGRAPHY

1. Kojda, G. and D. Harrison, *Interactions between NO and reactive oxygen species: pathophysiological importance in atherosclerosis, hypertension, diabetes and heart failure.* Cardiovasc Res, 1999. **43**(3): p. 562-71.
2. Kohen, R. and A. Nyska, *Oxidation of biological systems: oxidative stress phenomena, antioxidants, redox reactions, and methods for their quantification.* Toxicol Pathol, 2002. **30**(6): p. 620-50.
3. Suzuki, Y.J. and G.D. Ford, *Redox regulation of signal transduction in cardiac and smooth muscle.* J Mol Cell Cardiol, 1999. **31**(2): p. 345-53.
4. Stamler, J.S. and G. Meissner, *Physiology of nitric oxide in skeletal muscle.* Physiol Rev, 2001. **81**(1): p. 209-237.
5. Murad, F., *Nitric oxide signaling: would you believe that a simple free radical could be a second messenger, autacoid, paracrine substance, neurotransmitter, and hormone?* Recent Prog Horm Res, 1998. **53**: p. 43-59; discussion 59-60.
6. Pessah, I.N., *Ryanodine receptor acts as a sensor for redox stress.* Pest Manag Sci, 2001. **57**(10): p. 941-5.
7. Hare, J.M., *Nitric oxide and excitation-contraction coupling.* J Mol Cell Cardiol, 2003. **35**(7): p. 719-29.
8. Ignarro, L.J., *Nitric oxide. A novel signal transduction mechanism for transcellular communication.* Hypertension, 1990. **16**(5): p. 477-83.
9. Furchgott, R.F. and P.M. Vanhoutte, *Endothelium-derived relaxing and contracting factors.* Faseb J, 1989. **3**(9): p. 2007-18.
10. Gaston, B., et al., *Relaxation of human bronchial smooth muscle by S-nitrosothiols in vitro.* J Pharmacol Exp Ther, 1994. **268**(2): p. 978-84.
11. Rapoport, R.M., M.B. Draznin, and F. Murad, *Endothelium-dependent relaxation in rat aorta may be mediated through cyclic GMP-dependent protein phosphorylation.* Nature, 1983. **306**(5939): p. 174-6.
12. Stuart-Smith, K., D.O. Warner, and K.A. Jones, *The role of cGMP in the relaxation to nitric oxide donors in airway smooth muscle.* Eur J Pharmacol, 1998. **341**(2-3): p. 225-33.
13. Eu, J.P., et al., *Regulation of ryanodine receptors by reactive nitrogen species.* Biochem Pharmacol, 1999. **57**(10): p. 1079-84.

14. Xu, L., et al., *Activation of the cardiac calcium release channel (ryanodine receptor) by poly-S-nitrosylation.* Science, 1998. **279**(5348): p. 234-7.

15. Stoyanovsky, D., et al., *Nitric oxide activates skeletal and cardiac ryanodine receptors.* Cell Calcium, 1997. **21**(1): p. 19-29.

16. Paolocci, N., et al., *Positive inotropic and lusitropic effects of HNO/NO- in failing hearts: independence from beta-adrenergic signaling.* Proc Natl Acad Sci U S A, 2003. **100**(9): p. 5537-42.

17. Petroff, M.G., et al., *Endogenous nitric oxide mechanisms mediumte the stretch dependence of Ca2+ release in cardiomyocytes.* Nat Cell Biol, 2001. **3**(10): p. 867-73.

18. Stamler, J.S., et al., *S-nitrosylation of proteins with nitric oxide: synthesis and characterization of biologically active compounds.* Proc Natl Acad Sci U S A, 1992. **89**(1): p. 444-8.

19. Arnelle, D.R. and J.S. Stamler, *NO+, NO, and NO- donation by S-nitrosothiols: implications for regulation of physiological functions by S-nitrosylation and acceleration of disulfide formation.* Arch Biochem Biophys, 1995. **318**(2): p. 279-85.

20. Doyle, M.P., et al., *Oxidation and reduction of hemoproteins by trioxodinitrate(II). The role of nitrosyl hydride and nitrite.* J. Am. Chem. Soc., 1988. **110**(2): p. 593-9.

21. Kim, W.K., et al., *Attenuation of NMDA receptor activity and neurotoxicity by nitroxyl anion, NO.* Neuron, 1999. **24**(2): p. 461-9.

22. Wolosker, H., R. Panizzutti, and S. Engelender, *Inhibition of creatine kinase by S-nitrosoglutathione.* FEBS Lett, 1996. **392**(3): p. 274-6.

23. Fill, M., et al., *Role of the ryanodine receptor of skeletal muscle in excitation-contraction coupling.* Ann N Y Acad Sci, 1989. **560**: p. 155-62.

24. Fill, M. and J.A. Copello, *Ryanodine receptor calcium release channels.* Physiol Rev, 2002. **82**(4): p. 893-922.

25. Franzini-Armstrong, C. and A.O. Jorgensen, *Structure and development of E-C coupling units in skeletal muscle.* Annu Rev Physiol, 1994. **56**: p. 509-34.

26. Franzini-Armstrong, C. and F. Protasi, *Ryanodine receptors of striated muscles: a complex channel capable of multiple interactions.* Physiol Rev, 1997. **77**(3): p. 699-729.

27. Zucchi, R. and S. Ronca-Testoni, *The sarcoplasmic reticulum Ca2+ channel/ryanodine receptor: modulation by endogenous effectors, drugs and disease states.* Pharmacol Rev, 1997. **49**(1): p. 1-51.

28. Marks, A.R., *Intracellular calcium-release channels: regulators of cell life and death.* Am J Physiol, 1997. **272**(2 Pt 2): p. H597-605.

29. Marks, A.R., *Cardiac intracellular calcium release channels: role in heart failure.* Circ Res, 2000. **87**(1): p. 8-11.

30. Marks, A.R., *Ryanodine receptors/calcium release channels in heart failure and sudden cardiac death.* J Mol Cell Cardiol, 2001. **33**(4): p. 615-24.

31. Missiaen, L., et al., *Abnormal intracellular ca(2+)homeostasis and disease.* Cell Calcium, 2000. **28**(1): p. 1-21.

32. Phillips, R.M., et al., *Sarcoplasmic reticulum in heart failure: central player or bystander?* Cardiovasc Res, 1998. **37**(2): p. 346-51.

33. Balshaw, D., L. Gao, and G. Meissner, *Luminal loop of the ryanodine receptor: a pore-forming segment?* Proc Natl Acad Sci U S A, 1999. **96**(7): p. 3345-7.

34. Berchtold, M.W., H. Brinkmeier, and M. Muntener, *Calcium ion in skeletal muscle: its crucial role for muscle function, plasticity, and disease.* Physiol Rev, 2000. **80**(3): p. 1215-65.

35. McCarthy, T.V., K.A. Quane, and P.J. Lynch, *Ryanodine receptor mutations in malignant hyperthermia and central core disease.* Hum Mutat, 2000. **15**(5): p. 410-7.

36. Oyamada, H., et al., *Novel mutations in C-terminal channel region of the ryanodine receptor in malignant hyperthermia patients.* Jpn J Pharmacol, 2002. **88**(2): p. 159-66.

37. Williams, A.J., D.J. West, and R. Sitsapesan, *Light at the end of the Ca(2+)-release channel tunnel: structures and mechanisms involved in ion translocation in ryanodine receptor channels.* Q Rev Biophys, 2001. **34**(1): p. 61-104.

38. Berne, R.M. and M.N. Levy, *Physiology*. 4th edition ed. 1998: Mosby.

39. Protasi, F., et al., *Multiple regions of RyR1 mediumte functional and structural interactions with alpha(1S)-dihydropyridine receptors in skeletal muscle.* Biophys J, 2002. **83**(6): p. 3230-44.

40. Protasi, F., C. Franzini-Armstrong, and P.D. Allen, *Role of ryanodine receptors in the assembly of calcium release units in skeletal muscle.* J Cell Biol, 1998. **140**(4): p. 831-42.

41. Protasi, F., et al., *RYR1 and RYR3 have different roles in the assembly of calcium release units of skeletal muscle.* Biophys J, 2000. **79**(5): p. 2494-508.

42. Franzini-Armstrong, C., F. Protasi, and V. Ramesh, *Comparative ultrastructure of Ca2+ release units in skeletal and cardiac muscle.* Ann N Y Acad Sci, 1998. **853**: p. 20-30.

43. Nelson, M.T., et al., *Relaxation of arterial smooth muscle by calcium sparks.* Science, 1995. **270**(5236): p. 633-7.

44. Zorzato, F., et al., *Molecular cloning of cDNA encoding human and rabbit forms of the Ca2+ release channel (ryanodine receptor) of skeletal muscle sarcoplasmic reticulum.* J Biol Chem, 1990. **265**(4): p. 2244-56.

45. Takeshima, H., *Primary structure and expression from cDNAs of the ryanodine receptor.* Ann N Y Acad Sci, 1993. **707**: p. 165-77.

46. Takeshima, H., et al., *Primary structure and expression from complementary DNA of skeletal muscle ryanodine receptor.* Nature, 1989. **339**(6224): p. 439-45.

47. Nakai, J., et al., *Primary structure and functional expression from cDNA of the cardiac ryanodine receptor/calcium release channel.* FEBS Lett, 1990. **271**(1-2): p. 169-77.

48. Du, G.G. and D.H. MacLennan, *Functional consequences of mutations of conserved, polar amino acids in transmembrane sequences of the Ca2+ release channel (ryanodine*

receptor) of rabbit skeletal muscle sarcoplasmic reticulum. J Biol Chem, 1998. **273**(48): p. 31867-72.

49. Gao, L., et al., *Evidence for a role of C-terminal amino acid residues in skeletal muscle Ca2+ release channel (ryanodine receptor) function.* FEBS Lett, 1997. **412**(1): p. 223-6.

50. Wagenknecht, T. and M. Radermacher, *Three-dimensional architecture of the skeletal muscle ryanodine receptor.* FEBS Lett, 1995. **369**(1): p. 43-6.

51. Wagenknecht, T., et al., *Locations of calmodulin and FK506-binding protein on the three-dimensional architecture of the skeletal muscle ryanodine receptor.* J Biol Chem, 1997. **272**(51): p. 32463-71.

52. Wagenknecht, T. and M. Samso, *Three-dimensional reconstruction of ryanodine receptors.* Front Biosci, 2002. **7**: p. d1464-74.

53. Samso, M. and T. Wagenknecht, *Contributions of electron microscopy and single-particle techniques to the determination of the ryanodine receptor three-dimensional structure.* J Struct Biol, 1998. **121**(2): p. 172-80.

54. Brandt, N.R., et al., *Mapping of the calpain proteolysis products of the junctional foot protein of the skeletal muscle triad junction.* J Membr Biol, 1992. **127**(1): p. 35-47.

55. Grunwald, R. and G. Meissner, *Lumenal sites and C terminus accessibility of the skeletal muscle calcium release channel (ryanodine receptor).* J Biol Chem, 1995. **270**(19): p. 11338-47.

56. Du, G.G., et al., *Topology of the Ca2+ release channel of skeletal muscle sarcoplasmic reticulum (RyR1).* Proc Natl Acad Sci U S A, 2002. **99**(26): p. 16725-30.

57. Bhat, M.B., et al., *Functional calcium release channel formed by the carboxyl-terminal portion of ryanodine receptor.* Biophys J, 1997. **73**(3): p. 1329-36.

58. Lynch, P.J., et al., *A mutation in the transmembrane/luminal domain of the ryanodine receptor is associated with abnormal Ca2+ release channel function and severe central core disease.* Proc Natl Acad Sci U S A, 1999. **96**(7): p. 4164-9.

59. Gao, L., et al., *Evidence for a role of the lumenal M3-M4 loop in skeletal muscle Ca(2+) release channel (ryanodine receptor) activity and conductance.* Biophys J, 2000. **79**(2): p. 828-40.

60. Bhat, M.B., et al., *Deletion of amino acids 1641-2437 from the foot region of skeletal muscle ryanodine receptor alters the conduction properties of the Ca release channel.* Biophys J, 1997. **73**(3): p. 1320-8.

61. Sutko, J.L., et al., *The pharmacology of ryanodine and related compounds.* Pharmacol Rev, 1997. **49**(1): p. 53-98.

62. Sitsapesan, R. and A.J. Williams, *Regulation of current flow through ryanodine receptors by luminal Ca2+.* J Membr Biol, 1997. **159**(3): p. 179-85.

63. Gyorke, I. and S. Gyorke, *Regulation of the cardiac ryanodine receptor channel by luminal Ca2+ involves luminal Ca2+ sensing sites.* Biophys J, 1998. **75**(6): p. 2801-10.

64. Chen, S.R., L. Zhang, and D.H. MacLennan, *Characterization of a Ca2+ binding and regulatory site in the Ca2+ release channel (ryanodine receptor) of rabbit skeletal muscle sarcoplasmic reticulum.* J Biol Chem, 1992. **267**(32): p. 23318-26.

65. Du, G.G., V.K. Khanna, and D.H. MacLennan, *Mutation of divergent region 1 alters caffeine and Ca(2+) sensitivity of the skeletal muscle Ca(2+) release channel (ryanodine receptor).* J Biol Chem, 2000. **275**(16): p. 11778-83.

66. Hayek, S.M., et al., *Characterization of a calcium-regulation domain of the skeletal-muscle ryanodine receptor.* Biochem J, 2000. **351**(Pt 1): p. 57-65.

67. Hayek, S.M., et al., *A negatively charged region of the skeletal muscle ryanodine receptor is involved in Ca(2+)-dependent regulation of the Ca(2+) release channel.* FEBS Lett, 1999. **461**(3): p. 157-64.

68. Abramson, J.J. and G. Salama, *Sulfhydryl oxidation and Ca2+ release from sarcoplasmic reticulum.* Mol Cell Biochem, 1988. **82**(1-2): p. 81-4.

69. Abramson, J.J. and G. Salama, *Critical sulfhydryls regulate calcium release from sarcoplasmic reticulum.* J Bioenerg Biomembr, 1989. **21**(2): p. 283-94.

70. Marengo, J.J., C. Hidalgo, and R. Bull, *Sulfhydryl oxidation modifies the calcium dependence of ryanodine-sensitive calcium channels of excitable cells.* Biophys J, 1998. **74**(3): p. 1263-77.

71. Salama, G., J.J. Abramson, and G.K. Pike, *Sulphydryl reagents trigger Ca2+ release from the sarcoplasmic reticulum of skinned rabbit psoas fibres.* J Physiol, 1992. **454**: p. 389-420.

72. Prabhu, S.D. and G. Salama, *The heavy metal ions Ag+ and Hg2+ trigger calcium release from cardiac sarcoplasmic reticulum.* Arch Biochem Biophys, 1990. **277**(1): p. 47-55.

73. Salama, G. and J. Abramson, *Silver ions trigger Ca2+ release by acting at the apparent physiological release site in sarcoplasmic reticulum.* J Biol Chem, 1984. **259**(21): p. 13363-9.

74. Proenza, C., et al., *Identification of a region of RyR1 that participates in allosteric coupling with the alpha(1S) (Ca(V)1.1) II-III loop.* J Biol Chem, 2002. **277**(8): p. 6530-5.

75. Stange, M., A. Tripathy, and G. Meissner, *Two domains in dihydropyridine receptor activate the skeletal muscle Ca(2+) release channel.* Biophys J, 2001. **81**(3): p. 1419-29.

76. Sheridan, D.C., et al., *Truncation of the carboxyl terminus of the dihydropyridine receptor beta1a subunit promotes Ca2+ dependent excitation-contraction coupling in skeletal myotubes.* Biophys J, 2003. **84**(1): p. 220-37.

77. Masumiya, H., et al., *Localization of the 12.6-kDa FK506-binding protein (FKBP12.6) binding site to the NH2-terminal domain of the cardiac Ca2+ release channel (ryanodine receptor).* J Biol Chem, 2003. **278**(6): p. 3786-92.

78. Smith, J.S., E. Rousseau, and G. Meissner, *Calmodulin modulation of single sarcoplasmic reticulum Ca2+-release channels from cardiac and skeletal muscle.* Circ Res, 1989. **64**(2): p. 352-9.

79. Balshaw, D.M., et al., *Calmodulin binding and inhibition of cardiac muscle calcium release channel (ryanodine receptor).* J Biol Chem, 2001. **276**(23): p. 20144-53.

80. Fruen, B.R., et al., *Regulation of the RYR1 and RYR2 Ca2+ release channel isoforms by Ca2+-insensitive mutants of calmodulin.* Biochemistry, 2003. **42**(9): p. 2740-7.

81. Hamilton, S.L. and M.B. Reid, *RyR1 modulation by oxidation and calmodulin.* Antioxid Redox Signal, 2000. **2**(1): p. 41-5.

82. Zhang, J.Z., et al., *Oxidation of the skeletal muscle Ca2+ release channel alters calmodulin binding.* Am J Physiol, 1999. **276**(1 Pt 1): p. C46-53.

83. Eu, J.P., et al., *The skeletal muscle calcium release channel: coupled O2 sensor and NO signaling functions.* Cell, 2000. **102**(4): p. 499-509.

84. Sun, J., et al., *Cysteine-3635 is responsible for skeletal muscle ryanodine receptor modulation by NO.* Proc Natl Acad Sci U S A, 2001. **98**(20): p. 11158-62.

85. Sun, J., et al., *Classes of thiols that influence the activity of the skeletal muscle calcium release channel.* J Biol Chem, 2001. **276**(19): p. 15625-30.

86. Sun, J., et al., *Nitric oxide, NOC-12, and S-nitrosoglutathione modulate the skeletal muscle calcium release channel/ryanodine receptor by different mechanisms. An allosteric function for O2 in S-nitrosylation of the channel.* J Biol Chem, 2003. **278**(10): p. 8184-9.

87. Eager, K.R. and A.F. Dulhunty, *Activation of the cardiac ryanodine receptor by sulfhydryl oxidation is modified by Mg2+ and ATP.* J Membr Biol, 1998. **163**(1): p. 9-18.

88. Suko, J., H. Drobny, and G. Hellmann, *Activation and inhibition of purified skeletal muscle calcium release channel by NO donors in single channel current recordings.* Biochim Biophys Acta, 1999. **1451**(2-3): p. 271-87.

89. Abramson, J.J., et al., *Heavy metals induce rapid calcium release from sarcoplasmic reticulum vesicles isolated from skeletal muscle.* Proc Natl Acad Sci U S A, 1983. **80**(6): p. 1526-30.

90. Stoyanovsky, D.A., G. Salama, and V.E. Kagan, *Ascorbate/iron activates Ca(2+)-release channels of skeletal sarcoplasmic reticulum vesicles reconstituted in lipid bilayers.* Arch Biochem Biophys, 1994. **308**(1): p. 214-21.

91. Zaidi, N.F., et al., *Reactive disulfides trigger Ca2+ release from sarcoplasmic reticulum via an oxidation reaction.* J Biol Chem, 1989. **264**(36): p. 21725-36.

92. Trimm, J.L., G. Salama, and J.J. Abramson, *Sulfhydryl oxidation induces rapid calcium release from sarcoplasmic reticulum vesicles.* J Biol Chem, 1986. **261**(34): p. 16092-8.

93. Prabhu, S.D. and G. Salama, *Reactive disulfide compounds induce Ca2+ release from cardiac sarcoplasmic reticulum.* Arch Biochem Biophys, 1990. **282**(2): p. 275-83.

94. Pessah, I.N. and W. Feng, *Functional role of hyperreactive sulfhydryl moieties within the ryanodine receptor complex.* Antioxid Redox Signal, 2000. **2**(1): p. 17-25.

95. Pessah, I.N., K.H. Kim, and W. Feng, *Redox sensing properties of the ryanodine receptor complex.* Front Biosci, 2002. **7**: p. a72-9.

96. Feng, W., et al., *Transmembrane redox sensor of ryanodine receptor complex.* J Biol Chem, 2000. **275**(46): p. 35902-7.

97. Xia, R., T. Stangler, and J.J. Abramson, *Skeletal muscle ryanodine receptor is a redox sensor with a well defined redox potential that is sensitive to channel modulators.* J Biol Chem, 2000. **275**(47): p. 36556-61.

98. Jensen, D.E., G.K. Belka, and G.C. Du Bois, *S-Nitrosoglutathione is a substrate for rat alcohol dehydrogenase class III isoenzyme.* Biochem. J., 1998. **331 (Pt 2)**: p. 659-68.

99. Kanai, A.J., et al., *Beta-adrenergic regulation of constitutive nitric oxide synthase in cardiac myocytes.* Am J Physiol, 1997. **273**(4 Pt 1): p. C1371-7.

100. Hogg, N., *The biochemistry and physiology of S-nitrosothiols.* Annu Rev Pharmacol Toxicol, 2002. **42**: p. 585-600.

101. Menshikova, E.V., et al., *Nitric oxide prevents myoglobin/tert-butyl hydroperoxide-induced inhibition of Ca2+ transport in skeletal and cardiac sarcoplasmic reticulum.* Ann N Y Acad Sci, 1999. **874**: p. 371-85.

102. Lin, C.S., et al., *Analysis of neuronal nitric oxide synthase isoform expression and identification of human nNOS-mu.* Biochem Biophys Res Commun, 1998. **253**(2): p. 388-94.

103. Mashimo, H. and R.K. Goyal, *Lessons from genetically engineered animal models. IV. Nitric oxide synthase gene knockout mice.* Am J Physiol, 1999. **277**(4 Pt 1): p. G745-50.

104. Huang, P.L., et al., *Hypertension in mice lacking the gene for endothelial nitric oxide synthase.* Nature, 1995. **377**(6546): p. 239-42.

105. Lincoln, T.M., P. Komalavilas, and T.L. Cornwell, *Pleiotropic regulation of vascular smooth muscle tone by cyclic GMP-dependent protein kinase.* Hypertension, 1994. **23**(6 Pt 2): p. 1141-7.

106. Carvajal, J.A., et al., *Molecular mechanism of cGMP-mediated smooth muscle relaxation.* J Cell Physiol, 2000. **184**(3): p. 409-20.

107. Jaggar, J.H., et al., *Calcium sparks in smooth muscle.* Am J Physiol Cell Physiol, 2000. **278**(2): p. C235-56.

108. Fukao, M., et al., *Cyclic GMP-dependent protein kinase activates cloned BKCa channels expressed in mammalian cells by direct phosphorylation at serine 1072.* J Biol Chem, 1999. **274**(16): p. 10927-35.

109. Onoue, H. and Z.S. Katusic, *The effect of 1H-[1,2,4]oxadiazolo[4,3-a]quinoxalin-1-one (ODQ) and charybdotoxin (CTX) on relaxations of isolated cerebral arteries to nitric oxide.* Brain Res, 1998. **785**(1): p. 107-13.

110. Plane, F., et al., *Evidence that different mechanisms underlie smooth muscle relaxation to nitric oxide and nitric oxide donors in the rabbit isolated carotid artery.* Br J Pharmacol, 1998. **123**(7): p. 1351-8.

111. Pinsky, D.J., et al., *Mechanical transduction of nitric oxide synthesis in the beating heart.* Circ Res, 1997. **81**(3): p. 372-9.

112. Mohan, P., et al., *Myocardial contractile response to nitric oxide and cGMP.* Circulation, 1996. **93**(6): p. 1223-9.

113. Ziolo, M.T., H. Katoh, and D.M. Bers, *Positive and negative effects of nitric oxide on Ca(2+) sparks: influence of beta-adrenergic stimulation.* Am J Physiol Heart Circ Physiol, 2001. **281**(6): p. H2295-303.

114. Barouch, L.A., et al., *Nitric oxide regulates the heart by spatial confinement of nitric oxide synthase isoforms.* Nature, 2002. **416**(6878): p. 337-9.

115. Kobzik, L., et al., *Nitric oxide in skeletal muscle.* Nature, 1994. **372**(6506): p. 546-8.

116. Meszaros, L.G., I. Minarovic, and A. Zahradnikova, *Inhibition of the skeletal muscle ryanodine receptor calcium release channel by nitric oxide.* FEBS Lett, 1996. **380**(1-2): p. 49-52.

117. Massion, P.B., S. Moniotte, and J.L. Balligand, *Nitric oxide: does it play a role in the heart of the critically ill?* Curr Opin Crit Care, 2001. **7**(5): p. 323-36.

118. Haywood, G.A., et al., *Expression of inducible nitric oxide synthase in human heart failure.* Circulation, 1996. **93**(6): p. 1087-94.

119. Dawn, B. and R. Bolli, *Role of nitric oxide in myocardial preconditioning.* Ann N Y Acad Sci, 2002. **962**: p. 18-41.

120. Aghdasi, B., M.B. Reid, and S.L. Hamilton, *Nitric oxide protects the skeletal muscle Ca2+ release channel from oxidation induced activation.* J Biol Chem, 1997. **272**(41): p. 25462-7.

121. Thomas, D.D., et al., *The biological lifetime of nitric oxide: implications for the perivascular dynamics of NO and O2.* Proc Natl Acad Sci U S A, 2001. **98**(1): p. 355-60.

122. Kluge, I., et al., *S-nitrosoglutathione in rat cerebellum: identification and quantification by liquid chromatography-mass spectrometry.* J Neurochem, 1997. **69**(6): p. 2599-607.

123. Kharitonov, V.G., A.R. Sundquist, and V.S. Sharma, *Kinetics of nitrosation of thiols by nitric oxide in the presence of oxygen.* J Biol Chem, 1995. **270**(47): p. 28158-64.

124. Palmerini, C.A., et al., *Formation of nitrosothiols from gaseous nitric oxide at pH 7.4.* J Biochem Mol Toxicol, 2002. **16**(3): p. 135-9.

125. Gordge, M.P., et al., *Role of a copper (I)-dependent enzyme in the anti-platelet action of S-nitrosoglutathione.* Br J Pharmacol, 1996. **119**(3): p. 533-8.

126. Clancy, R.M. and S.B. Abramson, *Novel synthesis of S-nitrosoglutathione and degradation by human neutrophils.* Anal Biochem, 1992. **204**(2): p. 365-71.

127. Gordge, M.P., et al., *Copper chelation-induced reduction of the biological activity of S-nitrosothiols.* Br J Pharmacol, 1995. **114**(5): p. 1083-9.

128. Singh, R.J., et al., *Mechanism of nitric oxide release from S-nitrosothiols.* J Biol Chem, 1996. **271**(31): p. 18596-603.

129. Stubauer, G., A. Giuffre, and P. Sarti, *Mechanism of S-nitrosothiol formation and degradation mediated by copper ions.* J Biol Chem, 1999. **274**(40): p. 28128-33.

130. Megson, I.L., et al., *Prolonged effect of a novel S-nitrosated glyco-amino acid in endothelium-denuded rat femoral arteries: potential as a slow release nitric oxide donor drug.* Br J Pharmacol, 1997. **122**(8): p. 1617-24.

131. Gordge, M.P., J.S. Hothersall, and A.A. Noronha-Dutra, *Evidence for a cyclic GMP-independent mechanism in the anti-platelet action of S-nitrosoglutathione.* Br J Pharmacol, 1998. **124**(1): p. 141-8.

132. Jia, L., et al., *S-nitrosohaemoglobin: a dynamic activity of blood involved in vascular control.* Nature, 1996. **380**(6571): p. 221-6.

133. Hughes, M.N., *Relationships between nitric oxide, nitroxyl ion, nitrosonium cation and peroxynitrite.* Biochim. Biophys. Acta, 1999. **1411**(2-3): p. 263-72.

134. Wong, P.S., et al., *Reaction between S-nitrosothiols and thiols: generation of nitroxyl (HNO) and subsequent chemistry.* Biochemistry, 1998. **37**(16): p. 5362-71.

135. Salama, G., E.V. Menshikova, and J.J. Abramson, *Molecular interaction between nitric oxide and ryanodine receptors of skeletal and cardiac sarcoplasmic reticulum.* Antioxid Redox Signal, 2000. **2**(1): p. 5-16.

136. Salama, G. and A. Scarpa, *Enhanced Ca2+ uptake and ATPase activity of sarcoplasmic reticulum in the presence of diethyl ether.* J Biol Chem, 1980. **255**(14): p. 6525-8.

137. Moss, B., et al., *Host range restricted, non-replicating vaccinia virus vectors as vaccine candidates.* Adv Exp Med Biol, 1996. **397**: p. 7-13.

138. Moss, B., *Replicating and host-restricted non-replicating vaccinia virus vectors for vaccine development.* Dev Biol Stand, 1994. **82**: p. 55-63.

139. Menshikova, E.V. and G. Salama, *Cardiac ischemia oxidizes regulatory thiols on ryanodine receptors: captopril acts as a reducing agent to improve Ca2+ uptake by ischemic sarcoplasmic reticulum.* J Cardiovasc Pharmacol, 2000. **36**(5): p. 656-68.

140. Menshikova, E.V., E. Cheong, and G. Salama, *Low N-ethylmaleimide concentrations activate ryanodine receptors by a reversible interaction, not an alkylation of critical thiols.* J Biol Chem, 2000. **275**(47): p. 36775-80.

141. Grynkiewicz, G., M. Poenie, and R.Y. Tsien, *A new generation of Ca2+ indicators with greatly improved fluorescence properties.* J Biol Chem, 1985. **260**(6): p. 3440-50.

142. Miller, C., *Ion channel reconstitution*. 1986, New York: Plenum Press.

143. Colquhoun, D. and A.G. Hawkes, *The principles of the stochastic interpretation of ion-channel mechanism. In single channel recording.*, ed. B. Sakmann and E. Neher. 1995, New York: Plenum Press. 397-479.

144. Saftenku, E., A.J. Williams, and R. Sitsapesan, *Markovian models of low and high activity levels of cardiac ryanodine receptors.* Biophysic. J., 2001. **80**: p. 2727-2741.

145. Qin, F., A. Auerbach, and F. Sachs, *Maximum likelihood estimation of aggregated Markov processes.* Proc R Soc Lond B Biol Sci, 1997. **264**(1380): p. 375-83.

146. Qin, F., A. Auerbach, and F. Sachs, *Hidden Markov modeling for single channel kinetics with filtering and correlated noise.* Biophys J, 2000. **79**(4): p. 1928-44.

147. Qin, F., A. Auerbach, and F. Sachs, *A direct optimization approach to hidden Markov modeling for single channel kinetics.* Biophys J, 2000. **79**(4): p. 1915-27.

148. Clancy, R., A.I. Cederbaum, and D.A. Stoyanovsky, *Preparation and properties of S-nitroso-L-cysteine ethyl ester, an intracellular nitrosating agent.* J Med Chem, 2001. **44**(12): p. 2035-8.

149. Kanai, A.J., et al., *Shear stress induces ATP-independent transient nitric oxide release from vascular endothelial cells, measured directly with a porphyrinic microsensor.* Circ Res, 1995. **77**(2): p. 284-93.

150. Gergel, D. and A.I. Cederbaum, *Interaction of nitric oxide with 2-thio-5-nitrobenzoic acid: implications for the determination of free sulfhydryl groups by Ellman's reagent.* Arch Biochem Biophys, 1997. **347**(2): p. 282-8.

151. Konorev, E.A., B. Kalyanaraman, and N. Hogg, *Modification of creatine kinase by S-nitrosothiols: S-nitrosation vs. S-thiolation.* Free Radic Biol Med, 2000. **28**(11): p. 1671-8.

152. Kaasik, A., et al., *Nitric oxide inhibits cardiac energy production via inhibition of mitochondrial creatine kinase.* FEBS Lett, 1999. **444**(1): p. 75-7.

153. Hughes, M.N. and Wimbledon, *Chemistry of trioxodinitrates. 1. Decomposition of sodium trioxodinitrate (Angel's salt) in aqueous-solution.* J. Chem. Soc., Dalton, 1976: p. 703.

154. Shafirovich, V. and S.V. Lymar, *Nitroxyl and its anion in aqueous solutions: spin states, protic equilibria, and reactivities toward oxygen and nitric oxide.* Proc. Natl. Acad. Sci. U S A, 2002. **99**(11): p. 7340-5.

155. Loechler, E.L., Schneider, A. M., Schwartz, D. B., and Hollocher, T. C., J Am Chem Soc, 1987. **109**: p. 3076-3087.

156. Bonner, F.T., and Ravid, B., J. Inorg. Chem., 1975. **14**: p. 558-563.

157. Xia, Y., et al., *Electron paramagnetic resonance spectroscopy with N-methyl-D-glucamine dithiocarbamate iron complexes distinguishes nitric oxide and nitroxyl anion in a redox-dependent manner: applications in identifying nitrogen monoxide products from nitric oxide synthase.* Free Radic. Biol. Med., 2000. **29**(8): p. 793-7.

158. Bazylinski, D.A. and T.C. Hollocher, *Evidence from the Reaction between Trioxodinitrate(II) and ^{15}NO that Trioxodinitrate (II) decomposes into Nitrosyl Hydride and Nitrite in Neutral Aqueous Solution.* Inorg. Chem., 1985. **24**(25): p. 4285-4288.

159. Stoyanovsky, D.A., R.M. Clancy, and A.I. Cederbaum, *Decomposition of Sodium Trioxodinitrate (Angeli's Salt) to Hydroxyl Radical: An ESR Spin-Trapping Study.* J. Am. Chem. Soc., 1999. **121**(21): p. 5093-5094.

160. Field, R.J., N.V. Raghavan, and J.G. Brummer, *A pulse radiolysis investigation of the reactions of BrO2* with Fe(CN)64-, Mn(II), phenoxide ion, and phenol.* J. Am. Chem. Soc., 1982. **86**: p. 2443-2449.

161. Hage, J.P., A. Llobet, and D.T. Sawyer, *Aromatic hydroxylation by Fenton reagents {reactive intermediates [LxFe(II)OOH(BH+)], not free hydroxyl radical (HO*)}.* Bioorg. Med. Chem., 1995. **3**: p. 1383-1388.

162. Kaplin, A.I., et al., *Purified reconstituted inositol 1,4,5-trisphosphate receptors. Thiol reagents act directly on receptor protein.* J Biol Chem, 1994. **269**(46): p. 28972-8.

163. Gorbunov, N.V., et al., *Nitric oxide protects cardiomyocytes against tert-butyl hydroperoxide-induced formation of alkoxyl and peroxyl radicals and peroxidation of phosphatidylserine.* Biochem Biophys Res Commun, 1998. **244**(3): p. 647-51.

164. Oba, T., T. Murayama, and Y. Ogawa, *Redox states of type 1 ryanodine receptor alter Ca(2+) release channel response to modulators.* Am J Physiol Cell Physiol, 2002. **282**(4): p. C684-92.

165. Aghdasi, B., et al., *Multiple classes of sulfhydryls modulate the skeletal muscle Ca2+ release channel.* J. Biol. Chem., 1997. **272**: p. 3739-3748.

166. Hilkert, R., et al., *Properties of immunoaffinity purified 106-kDa Ca2+ release channels from the skeletal sarcoplasmic reticulum.* Arch Biochem Biophys, 1992. **292**(1): p. 1-15.

167. Zaidi, N.F., et al., *Disulfide linkage of biotin identifies a 106-kDa Ca2+ release channel in sarcoplasmic reticulum.* J Biol Chem, 1989. **264**(36): p. 21737-47.

168. Patel, R.P., et al., *Biochemical characterization of human S-nitrosohemoglobin. Effects on oxygen binding and transnitrosation.* J Biol Chem, 1999. **274**(22): p. 15487-92.

169. Hogg, N., *The kinetics of S-transnitrosation--a reversible second-order reaction.* Anal Biochem, 1999. **272**(2): p. 257-62.

170. Hogg, N., *Biological chemistry and clinical potential of S-nitrosothiols.* Free Radic Biol Med, 2000. **28**(10): p. 1478-86.

171. Wang, K., et al., *Equilibrium and kinetics studies of transnitrosation between S-nitrosothiols and thiols.* Bioorg Med Chem Lett, 2001. **11**(3): p. 433-6.

172. Liu, Z., et al., *S-Transnitrosation reactions are involved in the metabolic fate and biological actions of nitric oxide.* J Pharmacol Exp Ther, 1998. **284**(2): p. 526-34.

173. Scharfstein, J.S., et al., *In vivo transfer of nitric oxide between a plasma protein-bound reservoir and low molecular weight thiols.* J Clin Invest, 1994. **94**(4): p. 1432-9.

174. Saftenku, E., A.J. Williams, and R. Sitsapesan, *Markovian models of low and high activity levels of cardiac ryanodine receptors.* Biophys J, 2001. **80**(6): p. 2727-41.

175. Zahradnikova, A., M. Dura, and S. Gyorke, *Modal gating transitions in cardiac ryanodine receptors during increases of Ca2+ concentration produced by photolysis of caged Ca2+.* Pflugers Arch, 1999. **438**(3): p. 283-8.

176. Coll, R.J. and A.J. Murphy, *Sarcoplasmic reticulum CaATPase: product inhibition suggests an allosteric site for ATP activation.* FEBS Lett, 1985. **187**(1): p. 131-4.

177. Murphy, M.E. and H. Sies, *Reversible conversion of nitroxyl anion to nitric oxide by superoxide dismutase.* Proc. Natl. Acad. Sci. U S A, 1991. **88**(23): p. 10860-4.

178. Sharpe, M.A. and C.E. Cooper, *Reactions of nitric oxide with mitochondrial cytochrome c: a novel mechanism for the formation of nitroxyl anion and peroxynitrite.* Biochem. J., 1998. **332 (Pt 1)**: p. 9-19.

179. Hogg, N., R.J. Singh, and B. Kalyanaraman, *The role of glutathione in the transport and catabolism of nitric oxide.* FEBS Lett., 1996. **382**(3): p. 223-8.

180. Bartberger, M.D., J.M. Fukuto, and K.N. Houk, *On the acidity and reactivity of HNO in aqueous solution and biological systems.* Proc. Natl. Acad. Sci. U S A, 2001. **98**(5): p. 2194-8.

181. Bartberger, M.D., et al., *The reduction potential of nitric oxide (NO) and its importance to NO biochemistry.* Proc. Natl. Acad. Sci. U S A, 2002. **99**(17): p. 10958-63.

182. Miranda, K.M., et al., *Comparison of the reactivity of nitric oxide and nitroxyl with heme proteins. A chemical discussion of the differential biological effects of these redox related products of NOS.* J. Inorg. Biochem., 2003. **93**(1-2): p. 52-60.

183. Ohshima, H., I. Gilibert, and F. Bianchini, *Induction of DNA strand breakage and base oxidation by nitroxyl anion through hydroxyl radical production.* Free Radic. Biol. Med., 1999. **26**(9-10): p. 1305-13.

184. Kirsch, M. and H. de Groot, *Formation of peroxynitrite from reaction of nitroxyl anion with molecular oxygen.* J. Biol. Chem., 2002. **277**(16): p. 13379-88.

185. Ehrlich, B.E., et al., *The pharmacology of intracellular Ca(2+)-release channels.* Trends Pharmacol Sci, 1994. **15**(5): p. 145-9.

186. Mayrleitner, M., R. Schafer, and S. Fleischer, *IP3 receptor purified from liver plasma membrane is an (1,4,5)IP3 activated and (1,3,4,5)IP4 inhibited calcium permeable ion channel.* Cell Calcium, 1995. **17**(2): p. 141-53.

187. Mak, D.O. and J.K. Foskett, *Single-channel inositol 1,4,5-trisphosphate receptor currents revealed by patch clamp of isolated Xenopus oocyte nuclei.* J Biol Chem, 1994. **269**(47): p. 29375-8.

188. Zhuge, R., et al., *Spontaneous transient outward currents arise from microdomains where BK channels are exposed to a mean Ca(2+) concentration on the order of 10 microM during a Ca(2+) spark.* J Gen Physiol, 2002. **120**(1): p. 15-27.

189. ZhuGe, R., et al., *The influence of sarcoplasmic reticulum Ca2+ concentration on Ca2+ sparks and spontaneous transient outward currents in single smooth muscle cells.* J Gen Physiol, 1999. **113**(2): p. 215-28.

190. Bolz, S.S., et al., *Nitric oxide-induced decrease in calcium sensitivity of resistance arteries is attributable to activation of the myosin light chain phosphatase and antagonized by the RhoA/Rho kinase pathway.* Circulation, 2003. **107**(24): p. 3081-7.

191. Pabelick, C.M., et al., *S-nitrosoglutathione-induced decrease in calcium sensitivity of airway smooth muscle.* Am J Physiol Lung Cell Mol Physiol, 2000. **278**(3): p. L521-7.